ABSTRACT

KAYSER, MOHAMMAD. Investigation of Soil Erodibility using In Situ Erosion Evaluation Probe (ISEEP). (Under the direction of Professor Mohammed Gabr.)

Scour evaluation is a critical step for assessing the stability of several types of highway infrastructures during design and post construction stages as well as throughout the operational life of the structure. During the design stage, the knowledge of scour potential and depth is critical for specifying and designing various types of foundations and the development of their load carrying capacities. In addition, the knowledge of the progress of scour with time allows for the establishment of maintenance priorities and replacement schedules. Current techniques for assessing *in situ* erosion potential with depth require either the removal of soil samples for laboratory testing, thus limiting its utility to materials that can be sampled as such, or measuring erosion that has already occurred by monitoring changes in the mud-line elevation. The instruments used for non-invasive techniques range from simple steel sounding rods to remote sensing devices that employ electromagnetic waves and/or sonar with sound propagation. These approaches however only provide no data to estimate the potential of future erosion and scour. Therefore development of an affordable in situ device to provide data to estimate the soil erosion parameters is vital.

The overall objective of this study is the development of a procedure for assessing in situ soil erosion parameters with depth. The approach is developed based on data from the In Situ Erosion Evaluation Probe (ISEEP), which utilizes jetted water to advance a rod into the subsurface profile. The jet flow velocity and the advancement rate of the probe are correlated with a stream power value, which is then correlated with soil erodibility potential. Laboratory testing is performed to investigate the feasibility of the concept, and an approach for assessing the critical stream power and a detachment coefficient is proposed. Field tests are performed using ISEEP in both marine environment and riverine environment. Penetration rate vs. stream power plots are developed and the detachment coefficient, used in the computation of erosion magnitude with time, is obtained from these plots. Correlation of penetration rates with SPT N values is also explored to discern whether or not the ISEEP data reflect changes in soil density.

The influence of flow phenomena on the bed shear stress around cylinders is also investigated for live-bed and clear water scour, respectively, using Computational Fluid Dynamics (CFD) software FLOW-3D. Shear stress profiles with normalized scour depth are obtained from the simulations. The numerical model is calibrated through simulations of conditions observed from laboratory flume tests data reported in literature. Effect of sediment gradation on maximum shear stress and scour depth is also investigated for live bed scour. An equation that provides maximum shear stress around piers before scour starts is proposed based on the results of the numerical study. Parameters included in the equation include Reynolds number, mean flow velocity, fluid density and critical shields number. It is observed that maximum shear stress does not change with the change of soil gradation. However, equilibrium scour depth decreases with the increase of sediment gradation. Live-bed shear stress profile show that within a range of velocities used in the normalized shear profile follows similar trend, regardless of the velocity magnitude.

Computational fluid dynamics (CFD) software, FLOW-3D, is also used to assess the scour depth around a bridge pier. The results from modeling are compared with values that are based on ISEEP-estimated parameters and those calculated using empirical equations in literature. Estimated scour depths based on ISEEP data agree relatively well with the scour magnitudes obtained from the numerical analysis, as ISEEP data reflect the change in properties of the soil layer with depth. In contrast, the scour depth calculated from the empirical equations is underestimated, mainly because the equations have no provision for a layered soil profile. Correlations between scour magnitudes estimated by ISEEP parameters and those estimated through modeling illustrate viability of ISEEP's soil erosion parameters, as defined by a critical stream power and a detachment coefficient, in estimating scour magnitudes. Further validation of both the field testing procedure and data reduction approach, including the assessment of the approach applicability to soils that contain an appreciable percentage of fines, is recommended.

Investigation of Soil Erodibility using In Situ Erosion Evaluation Probe (ISEEP)

by
Mohammad Kayser

A dissertation submitted to the Graduate Faculty of
North Carolina State University
in partial fulfillment of the
requirements for the degree of
Doctor of Philosophy

Civil Engineering

Raleigh, North Carolina

2014

APPROVED BY:

Mohammed Gabr Committee Chair	Roy Borden
Shamim Rahman	Margery Overton
Elana Leithold	

BIOGRAPHY

Mohammad Kayser was born in Dhaka, Bangladesh. He received his bachelor degree in Civil Engineering from Bangladesh University of Engineering and Technology (BUET) in 2009. After receiving his Bachelor's degree, he moved to Fargo, North Dakota to start his Masters of Science study in Geotechnical engineering. His research in North Dakota State University was about investigation of soil uncertainty and its influences on seismic behavior of shallow foundations. Due to his massive interest in Geotechnical engineering he moved to North Carolina State University and started his Ph.D. in Civil Engineering with a Geotechnical focus. After finishing his Ph.D. he will start working as a Staff Engineer in Terracon Consultants Inc.

ACKNOWLEDGEMENTS

First and foremast I am grateful to the Almighty Allah for helping me to overcome all the obstacles I have faced during my doctoral journey. I would like to extend my appreciation to the Department of Homeland Security for funding the research. I am very much indebted to my advisor, Dr. Mohammed A. Gabr, for his constant guidance, encouragement and support during my doctoral research period. I consider myself very lucky for getting the opportunity to work with him. Completion of the work required for this degree would have been impossible without his assistance. I am also grateful to my dissertation committee members Dr. Roy H. Borden, Dr. Shamim Rahman, Dr. Margery Overton and Dr. Lonnie Leithold for their time and valuable input on my work.

I am very grateful to Yulian for helping me during our testing in the laboratory and field. In the Constructed Facilities laboratory, the guidance and support provided by Jerry Atkinson was very helpful during the research period.

Last but not the least I want to acknowledge the support I got from my family. I always missed my father, who passed away 13 years ago, during my doctoral journey. My mother was always concerned about me during my studies in the United States and this is also a big achievement for herself as well. I am also indebt to my brothers and sisters. Everything I am today and everything I have done, I owe to them. I would also like to express my gratitude to my friends for their encouragement.

TABLE OF CONTENTS

LIST OF FIGURES

ASSESSMENT OF IN SITU SCOUR PROFILE IN SAND USING A JET PROBE

ASSESSMENT OF SCOUR ON BRIDGE FOUNDATIONS BY MEANS OF IN SITU EROSION EVALUATION PROBE

DEVELOPMENT OF MAXIMUM SHEAR AND SHEAR STRESS PROFILE WITH PROGRESS OF SCOUR

APPLICABILITY OF IN SITU EROSION EVALUATION PROBE (ISEEP) TO FIELD CASES

LIST OF TABLES

CHAPTER 1
INTRODUCTION

Background

Scour evaluation is a critical step for assessing the stability of several types of highway infrastructures during design and post construction stages as well as throughout the operational life. According to Lagasse et al. (1997), there were 488,750 bridges over stream and river crossings in the United States with an annual cost for scour-related bridge failures estimated at $30 million. The knowledge of scour potential and depth is critical for specifying and designing various types of foundations and development of maintenance priorities and replacement schedules. Therefore, the monitoring and assessment of scour potential and the determination of the erosion rate of the soils that support these structures are needed not only during the design stage but also through the operational lifetime of such hydraulic structures. Within the purview of civil infrastructures, the assessment of scour and erosion rates is critical not only for bridge foundations but also for other structures such as culverts, dams, levees, and stream banks. Cases where such an evaluation was needed were for example cited for civil infrastructure by Seed et al. (2006), agricultural engineering by Hanson and Hunt (2007) and petroleum engineering by Vardoulakis et al. (1996).

The overall objective of this study is the development of a procedure for assessing in situ soil erosion parameters with depth. The approach is developed based on data from the In Situ Erosion Evaluation Probe (ISEEP), which utilizes jetted water to advance a rod into the subsurface profile. The jet flow velocity and the advancement rate of the probe are correlated with a stream power value, which is then correlated with soil erodibility potential. Laboratory testing is performed to show the feasibility of the concept and an approach for the estimation of a critical stream power and a detachment coefficient is developed. Field tests were performed using ISEEP in both marine environment and riverine environment. Penetration rate vs. stream power plots are developed and detachment coefficient is obtained from these plots Correlation of penetration rates with SPT N values is also explored.

The influence of flow phenomena on the bed shear stress around cylinders is also investigated for live-bed and clear water scour, respectively, using Computational Fluid Dynamics (CFD) software FLOW-3D. In general, numerical investigations of bridge pier flow have utilized steady Reynolds-Average Navier-Stokes (RANS) models with wall functions (e.g., see Olsen and Melaaen, 1993, Richardson and Panchang, 1998, Olsen and Kjellesvig, 1998, Wang and Jia, 2000, Ali and Karim, 2002, Salaheldin et al., 2004, Roulund et al., 2005). This method has been reported to be applicable for bridge piers and abutments of complex geometry at field-equivalent Reynolds numbers. For the case of a highly unsteady flow characterized by large-scale unsteady vortex shedding and pressure gradients, the use of the wall-function approach and validity of the law-of-the-wall near solid boundaries remains questionable. The main disadvantages of the RANS approach is that it cannot accurately predict massively separated flows and flows in which large adverse pressure gradient are present. Large Eddy Simulations (LES) using subgrid-scale models and fine meshes (e.g., Kirkil et al, 2008, Koken and Constantinescu, 2008a-b) have allowed the investigation of the role of coherent structures in the scouring process at bridge piers and abutments of simplified geometry. These simulations were shown to accurately predict the flow patterns and turbulence structure compared to other numerical methods.

Shear stress profile with normalized scour depth is obtained from the simulations. The numerical model is calibrated through simulations of conditions observed from laboratory flume tests data reported in literature. Effect of sediment gradation on maximum shear stress and scour depth is also investigated for live bed scour. An equation that provides maximum shear stress around piers before scour starts is proposed based on the results of the numerical study. The equation is proposed as a function of Reynolds number, mean flow velocity, fluid density and critical shields number. It is observed that maximum shear stress does not change with the change of gradation. However, equilibrium scour depth decreases with the increase of sediment gradation. Live-bed shear stress profile showed that within a range of velocities the normalized shear profile follows similar trend.

Computational fluid dynamics (CFD) software, FLOW-3D, is used to assess the scour depth around a bridge pier. The results from modeling are compared with values that are based on ISEEP-estimated parameters and those calculated using empirical equations in literature. Correlations between scour magnitudes estimated by ISEEP parameters and those estimated through modeling are presented and discussed.

Problem Statement

Current techniques for assessing in situ erosion potential with depth require either the removal of soil samples for laboratory testing in a device such as the Erosion Function Apparatus (EFA), developed by Briaud et al. (2001), thus limiting it's utility to cohesive materials. Other techniques provide data only on erosion that has already occurred by monitoring changes in the mud-line elevation with respect to time. The instruments used for these techniques range from simple steel sounding rods to remote sensing devices that employ electromagnetic waves and/or sonar with sound propagation. As shown by Lu et al. (2010), sophisticated approaches, such as acoustic Doppler and ground penetration radar, are costly and the equipments require frequent maintenance and repair. Therefore development of an affordable approach for providing in situ soil erosion parameters is vital, especially for soils that are difficult to sample in the field.

Furthermore, the occurrence of scour and erosion is a time dependent process. A logical approach for estimating scour depths is to use excess shear stress, while assessing the magnitude of the applied shear stress with time. For example, to estimate bridge pier scour, it is necessary to determine the shear stress or stream power at the pier and the changes in the shear stresses as a function of the depth of the scour hole. Using the shear stress magnitude and the soil erosion parameters, the scour magnitude can be computed with time. In this case, this is an iterative process whereby the computed shear stress is compatible with the depth of the scour hole. Wei et al. (1997) developed an equation to calculate maximum shear stress before scour starts, for cohesive soils and clear water scour for cohesionless soil. While the development of such an equation is a step in the right direction, the work can be improved by

considering the effect of soil parameters i.e. mean particle diameter, d_{50} or critical shields parameter, θ in the equation. There is a need assess maximum shear stress value around bridge piers for both live-bed scour and clear water scour for cohesionless soils and study the effect of sediment gradation ($\sigma = \sqrt{(d_{84}/d_{16})}$) on maximum shear stress around bridge piers and equilibrium scour depth.

Research Objectives

The overall objective of this study is the development of a procedure for assessing in situ soil erosion parameters with depth. The approach is developed based on data from the In Situ Erosion Evaluation Probe (ISEEP). The specific objectives of this study are as follows:

i. To develop a data reduction approach using the In Situ Erosion Evaluation Probe (ISEEP), and provide soil erosion parameters with depth. It has been proposed that a vertical probe employing a water jet will be used to provide data to estimate scour potential and erosion rates of sediments. The idea is that analysis of the probe penetration rate into the soil correlates with scour rate and hence, erosion potential,
ii. To validate the ISEEP methodology by performing extensive laboratory and field testing with the in situ device,
iii. To investigate influence of flow phenomena to the bed shear stress around cylinders for live-bed scour and clear water scour using Computational Fluid Dynamics (CFD) software FLOW-3D,
iv. To develop an equation that provides maximum shear stress around piers, as a function of Reynolds number, mean flow velocity, fluid density and critical shields number, before scour starts by performing numerical simulations,
v. To investigate normalized shear stress profile against normalized scour depth from numerical simulations, and,
vi. To evaluate scour of bridge piers, as an example application, with ISEEP estimated parameters and compare results with Computational Fluid Dynamics (CFD) software, FLOW-3D

Scope of the Dissertation

It was reported that more than 1,000 bridges have collapsed in the United States over the past thirty years, with about 60% of such failures caused by excess scour at the supporting foundation system (Briaud et al., 2001). These figures suggest the importance of understanding the scour mechanism around bridge piers and hence the maintenance priority of the bridge foundations. The specific scope includes: i) The presentation of the In Situ Erosion Evaluation Probe (ISEEP) and the proposed data reduction scheme, ii) The deployment of the device in the field to illustrate the viability of performing the approach and collecting data to estimate erosion parameters, iii) Investigation of influence of flow phenomena to the bed shear stress around cylinders for live-bed scour and clear water scour using Computational Fluid Dynamics (CFD) software FLOW-3D, and iv) Example application of the device to bridge pier and comparison of estimated sour values with those obtained from existing empirical formulations.

CHAPTER 2

ASSESSMENT OF IN SITU SCOUR PROFILE IN SAND USING A JET PROBE[i]

Mo Gabr, Ph.D., P.E., Department of Civil, Construction and Environmental Engineering, North Carolina State University, Campus Box 7908, Raleigh, North Carolina, 27695. phone (919) 515-7904. fax (919) 515-7908. e-mail: gabr@ncsu.edu
Cary Caruso, Department of Civil, Construction and Environmental Engineering, North Carolina State University, Campus Box 7908, Raleigh, North Carolina, 27695. phone (919) 830-5657. e-mail: cwcaruso@ncsu.edu
Austin Key, Department of Civil, Construction and Environmental Engineering, North Carolina State University, Campus Box 7908, Raleigh, North Carolina, 27695. e-mail: akey@ncsu.edu
Mohammad Kayser, Department of Civil, Construction and Environmental Engineering, North Carolina State University, Campus Box 7908, Raleigh, North Carolina, 27695. phone (919) 515-4233. e-mail: mfkayser@ncsu.edu

ABSTRACT

Work in this paper presents a device and a process for in situ assessment of erosion potential with depth. The proposed device is termed "In Situ Erosion Evaluation Probe" (ISEEP) based upon advancing a rod fitted with a truncated cone jet nozzle into the soil. As water exits the nozzle with controllable velocity and flow rate (induced by an external pump) the probe advances into the subsurface profile and the rate of advancement is measured. The jet flow velocity and the advancement rate of the probe are correlated with a stream power value, which is then correlated with soil erodibility potential. Laboratory testing is performed to show the feasibility of the concept and an approach for the estimation of a critical stream power and a detachment coefficient is presented. Numerical modeling and deployment of the device at North Carolina barrier island site after hurricane Irene demonstrated the applicability of the proposed concept. Correlations between scour magnitudes estimated by ISEEP parameters and those estimated through modeling and field observation are presented and illustrate viability of ISEEP's soil erosion parameters as defined by a critical stream power incipient value and a detachment coefficient.

[i] This chapter is a slightly modified version of the paper that has been published. Changes are noted in the manuscript

Gabr, M., Caruso, C., Key, A. and Kayser, M. 2012. Assessment of In Situ Scour Profile in Sand Using a Jet Probe. Geotechnical testing journal, 36 (2), 0149-6115.

INTRODUCTION

Scour evaluation is a critical step for assessing the stability of several types of highway infrastructures during design and post construction stages as well as throughout the operational life. Briaud (2002) suggested that 60% of bridge failures in the US are caused by excess scour under the bridge piers or abutments, leading to serious structural damage. During the design stage, the knowledge of scour potential and depth is critical for specifying and designing various types of foundations. During operational lifetime, assessment of scour potential and erosion rate is needed for development of maintenance priorities and establishing replacement schedules. Within the purview of civil infrastructures, the assessment of scour and erosion rates is critical not only for bridge foundations but also for other structures such as culverts, dams, levees, and stream banks. Cases where scour evaluation is needed were cited for civil infrastructure by Seed et al. (2006), agricultural engineering by Hanson and Hunt (2007) and petroleum engineering by Vardoulakis et al. (1996).

Shields (1936) described the initiation of motion of granular particles on the basis of flume testing. The results are for initial movement of noncohesive uniformly graded sediments on a flat bed. One of Shields' conclusions was that a critical shear stress (τ_c) existed below which particles will not be dislodged and moved. At low velocities, this critical shear stress represents the viscous drag imparted by the moving fluid to the bed particles, and is related to a critical velocity value. At higher velocities, the critical shear stress appears to be related to the pressure differential between the upstream and the downstream sides of the particle (Leopold, 1994). Shields determined that the critical shear stress varies as a function of the boundary Reynolds number (Re*) which was defined in terms of critical velocity and the particle diameter. Re* is also referred to as the grain shear Reynolds number. This approach mainly states that erosion will occur as long as a bed shear stress exceeding a critical value is

applied to the soil. Using a mean particle size, soil unit weight and fluid unit weight, the critical shear stress can be estimated from the Shields' diagram.

Briaud et al. (2001) and Seed et al. (2006) reported that sand may erode at rates of 10,000 mm/hr versus clay-type soils that may erode at 1 to 1,000 mm/hr. The major identified forms of soil erosion include surface erosion, mass erosion, and fluidization as presented, for example, by Partheniades (1965) and Mehta (1991). During bed erosion, all three modes may be present in some proportion, though one typically dominates (Mehta, 1991). For coarse, non-cohesive materials, surface erosion occurs when the applied shear stress is at or above the sediment's critical shear stress. For surface erosion, Briaud et al. (2001) reported the dominant means of particle motion (erosion) are sliding, rolling, and plucking. For cohesive soils, much of the erosion occurs in a process known as mass erosion. In mass erosion, material is transported away from the bed in the form of flocs or pods (cohesive groups) of grains. The rate of surface erosion also increases with the applied shear stress. Partheniades (1965) identified the macroscopic shear strength of the bed at which the sediment can fail along an entire plane below the surface, allowing all of the material above the failure plane to be transported downstream.

Current techniques for assessing in situ erosion potential with depth require either removal of soil samples for laboratory testing in a device such as the Erosion Function Apparatus (EFA) by Briaud et al. (2001), or limiting the measurements to the surface of the sediment using inverted flumes, e.g. Aberle et al. (2006), or the use of a vertical jets as presented by Hanson and Cook (2004). Using a thin-walled Shelby tube, soil samples are extracted from the field to obtain scour rate with EFA. Extracted soil samples are placed in the EFA and 1 mm protrusion from the flume bed is maintained before water flow starts. Once water flow starts, time required to erode 1 mm soil is recorded, and soil scour rate and applied shear stress are estimated. An erosion plot with time is developed at the end. It should be noted that the applied velocities in this case are analogous to bed shear velocity which can be substantially lower than the average stream velocity depending on the depth of flow. In a very recent study

Bloomquist et al. (2012) developed a laboratory tool called RETA (Rotating Erosion Testing Apparatus) to evaluate applied shear stress and soil erosion rate for rock and cohesive soil. In this device sample obtained from field is placed in a cylinder, forming an annular space which is filled with fluid. By rotating the cylinder, torque is produced over the surface area of the soil sample. Shear stress imparted by the flow is evaluated in terms of the torque applied, and measuring eroded soil mass and time duration of the test soil erosion rate was obtained. Erosion rate versus applied shear stress was presented using RETA apparatus for four different river sites. Bloomquist et al. (2012) concluded that results obtained in this study are site specific therefore cannot be extrapolated. Design scour depth, of a structure during its life time, obtained using RETA apparatus showed a very small value.

Stresses leading to Erosion

Several relationships have been developed to relate the velocity to the critical level of shear stresses. Regardless of the particular form of the equation describing such relation, these imply that the erosion rate can be assessed by knowing the effective surface area exposed to the moving fluid, the properties of the geomaterials, and the velocity of the flow. Among others, Julien (1995), Briaud et al. (2001), and Chaudhry (2008), summarized the forces governing the erosion process to include gravity, buoyancy, and viscous drag. Furthermore, Briaud et al. (2001) determined that the critical shear stress, (τ_c) at which sediment motion is initiated is related to the average particle diameter, d_{50} by:

τ_c (N/m^2) ~ d_{50} (mm) Equation 1

This equation is similar to Shields' (1936) equation, which was expressed as: τ_c (N/m^2) = 0.63d_{50} (mm) where: d_{50} = particle diameter (mm) corresponding to 50% finer fraction. Julien (1995) manipulated Shields' critical stress into dimensionless form, representing the ratio of the applied shear stress to the submerged weight of the particle at the moment of incipient motion. This dimensionless shear stress is also referred to as Shields' parameter which is given by τ^* in the following expression:

$\tau^* = \rho_m u^{*2}/[(\gamma_s-\gamma_m)d_s)]$ Equation 2

where: ρ_m is the mass density of the submerged mixture (solid and water), u* is the critical shear velocity, γ_s and γ_m are the unit weights of the sediment particle and the fluid mixture, respectively, and d_s is a representative particle size. Regardless of the particular form of the equation describing the shear stress, the concept is to estimate the erosion rate on the basis of applied shear stresses that exceed a critical value. Particle size is one of the controlling factors in defining the critical shear stress magnitude.

Impinging Jets

Scour downstream of many hydraulic structures such as culverts and spillways may be treated as analogues to jet scour. Doodiah et al. (1953), Sarma (1965), Beltaos and Rajaratnam (1974), Aderibigbe and Rajaratnam (1997), Hanson et al. (2002) and others have made contributions to this field. Most of these studies were concerned with describing the maximum scour depth, as the jet is held stationary on the surface. There is however little documentation of the erosion behavior produced by a jet that is embedded internally to the material. Niven and Khalili (1998a, 1998b, 2002) and Niven (2001) discussed the mechanics and application of vertical, internal jets in a series of papers with their analysis mainly concerned with in situ fluidization of sand beds for environmental site remediation. In this case, the internal diameter of the jet was 75 mm and it was operated at relatively high flow rates on the order of 5-13 l/s (80-206 gpm). Their conclusions included the following:

1. As an internal jet progresses into the soil, the shape of the fluidized zone remains constant for a given soil, and flow rate.
2 The fluidized zone transitions from an open, ellipsoidal form to a closed fluidized cavity at some critical depth.
3. The jet penetration depth (fluidization zone depth) is proportional to the jet velocity and may be explained by a Shields-type of relationship for the minimum particle Froude number.

Hanson et al. (2002) and Hanson and Cook (2004) presented the resulting stress distribution from impinging jet as shown in Figure 1. This is the case for soils with fines and the data

reduction approach was presented on the premise of the excess shear model, where erosion occurs once the shear stresses exceed a critical value. In application of impinging jet, the "potential core" is the part of the jet where water retains its original velocity. At distances greater than the potential core, it is postulated that the velocity decreases linearly with

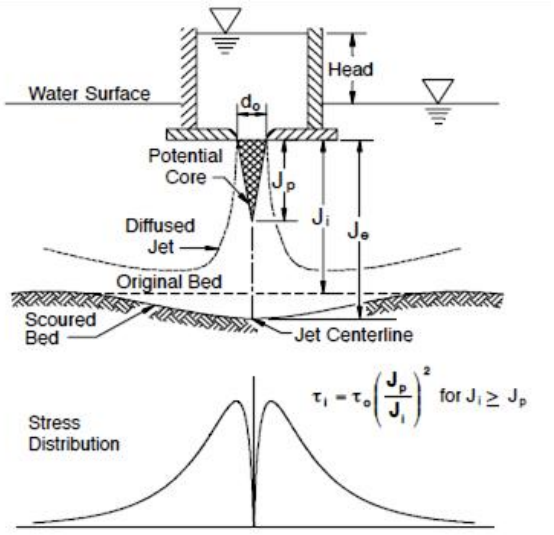

Figure 1. Schematic of Vertical Jet Apparatus and the Resulting Stress Distribution, from Hanson and Cook (2004)

increasing distance from the jet orifice. The shear stress applied to a surface within the potential core of the jet is expressed by Hanson et al. (2002) and Hanson and Cook (2004) as:

$\tau_o(N/m^2) = C_f \rho U_0^2$ Equation 3

where: τ_o= applied shear stress to bed in N/m^2, U_0 = average velocity of water at the tip (m/s), ρ = density (kg/m^3), and C_f is a friction coefficient =0.00416

Hanson and Cook (2004) used estimates of the asymptotic state of depth of scour to derive an expression for τ_c. Their ability to accomplish this task was based on the realization by Stein et al. (1993) that, for a fixed jet, as the depth of a scour hole increased, it would reach a depth

where the horizontal shear stress becomes equal to τ_c and no more scour takes place. When the soil-water interface is within the potential core region of the jet, the depth of the score hole was assumed to increase in a linear fashion since the velocity within the core is constant. As the erosion depth increases, the distance between the jet orifice and the soil surface increases, and the rate of change decreases, until equilibrium is reached. In Hanson and Cook's formulation, once an estimate of the ultimate depth of scour is obtained, the critical shear stress (τ_c) is expressed as:

$$\tau_c = \tau_0(J_p/J_e)^2 \qquad \text{Equation 4}$$

where: τ_c = critical shear stress, J_p = erosion depth equal to length of potential core, J_e = ultimate depth of scour, and τ_0 = Maximum shear stress at nozzle, or within the potential core.

The rate of erosion is then defined on the basis of the excess shear model, to describe the mass rate of erosion per unit area, or erosion rate (E) as a function of shear stresses exceeding the critical value as follows, Mehta (1991):

$$E = k_d (\tau - \tau_c)^{\alpha} \qquad \text{Equation 5}$$

The k_d coefficient, often called the detachment rate coefficient, and is basically the erosion rate normalized with respect to shear stresses leading to such a rate, and α is usually assumed to be 1 (Hanson and Cook 2004). The Hanson and Cook's approach has been codified as ASTM standard D5852 (ASTM, 1999). On the other hand, Annandale and Parkhill (1995) presented the concept of "Stream Power" as an estimate of the magnitude of the induced flow erosive potential. They indicated this concept is especially useful in the case of turbulent flow regimes. The input to a system is represented by an applied stream power, P, in Watts per unit area, and is given below for a flow situation with a head drop, H (Annandale, 2006):

$P = \gamma qH$, or in terms of shear stresses as $P = \tau Uo$ Equation 6

where: P is in the unit of Watts/m^2 (1 Watt = 1 N.m per sec or Kg.m^2 per sec ^{3}), γ = unit weight of water, q = discharge per unit area, and H = energy head, U_o = induced velocity. Annandale (2006) also expressed P in terms of τ for the case of impinging jet and indicated that such an approach accounts for the near boundary turbulent effect and should be used for reducing data from the impinging jet configuration. Based on derivations from the boundary layer theory, Annandale (2006) recommended that the friction factor, C_f (see Equation 3), to estimate the shear stress value, is equal to 0.016.

PROPOSED DEVICE CONCEPT

The proposed approach is based on assessment of scour potential with depth by applying a vertical water jet and monitoring the rate of advancement and depth of erosion hole. A prototype ISEEP (In Situ Erosion Evaluation Probe) has been constructed as a simple stainless steel tubes fitted with truncated cone tip. The concept draws from the approach by Hanson et al. (2002), and has been tested in sand. The cone-tipped vertical probe is attached to a digitally controlled, centrifugal pump that provides controllable and repeatable water velocity at the tip, with sustained flow rate against induced back pressure. As the water jet is induced through the cone tip, it mobilizes the soil particles. The sand particles are in a liquefied state while being transported from the annulus to the surface. The probe advances once an erosion of a sufficient area of soil beneath the tip occurred. During this process, the sand is displaced into the annulus, and the erosion process continued. This process is similar to that reported by Smith (2003) during the use of jets for pile installations. The magnitude of advancement of the probe is recorded with time. Photographs of the probe and the tip are shown in Figure 2.

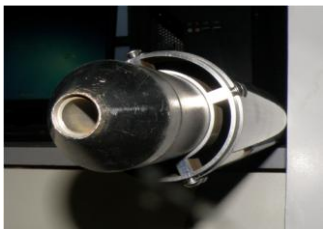

(a) Scale 1 cm = 5 cm (b) Scale 1 cm = 20 cm (c) Scale 1 cm = 5 cm

Figure 2. Probe with (a) Outer Shroud, (b) Bottom end and (c) Tips

The probe has a stainless steel body with several removable stainless steel tips. Each section is 1.52 m (5 ft) with a diameter of 50 mm (2.0 inch), so that it may be broken down for transport. The probe has an outer sheathing that is 76 mm (3.0 inch) in diameter with a wall thickness of 1.65 mm (0.065 inch). This is implemented to dissipate the pore water pressure in the tip area. The flow pump is a Gould GLSSV2 variable speed centrifugal pump coupled to an ITT PumpSmart variable speed controller. Several tips and configurations were constructed and tested. Results in this paper are reported from testing with 60° truncated cone tip with a 19 mm orifice (3/4 in). The probe is marked with 1 cm intervals, and the test runs are videotaped where the image is later processed for estimation of the penetration rate. The system is capable of applying a flow rate of 2000 ml/sec (32 gpm) and velocities as high as 12 m/s depending on the tip size.

EXPERIMENTAL PROGRAM

The laboratory testing is conducted in a liquefiable circular pit with a diameter of approximately 3 m (9.5 ft) and a depth of 6 m (20 ft). Located within the bottom most 18 inches of the pit are water inlet and drain outlet for infusing and draining water as a means for regeneration of the sand bed. These lie within a filter bed consisting of 9 inches of #57 stone overlain by 9 inches of 'pea' gravel. Figure 3 shows the Probe set up in the test pit prior to testing.

Test Soil

The test sand originates from a quarry at Drowning Creek near Hoffman, NC, and is a quartzite sand that was mined from underwater alluvial deposit. The grain size distribution (performed in triplicate) is shown in Figure 4, and other properties are given in Table 1. The results from the nuclear gage measurements showed that during the testing, the moisture content was between 10% and 15%, with the water table near the surface. The unit weight of the sand in place was on the average measured to be 14 KN/m^3, corresponding to an in-place relative density of 26%.

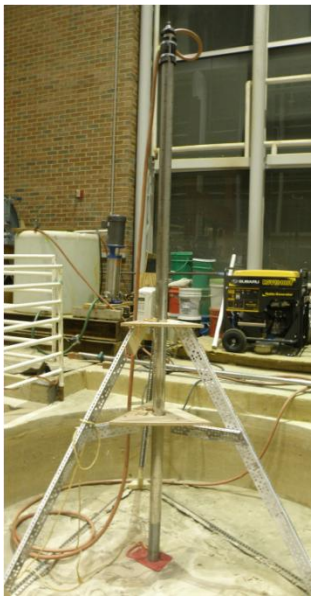

Figure 3. Photograph of the Test Setup Showing the Probe Prior to Testing in the Sand Pit

Table 1. Properties of Test Sand

Min. Unit Weight (KN/m^3)	Max. Unit Weight (KN/m^3)	D_{50} (mm)	Cu	$\phi°$
13	17.8	0.3	1.5	31

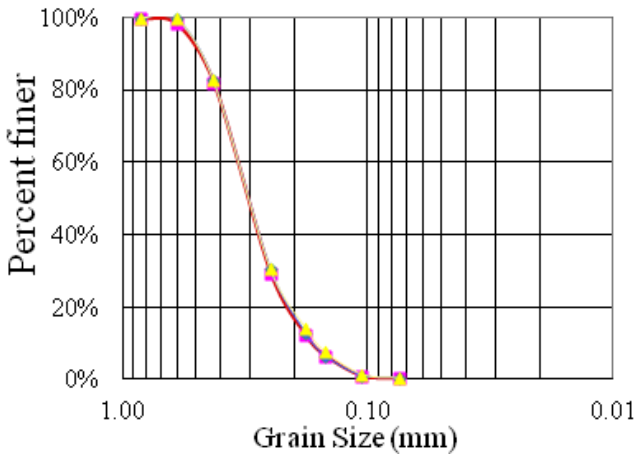

Figure 4. Grain Size Distribution of Test Sand

Results from repeatability testing on penetration rate are shown in Figure 5. These two tests were run when the water table was maintained at a depth of 1.35 m below the surface. The tests were run on two different days and the pit was drained and refilled between the runs. Both tests were run at a pump rpm of 1800, which in this case corresponded to a jet velocity of 2.65 m/s. The results show reasonable repeatability of the testing approach.

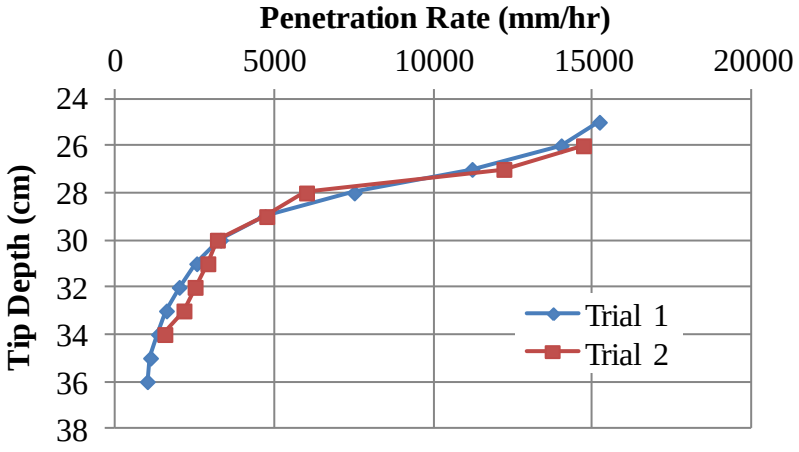

Figure 5. Results from Repeatability Test at Flow Velocity - 2.65 m/s

Experimental Results

Scour profile of the sand bed at two different times are showed in Figure 6. Data from 101 penetration runs are shown in Figure 7. The duration of run was varied from 15 to 60 sec to assess the minimum time period needed to record a penetration rate that is representative for

(a) (b)

Figure 6. Depth Test Scour Profile (a) at t = 10 sec and (b) After the Test.

layer. In this case, the velocity of flow was also changed each time by changing the flow rate, with the diameter of the tip being the same for all cases (19 mm). Due to the speed with which depth changes occurred during experimental measurements of the erosion rate, data are collected through the use of videotaping. Images are recorded and then transferred to a computer. Measurements were made by slowing the playback speed and using image processing software that allowed the timing interval to be 1/30 second (representing the time interval between the neighboring frames of the digital video signal). The data are tabulated and the output is exported as an EXCEL file. Depth of penetration at 15 sec and 30 sec does not provide a reliable measurement of penetration depth since small time durations have much more fluctuation and higher error possibilities. Data in Figure 7 show that slope made by 45 sec and 60 sec penetration depth are similar, therefore for a given velocity, a depth of penetration with a run time duration of 45 sec seems to provide sufficient information on the

rate of penetration.

For clarity, only the averages of the penetration rate at a given velocity for each of the test time duration are shown in Figure 8. As mentioned earlier, a testing duration of 45 sec allows the collection of sufficient information as well as averaging out the measurement uncertainties associated with the onset of the probe motion and the ability to accurately capture the data in the initial seconds of the run.

The penetration rate (cm/sec) estimated at 45 seconds is close to that estimated at 60 seconds with smaller error bars. Relative differences between these two rates fall within a range of 1% to 12%. The penetration rate is increased with increasing velocity. For example, at 45 second data, the rate of penetration is increased from 1.6 to 2.5 cm/s as the jet velocity is increased by approximately 40% (from 2.2 m/s to 3.1 m/s).

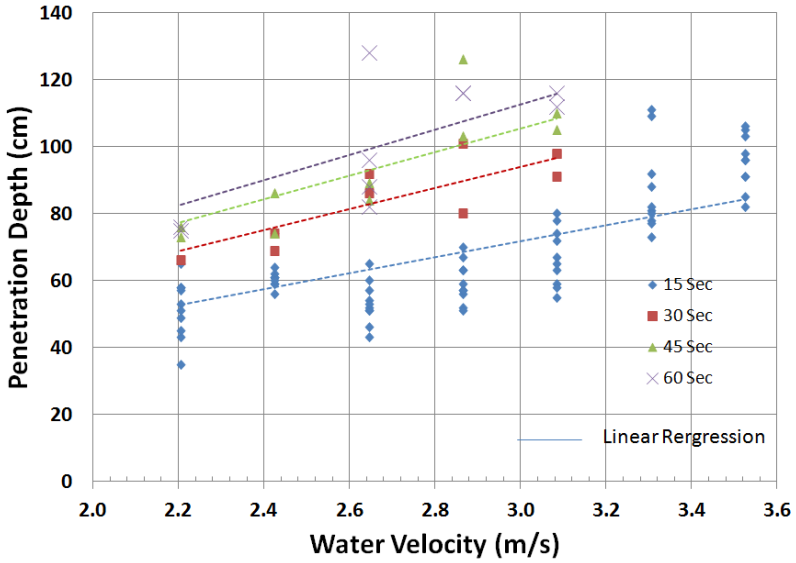

Figure 7. Measured Data Showing Change of Penetration Depth with Flow Velocity and Test Duration

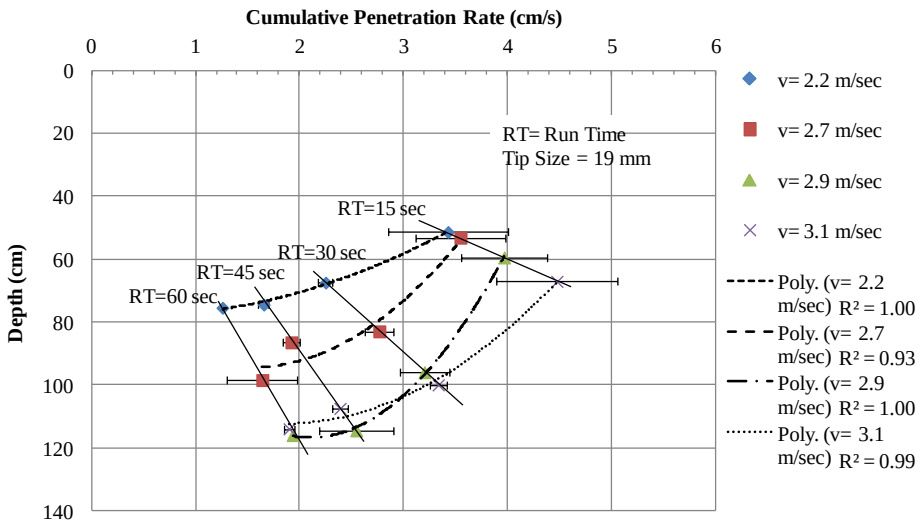

Figure 8. Average of Penetration Rate with Error Bars (One Standard Deviation of the Cumulative Penetration Rate) for Various Test Velocities and Run Time

INTERPRETATION OF TEST DATA

The results showing the rate of penetration are plotted in Figure 9 as a function of the stream power (P), which is computed using Equation 6. The logic of this plot is to extrapolate to zero penetration depth in order to assess the critical stream power value (P_c) at which no erosion will occur. Extrapolation of the data from the three testing periods of 30, 45, and 60 seconds shows a P_c value that ranges from 22-26 Watts/m^2. The "15 sec data" were not extrapolated since this run time is not sufficient to provide a reliable measurement of the penetration rate, as observed from the testing results. In addition to the "depth" testing, five independent surface tests were performed on the same sand bed. In these tests, the jet was kept stationary and the depth of the scoured hole was measured with time until the maximum depth of scour is achieved under the applied jet velocity. The critical velocity corresponding to the maximum scour depth was computed using the procedure by Hanson and Cook (2004). The critical stream power was then computed based on the critical velocity times the

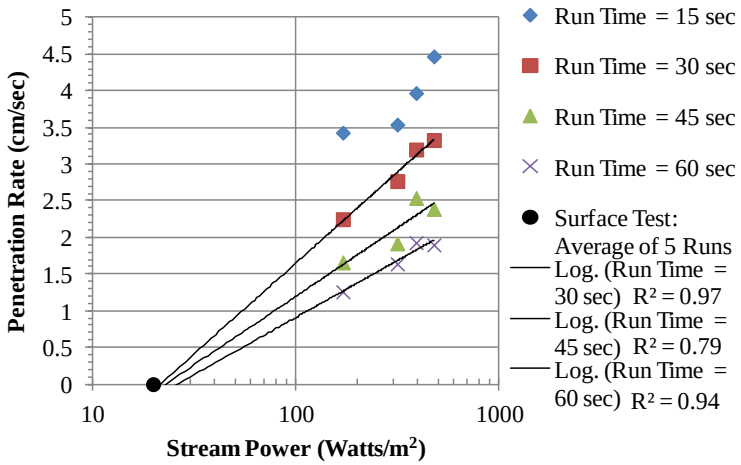

Figure 9. Extrapolation of the Stream Power to Assess Critical Value (P_c)

maximum scour depth. Results from these five surface tests yielded an average P_c value of 20 Watts/m^2. This value is reasonably within the range of values obtained through the extrapolation approach. Figure 10 shows the equivalent penetration rate per stream power function for the averaged test data. The slope of these lines provides a parameter equivalent to the detachment rate coefficient (k_d) proposed by Mehta (1991) and Hanson and Cook (2004). This coefficient, in terms of P, was designated by Annandale (2006) as k_d'. The k_d' ranged from 0.0024 to 0.0037 cm/s per unit power per unit area (Watts/m^2). The lower value of 0.0024 was obtained at the run times of 45 and 60 seconds.

Based on the results of testing in the sand pit, the measured parameters from the probe testing are a P_c value = 24 Watts/m^2 and k_d' = 0.0024 cm/s per Watts/m^2. These two values are used in conjunction with an applied stream power to compute the erosion rate in a fashion similar to the excess shear model as follows (Annandale 2006):

$$E = k_d' (P_{applied} - P_c) \qquad \text{Equation 7}$$

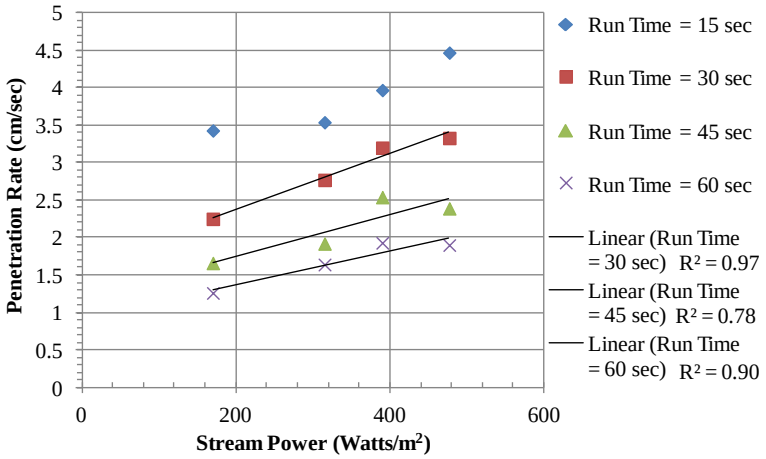

Figure 10. Assessment of k_d' through the Slope of the Penetration Rate versus Stream Power for the Various Run Times of 15, 30, 45 and 60 Sec

COMPARISON WITH NUMERICAL SIMULATION

The computational fluid dynamics (CFD) software Flow-3D was used to perform numerical simulations of a flow and scour problem, with the problem configuration shown in Figure 11. The geometry of the bed was 15 m in length, 10 m in width and 3 m in depth. The bed consisted of sand with a grain size distribution similar to the one used in the experimental program. A uniform mesh with 0.30 m spacing was used in the numerical simulation with a total of 40,429 cells. "Sediment Scour" model and "Gravity" model were activated. Gravity model was activated by specifying gravity component of 9.8 m/s^2 in z direction. Fluid flow was induced from the upstream boundary with a specified velocity that was varied from 1 m/s to 4 m/s with a 1 m constant head at the left boundary. Table 2 shows value of input parameters used in the sediment scour model. The computed Reynolds number for the flow regime is 300 using a D_{50} = 0.3 mm and a velocity = 1 m/s. Julien (1995) indicated for particle motion in Newtonian fluid, the drag coefficient (DC) is approximately 1.5 for a Reynolds number equal to or greater than 300. The entrainment coefficient (EC) describes lifting of the sediments in the bulk flow of fluid and sediment erosion at a given shear stress level. The bed load coefficient (BC) indicates the transport of heavier particles along the top

of the packed bed by the flow of water. In that process BC predicts the rate of bed load transport at a given shear stress higher than the critical shear stress. The DC, EC, and BC values used in the base case numerical simulation, to use in conjunction with ISEEP data, were 1.5, 0.018 and 5.7 respectively. These are values most commonly specified for sand (Mastbergen and Von den Berg, 2003, Ribberink, 1998, and Engelund and Hansen, 1967). The "Critical Shields Parameter" was kept blank in the numerical simulation since FLOW-3D can be used to compute the number from the Shields curve (Brethour and Burnham, 2010).

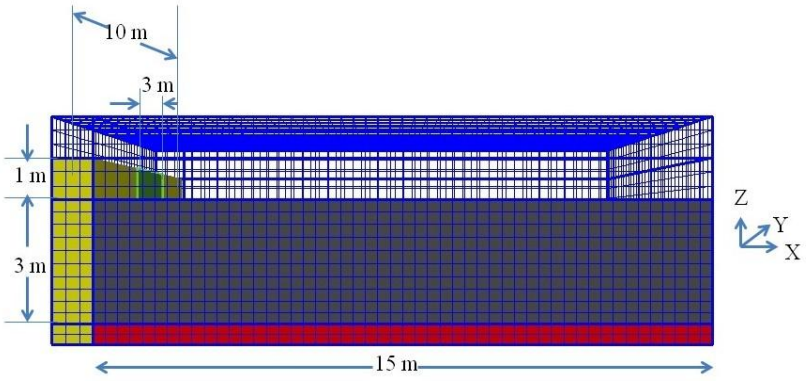

Figure 11. "Discretized Domain for Numerical Simulation of Scour with Sand Bed and 1m Outfall (water flowing from the 3 m wide boundary, shown as "green". The 1 m high "yellow" plate separates water source from the landform bed, "red" area indicates end boundary of the bed and soil bed is colored "grey")

Table 2. Parameters used in the Numerical Simulation

Parameter	Value	Reference
Density	1500 Kg/m^3	
Drag Coefficient (DC)	1.5	Engelund and Hansen (1967)
Entrainment Coefficient (EC)	0.018	Mastbergen and Von den Berg (2003)
Bed Load Coefficient (BC)	5.7	Fernandez and Van Beek (1976), Ribberink (1998)
Angle of Repose	31º	

The flow regime was simulated with time and the results provided erosion profile and maximum erosion depth for the various velocities used in the simulations. Each run took approximately 70 minutes. Scour profile in X-Z direction at two different times are shown in Figure 12. The erosion depth was also estimated using the parameters from the probe testing, in accordance to Equation 7.

The applied stream power from the simulated flow regime was computed in accordance with Equation 6. The simulated and computed scour depths from both approaches agree relatively well as shown in Figure 13, especially when using the DC value = 1. A larger scour depth is computed for the case with a DC equal to 1.5 at the larger velocities of 3.5 m/s and 4 m/s (corresponding to stream power values of 687 watts/m^2 and 883 watts/m^2). The velocity used in conjunction with scour depth computations using the probe data was the initial velocity since normally changes in velocity due to landforms changes is not known in advance. Scour depth obtained from Flow 3D simulation (with DC = 1.5 and DC = 1, other input parameters are mean value), for a velocity range of 1 m/s to 3.5 m/s (Stream power 200 watts/m^2 to 687 watts/m^2), differs from ISEEP estimated depth within a range of 2% to 9%. Therefore the comparative data in Figure 13 show the viability of the proposed approach for data reduction using the probe data.

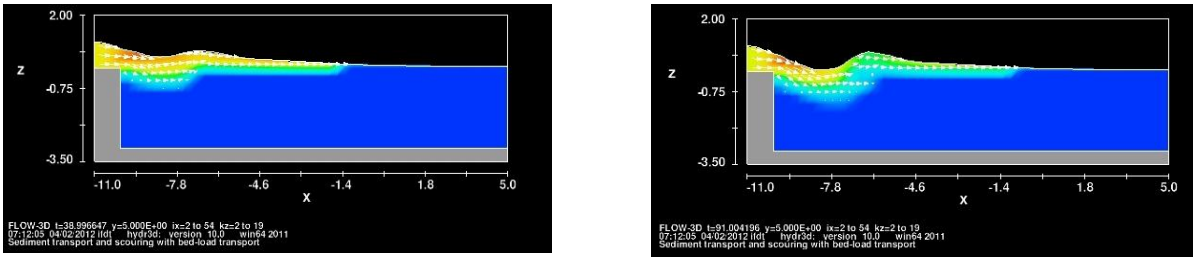

(a) (b)

Figure 12. Centerline Scour Profile in X-Z direction at (a) Time, t = 39 sec and (b) t = 91 sec

FIELD APPLICATION

Field testing was conducted at outer banks barrier island site, along NC-12, that was breached during Hurricane Irene. The occurrence of Hurricane Irene caused the erosion

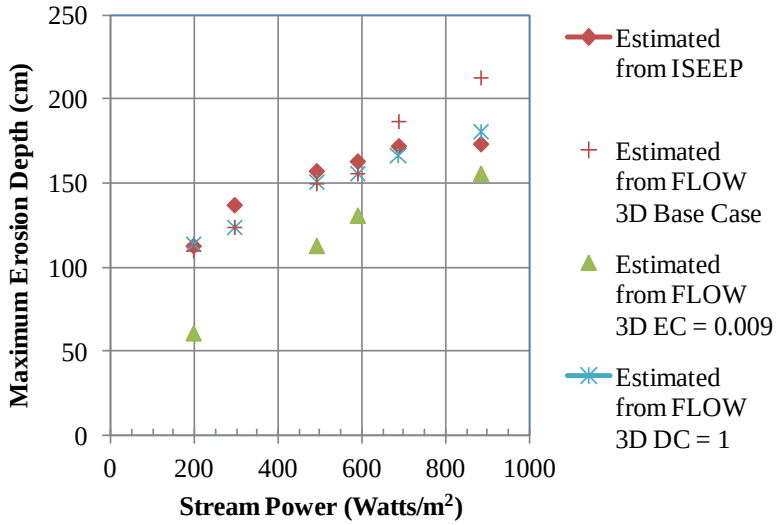

Figure 13. Comparison of Maximum Scour Depth versus Time based on Numerical Simulations and Probe Data

of 274 m (900 ft) section of NC 12[ii]. The estimated erosion rates were up to 4 m/hr with the higher rates occurring in a narrow time window of less than 2 hours (Overton et al. 2012). Figure 14 shows a photograph of one of three breach locations (left photo; with a temporary bridge installed) and the ISEEP set up (right photo) prior to the testing at the same location. The grain size distribution of the site soil is shown in Figure 15. The test soil at the site has a D_{50} of 0.32 mm with some of the samples include organic materials and shells, and lead to an indication of a coarser distribution, as shown in Figure 15. The sand is poorly graded with a coefficient of uniformity of approximately 1.5. According to NCDOT (2011) the sand is

[ii] This statement has been changed to correct for an error in the published version of the paper

described as loose, gray, fine sand (A-3) with uncorrected N-value of 20 blows per foot near the surface reducing to zero at a depth of 4.5m.

Figure 14. Location of Breach Along NC-12 and Set Up for Testing Using ISEEP

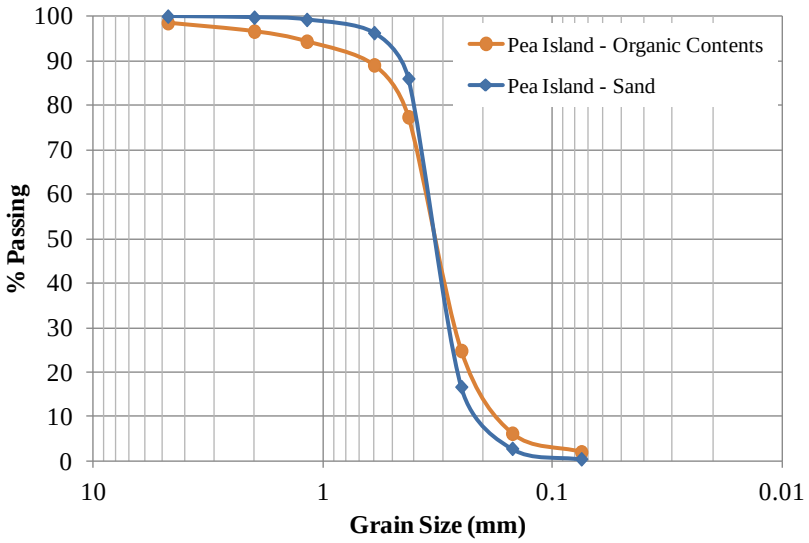

Figure 15. Grain Size Distribution of Test Site- Pea Island

The data from test runs at three different jet velocities are presented in Figure 16. The three penetration profiles were obtained within 1 m from each other. Penetration depth is shown to be dependent on the velocity level, with a lower rate of penetration observed in the top 0.5 m of the test profile. It is interesting to note that this is consistent with the observation from the standard penetration test N-value where lower values are obtained with depth. The higher N-values near the top are a manifestation of the organic (root/shells) content of the layer.

In order to estimate the critical value of the stream power for each case, the penetration rate is plotted versus the natural log of the stream power and extrapolation is performed to a zero penetration rate as shown in Figure 17. In the profile depth range of 0-0.5 m, the P_c value is 200 Watts/m^2 and drops to 45 watts/m^2 thereafter within the test depth.

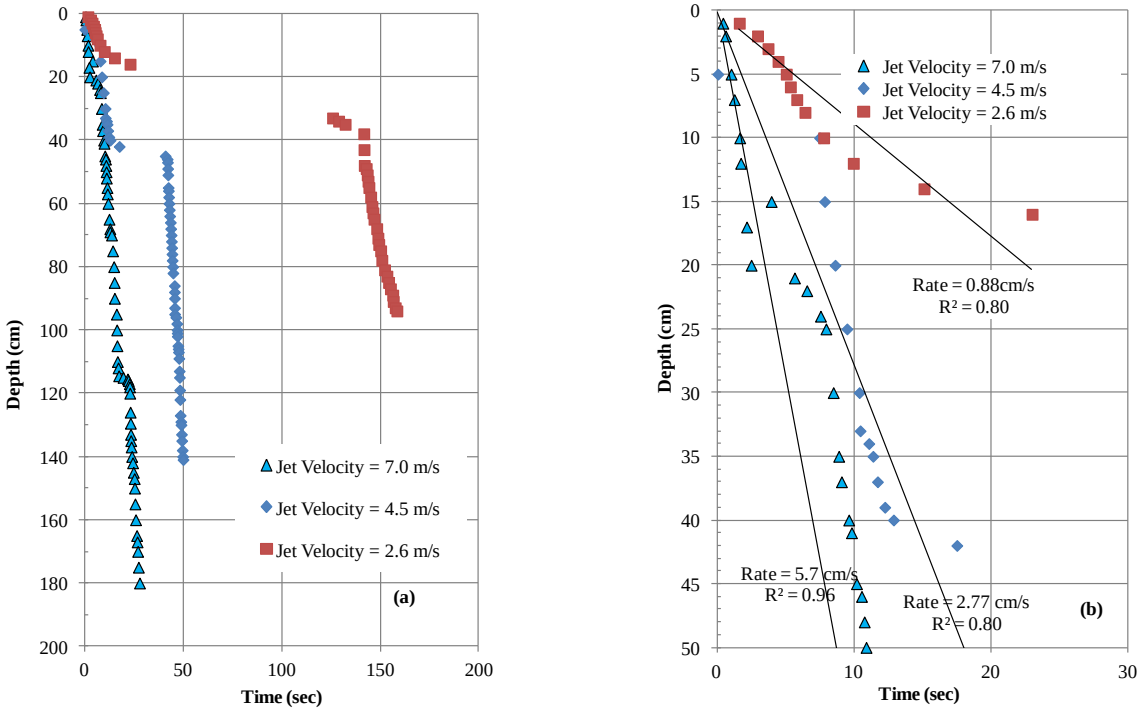

Figure 16. Penetration Depth as a Function of Time: a) Full Penetration Profile and b) Magnification of the Initial 0.5 m Depth

The value of k_d' is obtained as the slope of the penetration rate versus stream power on a natural scale plot. Using the best fit linear interpolation lines, these values are 0.0009 and 0.001 cm/s per watts/m^2, for the two depth ranges, respectively.

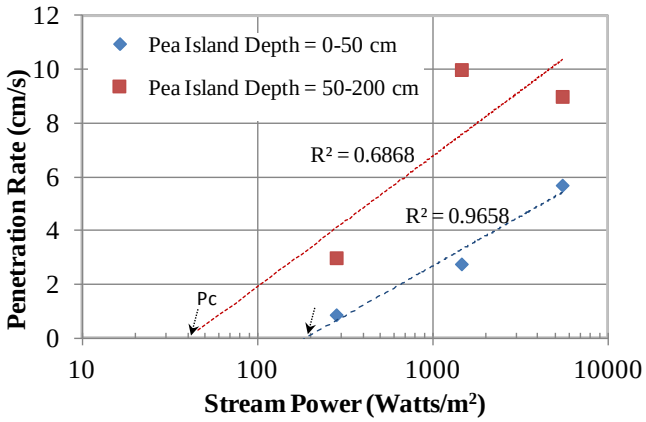

Figure 17. Extrapolation to Estimate the Critical Value of Stream Power at which Onset of Erosion Occurs

Illustrative Example

The estimated parameters are used to assess the erosion depth associated with NC-12 breach. The bed shear stresses are evaluated based on Julien (1995) as:

$$\tau_b = \rho U_*^2 \qquad \text{Equation 8}$$

Where U_* = bed shear velocity and ρ = fluid density.

Although there are various approaches for defining τ_b, depending on the application, Biron et al. (2004) compared various approaches and concluded that in a simple boundary configuration, Equation 8 is widely accepted for estimating the bed shear stresses. For turbulent flow, the U_* was expressed by Julien (1995) as a function of the water surface velocity (U), flow depth (h), and grain characteristic (d_{90}) as follows:

$$U_* = \frac{U}{5.75 Log(\frac{6.1h}{d_{90}})} \qquad \text{Equation 9}$$

The use of this equation provides the bed shear velocity as a function of the water surface velocity and therefore yields a lower value as the flow depth is increased.

Estimation of erosion rate with time was performed using parameters from the field testing. A d_{90} = 0.45 mm along with an average flow velocities of 3 m/s and 4/s were used in the illustrative example. The depth of flow was assumed to vary from 0.1 m to 2 m simulating a rising water level with time. The P_c parameter is taken as 200 watts/m^2 for elevation from 0-0.5 m below ground surface, and 42 watts/m^2 thereafter per the data in Figure 17. The k_d' is taken as 0.0009 cm/s per watts/m^2.

The estimated erosion rate is shown in Figure 18 for the two velocity magnitudes of 3 m/s and 4 m/s. At surface flow velocity of 3 m/s, the estimated erosion rate is 0.5 m/hr for depth of flow =0.5 m and increase to nearly 3 m/h at surface flow velocity of 4m/s for the same depth of flow. To estimate the depth of erosion, one needs the rate of water level rise as well as surface flow velocity. It is of interest to note that assuming an average flow depth of 0.5 m, a 4.5 m breach is estimated to occur in approximately 1.5 hours for a 4 m/s flow velocity and in 9 hours for 3 m/s flow velocity.

SUMMARY AND CONCLUSIONS

An approach for assessing the scour potential with depth is proposed through the use of a vertical probe employing a water jet. Results from large scale laboratory testing, field testing and modeling using sand as the test soil are presented and discussed. The probe, termed ISEEP, has been tested in sand across a range of water velocities and flow rates, and a proposed procedure for data reduction, based on the stream power approach by Annandale (1995, 2006), is presented. Field deployment served to illustrate the viability of performing the approach and collect data to estimate erosion parameters. One advantage of ISEEP is the ability to quickly deploy it and collect data (less than an hour once on site), and being self contained with all equipment necessary fitting well in a full size Van. An illustrative example is presented demonstrating the application of the proposed approach for assessing erosion depth. Based on the findings of this study, the following observations are advanced:

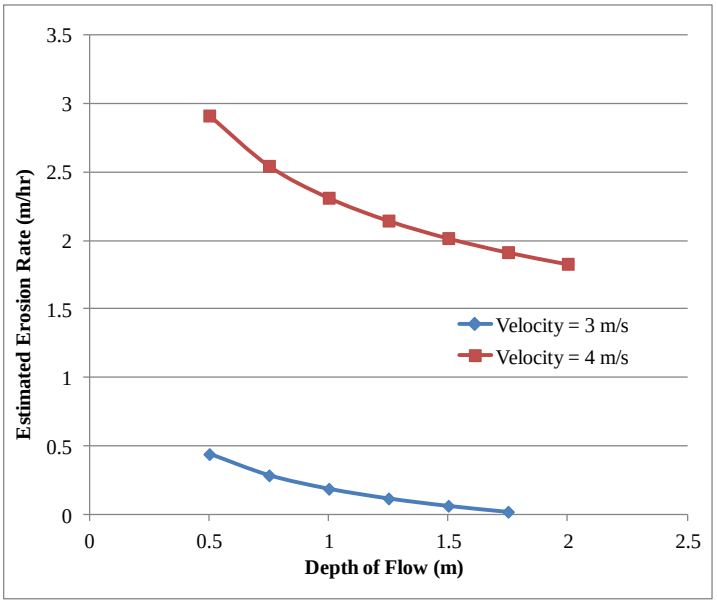

Figure 18. Estimate of Erosion Rate Based on ISEEP Measurements and Data from Pea Island, North Carolina

1. The viability of obtaining various penetration rates of the probe with increasing jet velocity is demonstrated. The rate of advancement was correlated to the vertical velocity of the water and provides an indication of the erosion potential of the soil. Data indicated a minimum of 45 sec run time is needed to obtain a repetitive rate.
2. The data reduction approach illustrated the viability of obtained soil erosion parameters in terms of critical stream power and modified detachment coefficient.
3. The probe is capable of applying various velocities at the same flow rate as well as various flow rates at the same velocity through changing the size of the jet orifice. This feature is important when erosion through "cutting" versus particle mobilization is induced as in the case of fine grained soils.
4. The combined probe and outer sheathing has a weight of approximately 15 kg per m. Assuming a dynamic coefficient of friction of 0.25-0.35, at 1m depth, the skin friction force is estimated equal to 7-10 kg. The probe is in continuous movement and the amount of skin friction force is estimated to be less than the weight of the probe for

the test sand. A stick-slip behavior was however observed at times. The issue of skin friction is assessed during the testing and measures to reduce the skin friction (such as friction reducers, special coatings) are being investigated.

5. Testing has been conducted in sand since these types of soils are the most difficult to sample in the field and the simpler to test in a laboratory setting with reconstituted samples. The approach need to be validated in soil with a significant fines content as the mode of erosion will no longer be particulate in nature and the set of parameters in terms of velocity/flow rate value to advance the probe will need to be evaluated.

REFERENCES

Aberle, J., Nikora, V., and Walters, R., 2006, "Data Interpretation for in Situ Measurements of Cohesive Sediment Erosion," *Journal of Hydraulic Engineering*, Vol. 132, No. 6, pp. 581-588.

Aderibigbe, O. and Rajaratnam, N., 1997, "Erosion of Loose Beds by Submerged Circular Impinging Vertical Turbulent Jets," *Journal of Hydraulic Research/De Recherches Hydrauliques*, Vol. 35, No. 4, pp. 567-574.

Annandale, G. W. and Parkhill, D. L., 1995, "Stream Bank Erosion: Application of the Erodibility Index Method," *International Water Resources Engineering Conference Proceedings*, Vol. 2, pp. 1570-1574.

Annandale, G.W., 2006, Scour Technology: Mechanics and Practice, McGraw Hill, New York, pp. 430.

ASTM Standard D5852-95, 1999, "Standard Test Method for Erodibility Determination of Soil in the Field or in the Laboratory by the Jet Index Method," *Annual Book of ASTM standards*, Vol. 04.08, ASTM International, West Conshohocken, PA, pp. 686-690.

Bloomquist, D., Sheppard, M., Schofield, S. and Crowley, R. 2012, "The Rotating Erosion Testing Apparatus (RETA): A Laboratory Device for Measuring Erosion Rates versus Shear Stresses of Rock and Cohesive Materials." *Geotechnical Testing Journal*, Vol. 35, No. 4, pp. 641-648.

Beltaos, S. and Rajaratnam, N., 1974, "Impinging Circular Turbulent Jets," *Journal of Hydraulic Engineering*, Vol. 100, No. 10, pp. 1313-1328.

Biron, P. M., Robson, C., Lapointe, M. F., and Gaskin, S. J., 2004, "Comparing Different Methods of Bed Shear Stress Estimates in Simple and Complex Flow Fields," *Earth Surface Processes and Landforms*, Vol. 29, pp. 1403–1415.

Brethour, J. and Burnham, J., 2010, "Modeling Sediment Erosion and Deposition with the FLOW-3D Sedimentation and Scour Model," *Flow Science Technical Note*, FSI-10-TN85, pp. 1-22.

Briaud, J. L., Ting, F.C.K., Chen, H.C., Cao, Y., Han, S.W., and Kwak, K.W., 2001, "Erosion Function Apparatus for Scour Rate Predictions," *Journal of Geotechnical and Geoenvironmental Engineering*, Vol. 127, No. 2, pp. 105-113.

Briaud, J. L., 2002, TTI Researcher, V38, #4.

Chaudhry, M. H., 2008, Open Channel Flow, 1st Edition, Springer-Verlag, New York.

Doddiah, D., Albertson, M. L., and Thomas, R., 1953, "Scour from Jets," *Proceedings Minnesota International. Hydrology Convention*, International Association for Hydraulic Research, Minneapolis, 161–169.

Engelund, F. and Hansen, E., 1967, "A Monograph on Sediment Transport to Alluvial Streams," Copenhagen, Tenik Vorlag.

Fernandez, L. R. and Van Beek, R., 1976, "Erosion and Transport of Bed-load Sediment," *Journal of Hydraulic Research*, Vol. 14, No. 2, pp. 127-144.

FLOW-3D, 2000, User Manual. Flow Science, Inc.

Hanson, G. J. and Cook, K. R., 2004, "Apparatus, Test Procedures, and Analytical Methods to Measure Soil Erodibility in Situ," *Applied Engineering in Agriculture*, Vol. 20, No. 4, pp. 455-462.

Hanson, G. J. and Hunt, S. L., 2007, "Lessons Learned Using Laboratory Jet Method to Measure Soil Erodibility of Compacted Soils," *Applied Engineering in Agriculture*, Vol. 23, No. 3, pp. 305-312.

Hanson, G. J., Robinson, K. M., and Cook, K. R., 2002, "Scour Below an Overfall: Part II. Prediction," *Transactions of the American Society of Agricultural Engineers*, Vol. 45, No. 4, pp. 957-964.

Julien, P. Y., 1995, Erosion and Sedimentation, Press Syndicate of the University of Cambridge, New York, NY.

Leopold, L., 1994, A View of the River, Harvard University Press, Cambridge, Massachusetts, pp. 193.

Mastbergen, D.R. and Van den Berg, J.H., 2003, "Breaching in Fine Sands and the Generation of Sustained Turbidity Currents in Submarine Canyons," *Sedimentology*, Vol. 50, pp. 625-637.

Mehta, A. J., 1991, "Review Notes on Cohesive Sediment Erosion," In: N.C. Kraus, K.J. Gingerich, and D.L. Kriebel, (eds.), Coastal sediment '91, *Proceedings of Specialty Conference on Quantitative Approaches to Coastal Sediment Processes*, pp. 40–53.

Niven, R. K. and Khalili, N., 1998a, "In Situ Fluidization by a Single Internal Vertical Jet," *Journal of Hydraulic Research*, Vol. 36, No. 2, pp. 199-228.

Niven, R. K. and Khalili, N., 1998b, "In Situ Multiphase Fluidization (" Upflow Washing") for the Remediation of Hydrocarbon Contaminated Sands," *Canadian Geotechnical Journal*, Vol. 35, No. 6, pp. 938-960.

Niven, R. K., 2001, "In Situ Fluidization for Solids Addition to Permeable Reactive Barriers," *2001 International Containment and Remediation Technology Conference and Exhibition*, Orlando, FL, June, pp. 10-13.

Niven, R. K., and Khalili, N., 2002, "In Situ Fluidization for Peat Bed Rupture, and Preliminary Economic Analysis," *Journal of contaminant hydrology*, Vol. 59, No. 1-2, pp. 67-85.

Overton, M., Kurum, M., and Clinch, A., 2012, "Engineered and Evolving Landforms," *The Coastal Hazards Center Research annual meeting*, January, Chapel Hill, N.C, January.

Partheniades, E., 1965, "Erosion and Deposition of Cohesive Soils," *Journal of the Hydraulics Division*, Vol. 91, No.1, pp. 105-139.

Ribberink, J. S., 1998, ''Bed-load Transport for Steady Flows and Unsteady Oscillatory Flows,'' *Coastal Engineering*, Vol. 34, pp. 59– 82.

Sarma, K. V. N., 1965, "Simple Empirical Formula for Scour under Vertical Jets," *Irrigation and Power (India)*, Vol. 22, No. 1, pp. 27-33.

Seed, R. B., and 34 others, 2006, "Investigation of the Performance of the New Orleans Flood Protection Systems in Hurricane Katrina on August 29, 2005," Report to National Science Foundation under Grants No. CMS-0413327 and CMS-0611632.

Shields, A., 1936, Anwendung der aenlichkeitsmechanik und der turbulenzforschung auf die geschiebebewegung. Mitteilungen der Preussischen Versuchsanstalt fur Wasserbau und Schiffbau, Berlin, Germany, translated to English by W. P. Ott and J. C. van Uchelen, CalTech, Pasadena, CA.

Smith, A. (2003) “Jetting Techniques for Pile Installation and Environmental Impact Minimization,” M. S. Thesis, North Carolina State University, Raleigh, 155pp.

Stein, O. R., Alonso, C. V., and Julien, P. Y., 1993, “Mechanics of Jet Scour Downstream of a Headcut,” *Journal of Hydraulic Research,* Vol. 31, No. 6, pp. 723-738.

Vardoulakis, I., Stavropoulou, M., and Papanastasiou, P., 1996, “Hydro-mechanical Aspects of the Sand Production Problem,” *Transport in Porous Media,* Vol. 22, pp. 225–244.

CHAPTER 3

ASSESSMENT OF SCOUR ON BRIDGE FOUNDATIONS BY MEANS OF IN SITU EROSION EVALUATION PROBE[iii]

M. Kayser[1] and M. A. Gabr[2]

[1]Graduate Research Assistant
Department of Civil, Construction and Environmental Engineering
North Carolina State University
Raleigh, NC 27695-7908
E-mail: mfkayser@ncsu.edu
Fax: 919-515-7908

[2]Professor, Ph.D., P.E.
Department of Civil, Construction and Environmental Engineering
North Carolina State University
Raleigh, NC 27695-7908
E-mail: gabr@eos.ncsu.edu
Phone: 919-515-7904
Fax: 919-515-7908

Kayser, M. and Gabr, M. (2013). "Assessment of Scour on Bridge Foundations by Means of In Situ Erosion Evaluation Probe." Transportation Research Record: Journal of the Transportation Research Board, 2335(1), 72-78.

[iii] This chapter is a slightly modified version of the paper that has been published. Changes are noted in the manuscript

ABSTRACT

The work in this paper presents the use of an *in situ* erosion evaluation probe (ISEEP) to assess scour depth at bridge piers. Numerical modeling and deployment of the device at a North Carolina Outer Banks site damaged by Hurricane Irene in 2011 demonstrates the applicability of the proposed concept. Computational fluid dynamics software, FLOW-3D, was used to assess the scour depth at a bridge pier, and the results are compared with values based on ISEEP-estimated parameters by using an excess-stream power model. The scour depth was also calculated from empirical equations that assume the same conditions as those used in the numerical analysis. Parametric analysis using FLOW-3D indicates that of the parameters for defining the scour depth, the entrainment coefficient (C_e) had the largest effect, whereas the drag coefficient (C_d) had the smallest effect on the scour magnitude within the range of values used included in this analysis. The estimated scour depths that were based on ISEEP data agree relatively well with the scour magnitudes obtained from the numerical analysis, as the ISEEP data reflected the changes in the properties of the sand layer in terms of depth. In contrast, the scour magnitude calculated from the empirical equations underestimated the scour depth, mainly because these equations had no provision for a layered soil profile. Further validation of both the field testing procedure and data reduction approach, including the assessment of the applicability of soils that contain an appreciable percentage of fines, is recommended.

INTRODUCTION

According to Lagasse et al. (*1*), there were *488,750 bridges* over stream and river crossings in the United States with the *cost* for scour-related *bridge* failures estimated at *$30 million* annually. Furthermore, it was reported that more than 1,000 bridges have collapsed in the United States over the past thirty years, with about 60% of such failures caused by excess scour at the supporting foundation system (*2*). Therefore, the monitoring and assessment of scour potential and the determination of the erosion rate of the soils that support these structures are needed tasks during the design, operation, and lifetime of such hydraulic structures. In addition to being critical in the initial design phase, these erosion magnitude

and rate data are also needed to develop maintenance priorities and establish replacement schedules.

Current techniques for assessing *in situ* erosion potential with depth require either the removal of soil samples for laboratory testing in a device such as the *Erosion Function Apparatus* (EFA), developed by Briaud et al. (*2*) or the measurement of erosion that has already occurred by monitoring of changes in the mud line elevation with respect to time. The instruments used for measuring changes in the mud line elevation range from simple steel sounding rods to remote sensing devices that employ electromagnetic waves, laser beams and sonar with sound propagation. As shown by Lu et al. (*3*), sophisticated approaches, such as acoustic Doppler and ground penetration radar, are costly and their equipments require frequent maintenance and repair.

For the measurement of scour rate in the field, Hanson et al. (*4*) and Hanson and Cook (*5)* reported the use of vertical jets for taking surface measurements of erosion potential. Those authors presented a framework for rendering the stress caused by an impinging jet in the form of applied shear stress. In this case, a *potential core* is defined as the part of the jet where water retains its original nozzle velocity. The jet deflects once it reaches the soil surface and therefore applies shear stress (τ) to the soil. This stress is expressed by Hanson and Cook (*5*) as

$$\tau = C_f \rho U_0^2 \qquad (1)$$

where τ = applied shear stress to bed in (N/m^2); U_0 = average velocity of water at the tip (m/s); ρ = density (kg/m^3); and C_f = friction coefficient = 0.00416.

The rate of erosion is then estimated on the basis of excess shear, as presented by the Mehta model (*6*). In contrast, Annandale presented the concept of *stream power* as an estimate of the flow erosive potential and indicated that this concept is especially useful in the case of turbulent flow (*7*). Annandale noted that for jet testing, the flow is turbulent, and the input to the system is better represented by stream power (P) in Watts (W) per unit area (1 W = 1 N-m/s or kg-m^2/s^3), as follows (*7*):

$P = \gamma qH$, or in relation to shear stress, $P = \tau U_o$ (2)

where γ = unit weight of water; q = discharge per unit area; H = energy head; and U_o = induced velocity. Furthermore, on the basis of boundary layer theory, Annandale recommended that the C_f parameter in Equation 1 is assumed to be 0.016 through the analysis of the near-boundary turbulent layer (*7*).

Gabr et al. (*8*) presented a prototype device, termed *ISEEP* (*in situ* erosion evaluation probe) to assess soil erosion parameters in terms of depth. The concept draws from the approach taken by Hanson et al. (*4*) and utilizes the stream power concept introduced by Annandale (*7*) for the data reduction scheme. A prototype ISEEP has been constructed by attaching simple stainless steel tubes fitted with a truncated cone tip. The cone-tipped vertical probe is attached to a digitally controlled centrifugal pump that provides controllable and repeatable water velocity at the tip, with a sustained flow rate against any induced backpressure.

The critical stream power (P_c) and the soil detachment rate coefficient (k_d') are assessed as the scour parameters on the basis of ISEEP data. These two values (P_c and k_d') are used in conjunction with the applied stream power ($P_{applied}$) to compute the rate of erosion (E) in a fashion similar to the excess shear model, as follows (*7*):

$$E = k_d' (P_{applied} - P_c) \quad (3)$$

From the results from tests conducted in a sand pit, the measured parameters obtained from the probe testing are P_c = 20 Watt/m^2 and k_d' = 0.0014 cm/sec per Watt/m^2 for sand with D_{50} = 0.30 mm. The viability of obtaining various penetration rates using the probe with an increasing jet velocity is demonstrated in this work. Results also indicate that the probe is capable of applying various velocities with the same flow rate as well as various flow rates at the same velocity by changing the size of the jet orifice (*8*).

The issue of bridge pier scour also has been studied via laboratory flume testing, field tests, and numerical modeling using computational fluid dynamics (CFD) models (*9-19*).

Parameters such as stream velocity, depth of fluid and geometric dimensions of a given structure have been varied in the laboratory to simulate various site conditions (*9-12*). Melville and Coleman have presented details about the mechanisms of local scour at bridge piers (*9*). Laursen and Toch (*10*), Shen et al. (*11*), and Melville and Sutherland (*12*) varied the depth of flow, stream velocity, angle of attack, pier shape and grain size in laboratory flume to study scour depth at a bridge pier and developed empirical equation based on the laboratory results. Melville also evaluated local scour at bridge piers by performing field tests at four different sites, and considered flow depth, flow velocity, pier shape and sediment size as variables (*13*). Scour depth measurements obtained in the field matched reasonably well with the empirical equation proposed by Shen et al. (*11*). Richardson and Davis also recommended equations that they developed from the results of an experimental study and that are currently implemented in *Hydraulic Engineering Circular* No. 18 (HEC-18) (*14*). Mueller (*15*) used 224 measurements of scour at 90 bridge piers in the United States, and compared the results from 22 scour empirical equations and recommended the use of HEC-18 equation for assessment of scour at bridge piers. In addition to the experimental studies, flow around a circular pier has been simulated by several researchers (*16-19*) by means of various CFD models.

This paper presents a case study for the assessment of scour potential with depth using ISEEP data. Field tests were conducted at the North Carolina Outer Banks at the site of a breach that occurred during Hurricane Irene in August 2011, where a temporary bridge is now installed. The soil detachment rate coefficient (k_d') and critical stream power (P_c) are evaluated based on the field data. CFD software, FLOW-3D, is used to perform the numerical simulations of the scour magnitude at the pier foundation, and the results are compared with those computed based on the ISEEP data. A parametric study is performed to illustrate the applicability of the data collected from the ISEEP in relation to the magnitude of scour computed by using the numerical approach. Results based on the ISEEP data are also compared with scour depth estimated from empirical equations reported in the literature for assessing local scour at bridge piers.

FIELD TESTING

Field tests were conducted at a site along NC-12 that was breached during Hurricane Irene in 2011. Flooding from Hurricane Irene eroded a 274-m section of NC-12 within the Pea Island National Wildlife Refuge[iv]. This erosion was caused by high water backwash from the sound side of the island. The maximum depth of the breach was estimated at approximately 4 m, with flow velocities ranging from 0.5 to 1 m/s and some instances of flow velocities as high as 4 m/s (M. Kurum and M. Overton, personal communication, 2012). An estimated erosion rate up to 4 m/h, occurring in a narrow window of less than 2 h, was used for the site-based modeling. Repairs to render NC-12 operational consisted of building a temporary bridge approximately 200 m long. The two-lane bridge is founded on 12 footings (bents) supported by 82 piles. This bridge is a temporary solution (but is expected to function for several years) until a permanent one is implemented.

Figure 1 shows a photograph of the breach location, with the temporary bridge installed and the ISEEP setup in the field. Samples for the grain size distribution were collected from the soil that washed out of the hole during ISEEP testing. The first patch sample was collected from a depth approximately 0.5 m, and the second patch, from a depth between 0.5 m and 1.5 m. As Figure 2 shows, the test soil at the site has a D_{50} = 0.32 mm with some of the shallower samples containing organic materials and shells that indicate an even coarser distribution.

The test procedure follows that described by Gabr et al. (*8*). To estimate the critical stream power (P_c) at two depths, the penetration rate is plotted against the natural log of the stream power, and extrapolation is performed to a zero penetration rate, as shown in Figure 3. In the depth range of 0 to 0.5 m, the P_c value is 200 W/m^2, and drops to 42 W/m^2 after 0.5 m within the test depth. The road was severely damaged at this location where an inlet opened. The uncorrected N-values (standard penetration resistance), below the debris of the pavement material, decrease from 20 near the surface to 6 at 4.6 m and then to weight of hammer at 6 m (North Carolina Department of Transportation 2011 boring log, unpublished data). The

[iv] This statement has been changed to correct for an error in the published version of the paper

(a) (b)

Figure 1. (a) Temporary Bridge along NC-12 at Location of Breach and (b) ISEEP Setup for Field Testing.

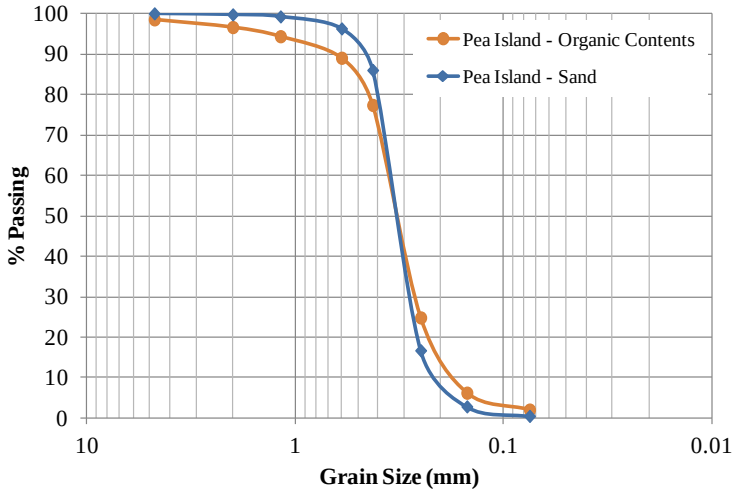

Figure 2. Grain Size Distribution for Pea Island Test Site.

values of k_d' is obtained by using best-fit linear interpolation between the penetration rate and the log of the stream power. The linear equation takes the form of Penetration Rate = c + b log (Stream Power). Differentiation of this equation with respect to stream power yields the value of k_d' per given stream power range. For example, for the stream power range of 300-400 W/m^2, the k_d' value is 0.007 cm/s/W/m^2 at a depth range of 0 to 50 cm.

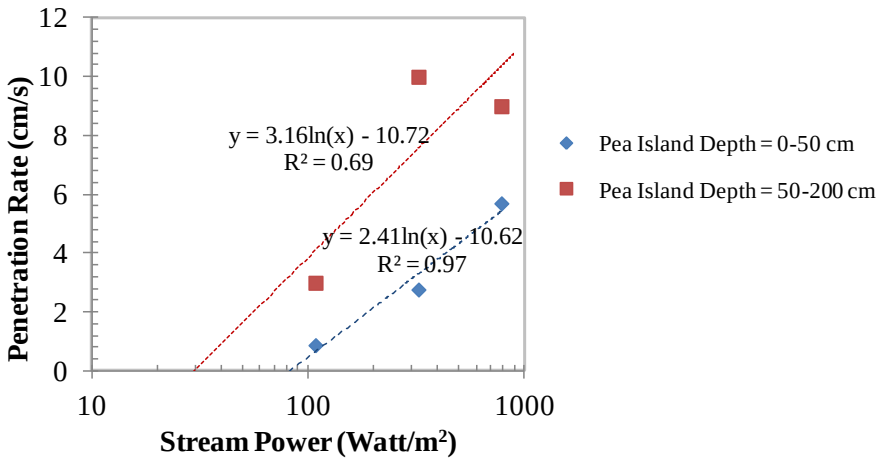

Figure 3. Extrapolation to Estimate Critical Value of Stream Power at Onset of Erosion.

NUMERICAL MODELING

The CFD software, FLOW-3D, is used to perform numerical simulations of scour at bridge piers. FLOW-3D (*20*) is based on the fundamental laws of mass, momentum and energy conservation. It simulates the flow process using the standard Navier-Stokes flow equation. The domain is discretized using finite difference blocks, and the governing equation is solved for each computational cell. The fractional area-volume obstacle representation (FAVOR) method is utilized for modeling solid obstacles within the domain (*21*).

Scour Model

A model of sediment scour turbulence can be used to simulate the scour around a cylindrical bridge pier. According to Brethour and Burnham (*22*), the sediment scour model can simulate the deposition and entrainment of sand, silt and other non-cohesive soils as suspended and packed sediment. According to FLOW-3D (*20*), suspended sediments are typically of low concentration and advect with fluid. Packed sediments exist in the computational domain at the critical packing fraction, as defined by the user. The input parameters of the sediment scour model are diameter and density of the sediment (d, ρ), the critical Shields parameter, drag coefficient (C_d), entrainment coefficient (C_e), bed load coefficient (C_b) and angle of repose (ϕ). When the critical Shields parameter is not assigned during the numerical simulation, FLOW-3D calculates the value from the Shields curve (*22*). The definitions of C_e, C_d, and C_b are as follows:

1. C_e describes the lifting of the sediment in the bulk flow of fluid. According to FLOW-3D (*20*), the entrainment coefficient predicts the rate of sediment erosion at a shear stress higher than the critical shear stress.

2. C_d quantifies the resistance of the sand particles to the fluid flow. Engelund and Hansen (*23*) proposed the following equation for natural sands and gravels based on laboratory measurements:

$$C_d = \frac{24}{R_e} + 1.5 \qquad (4)$$

3. C_b is a bed load coefficient indicating the transport of heavier particles along the top of the packed bed by the flow of water.

For a large Reynolds number signifying turbulent flow, the C_d is approximately equal to 1.5. C_b is related to the transport of heavy particles along the top of the packed bed by the flow of water. In this process, the bed load coefficient is used to predict the rate of transport at a shear stress higher than the critical shear stress. The default value of the bed load coefficient is 8.0 in FLOW-3D (*20*), which follows the Meyer-Peter and Muller (*24*) equation. Nnadi and Wilson (*25*) reported a C_b value of 12 for a sheet flow regime, and

Ribbernik (*26*) suggested a C_b of 5.7 for bed load data that are very close to the incipient motion. A typical C_b for sand and gravel is 5.7 (*26, 27*).

Table 1 provides values of the different parameters used for sandy soil. These value ranges are used as input parameters in the sediment scour model. As explained earlier, the value cell of the Critical Shields Parameter is blank in the table for the numerical simulations because the number is computed from the Shields curve (*22*). The C_d value was varied from 1.0 to 2.0 (*28, 29*), the C_e value was varied from 0.009 to 0.036, and the C_b value was varied from 4 to 8. These ranges are assumed on the basis of the consideration of the data found in the literature.

Table 1. Parameter Values Used in Numerical Simulations

Parameter	Value
Density, ρ	1500 Kg/m^3
Critical Shields Parameter	na
Drag Coefficient, C_d	1 to 2
Entrainment Coefficient, C_e	0.009 to 0.036
Bed Load Coefficient, C_b	4 to 8
Angle of Repose, Φ	31º

FLOW-3D has five different models for simulating turbulent flow: Prandtl's mixing-length theory, one-equation turbulent energy (k), two-equation turbulent energy (k-ε), renormalization group and the large eddy simulation. The renormalization group model is used in this study because it can describe low intensity turbulence flow with strong shear regions more accurately than the other models (*30*) and, in this case, seems to better fit the jetting scheme.

Model Geometry

Similar to the Pea Island bridge site, the modeled bed consists of sand in two layers, with the grain size distributions obtained from the field. As Figure 4 shows, the domain configuration consists of a sand bed 30 m long, 20 m wide and 4 m deep. A uniform mesh with 0.50-m spacing was used for the numerical simulation, with 48,392 cells. The *sediment scour* model, *viscosity and turbulence* model and *gravity* model were then activated. The gravity model was activated by specifying the gravity component of 9.8 m/s^2 in the z direction. Fluid flow was induced from the upstream boundary with a specified velocity that was varied from 0.45 m/s to 0.9 m/s, with a constant depth of flow of 1.0 m. Two cylindrical piers, 3 m in height from the surface and 1.22 m in diameter, were simulated to assess the local scour. The center-to-center spacing between the piers was 3 m.

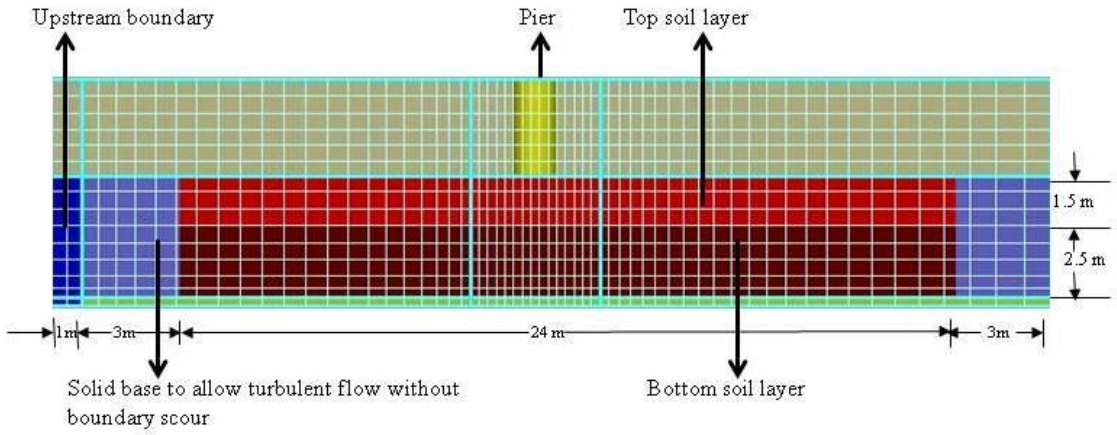

Figure 4. Discretized Domain for Numerical Simulation of Scour around Piers with Sand Bed and 1 m Outfall-Side View.

Simulation Results

The flow regime was simulated with time, and the results from the numerical modeling include data for bed shear stress, the erosion profile, and the maximum erosion depth as a function of flow velocity. By using the bed shear stress data computed from the model, the erosion rate at the pier was calculated using from Equation 3 on the basis of the parameters used in the ISEEP field testing.

Effect of Model Parameters

Figure 5 presents a comparison between the maximum scour depth measurements obtained on the basis of ISEEP parameters and the values computed using FLOW-3D, with a range of the C_e, C_b, and C_d parameters. Figures 5a, 5b and 5c present the simulated and computed scour depths obtained from both approaches. The excess shear stress value (therefore the stream power) was varied by changing the applied velocity in the upstream channel. The flow velocity was varied from 0.45 m/s to 0.9 m/s, which corresponds to stream power values in the range of 125 W/m^2 to 850 W/m^2. The C_e, C_b, and C_d values used for estimating the shear stress, and to use in conjunction with the ISEEP data, are 0.018, 5.7, and 1.5, respectively. These values are most commonly specified for sand and are within the range of values specified in Table 1 (*23, 26, 31*).

Figure 5a shows the effect of the entrainment coefficient, C_e, on the computed scour depth as a function of stream power. C_e was varied from 0.009 to 0.036. The figure shows that as C_e value increases, the scour depth also increases. The maximum scour depth for C_e = 0.009, whereas such a limit was not reached for the C_e value of 0.036 within the range of stream power values used in the analysis. Mastbergen and Von den Berg (*31*) indicated that the rate of erosion is linearly proportional to the entrainment coefficient. However, such a linear trend is not observed in Figure 5a. For example, the scour depth increases 70% for C_e = 0.036 versus C_e = 0.009 at a stream power = 600 W/m^2.

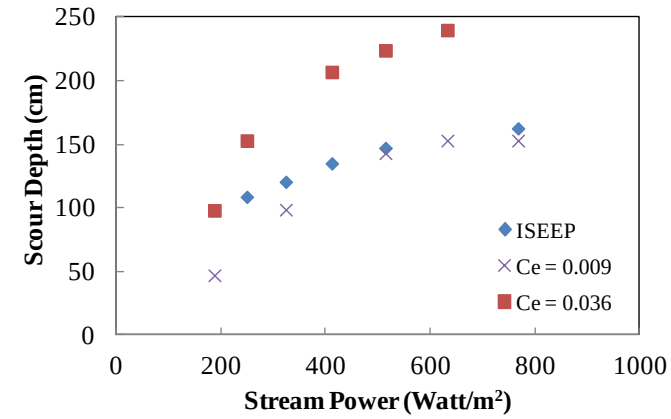

(a)

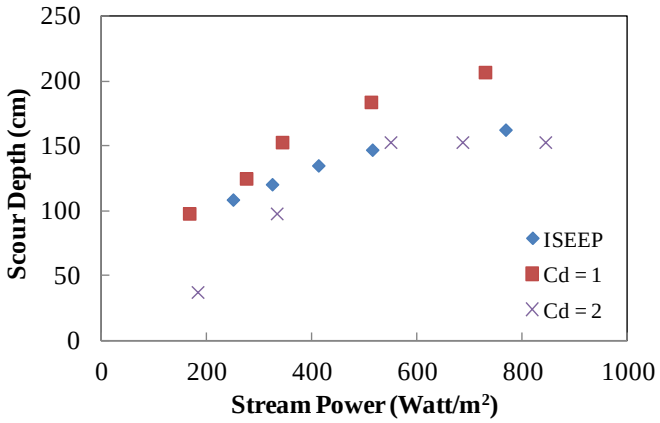

(b)

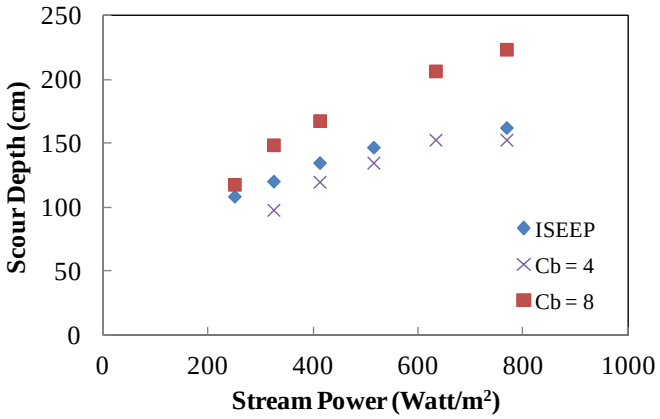

(c)

Figure 5. Comparison of Maximum Scour Depth around Bridge Piers Versus Stream Power Obtained from ISEEP Tests and Coefficients for (a) Entrainment (C_e) (b) Drag (C_d) and (c) Bed Load (C_b).

Figure 5b shows the effect of the drag coefficient, C_d, on scour depth. With an increase in the C_d, the magnitude of the scour depth decreases. The C_d value represents the resistance of the sand particles to the fluid flow and thus the observed reduction in the maximum scour depth under the same stream power value with an increasing C_d. At a stream power value of 600 W/m^2, the depth of scour decreases by 25% when C_d is doubled.

Figure 5c shows the effect of the bed load coefficient, C_b. The C_b parameter reflects the rate of bed load transport relative to the critical shear stress, and was varied from 4 to 8. Figure 5c shows that with an increase in the C_b value, the depth of scour increases. At a stream power value of 600 W/m^2, the depth of scour increases by 25% when C_b is doubled. As presented by Ribberink (*26*), the transport of heavy particles from the top of the bed in the direction of the fluid flow increases with higher C_b values and, therefore, the scour depth increases.

The results of the analyses indicate that among the three input parameters, the entrainment coefficient has the largest effect on scour depth, whereas the drag coefficient has the smallest effect. Figures 5a, 5b and 5c, also show that the computed scour depth measurements that are based on ISEEP data are within the values obtained from the FLOW-3D results, with the best match observed for the case of C_e, C_d and C_b values of 0.009, 2 and 4, respectively.

COMPARISON WITH EMPIRICAL EQUATIONS

Various approaches exist for empirically assessing bridge pier scour. Melville and Sutherland (*12*) suggested a maximum scour depth (d_s) to pier diameter (b) ratio of 2.4 in laboratory flume tests. Ettema (*32*) found that scour depth becomes independent of depth of flow (y) when the ratio of depth of flow to pier diameter ratio is greater than 3. Table 2 shows empirical equations to estimate the maximum scour depth in sandy soil; these equations have a provision for flow velocity and, therefore, can be used for comparison with results obtained from the numerical analyses and ISEEP predictions.

Table 2. Empirical Equations to Estimate Local Scour around Bridge Piers

Reference	Equation	Comments
Shen et al. (*11*)	$d_s = 0.000223\ (Vb/\upsilon)^{0.619}$	V = flow velocity, υ = kinematic viscosity of water $= 1 \times 10^{-6}\ m^2/s$
Richardson and Davis (*14*)	$d_s/b = 2K_sK_{theta}K_3K_4(y/b)^{0.35}Fr^{0.43}$	K_s = shape factor, K_{theta} = inclination factor, K_3 = factor for mode of sediment transport, K_4 = factor for armoring by bed material, Fr = Froude number
Breusers et al. (*33*)	$d_s/b = f\ (V/V_c)(2\tanh(y/b))K_sK_{theta}$	$f\ (V/V_c) = 0,\ V/V_c \leq 0.5$ $= (2V/V_c\text{-}1),\ 0.5 < V/V_c \leq 1$ $= 1,\ V/V_c > 1$ V_c = Critical velocity
Jain and Fischer (*34*)	$d_s/b = 1.86(y/b)^{0.5}(Fr - Fr_c)^{0.25}$	Fr_c = Critical Froude Number

Other empirical equations by Laursen and Toch (*10*), Melville and Sutherland (*12*), and Melville (*35*) were developed on the basis of only depth of flow and geometric dimensions. Therefore, these equations are not used in this study because comparisons with ISEEP-evaluated scour are not possible. Table 3 presents the input parameters and factors that are required to calculate scour depth using the empirical equations in relation to the methodology employed to estimate the input parameters.

Figure 6 presents a comparison of scour depth normalized by the pier diameter, from empirical equations, FLOW-3D, and ISEEP data. The stream power is varied by changing the flow velocity from 0.5 to 0.9 m/s. Figure 6 indicates that the simulated and computed scour depths obtained from both ISEEP and FLOW-3D agree relatively well. However, with an increase in stream power, the estimated scour magnitude values derived from ISEEP and FLOW-3D divert from the values estimated using the empirical equations. The difference in scour depth increases with the increase in flow velocity, (i.e., stream power). For a stream

power value of 800 W/m^2, the difference of scour depth to the pier diameter ratio is approximately 25% on the basis of the results from the empirical equations versus those assessed through the ISEEP data, with the magnitude of scour depth underpredicted by the empirical equations.

Table 3. Parameters used in the Empirical Equations

Parameter	Comments
V_c = Critical velocity	Calculated using $V_c/u_{*c} = 5.75 \log (5.53y/d_{50})$, where shear velocity $u_{*c} = 0.03(d_{50})^{1/2}$ and y = depth of flow (*12*)
Fr = Froude number	$Fr = V/(gy)^{0.5}$, where V is flow velocity and g is gravitational acceleration
K_s = shape factor	$K_s = 1$ for circular piers (*12*)
K_{theta} = inclination factor	$K_{theta} = 1$ for angle of attack 0 degree (*12*)
K_3 = factor for mode of sediment transport	From Richardson and Davis (*14*), when $V/V_c > 1$ the scour in the channel bed is live-bed scour (which is the movement of the bed material from the upstream to the pier hole) and $K_3 = 1$.
K_4 = factor for armoring by bed material	According to Richardson and Davis (*14*), for a $d_{50} < 2$ mm $K_4 = 1$. This study was performed with $d_{50} = 0.32$ mm. Therefore $K_4 = 1$.

The difference in the estimated depths of scour may be explained by the fact that the results that are based on the ISEEP data and FLOW-3D account for a two-layer soil system, whereas the empirical equations have been developed for a single-layer system and do not explicitly include soil properties in the equations. By the time the scour depth exceeds 1.5 m, the grain size distribution of the looser sand in the second layer controls the rate and, therefore, the difference.

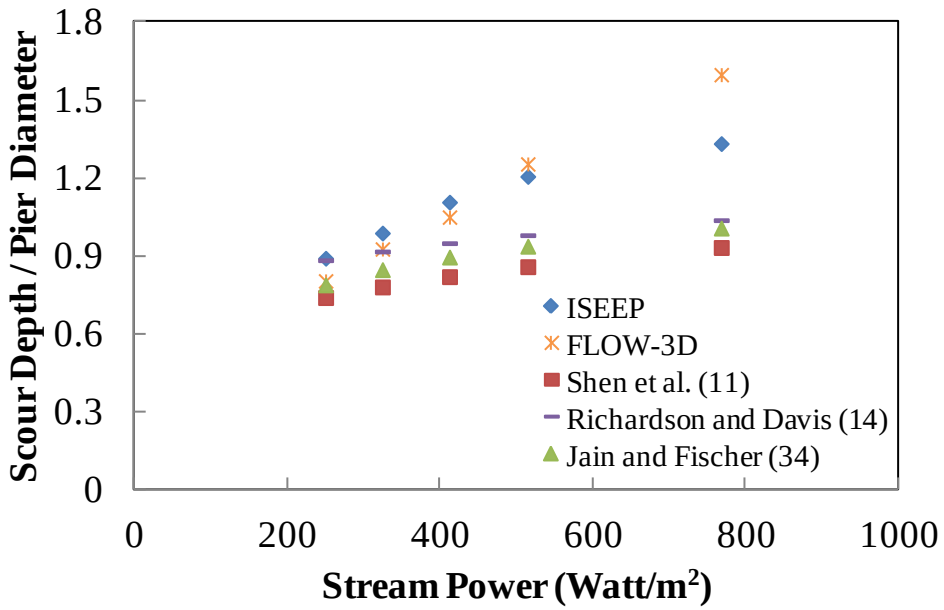

Figure 6. Ratio of Scour Depth to Pier Diameter Versus Stream Power for ISEEP Data and FLOW-3D from Empirical Equations from Literature.

SUMMARY AND CONCLUSIONS

This paper presents a case study that illustrates the use of an in situ device- ISEEP-that is used to assess the scour potential in relation to depth at a bridge site. The CFD software, FLOW-3D, is used to study the potential scour magnitude at a bridge pier with soil properties obtained from a site at a North Carolina Outer Banks site, where a breach occurred during Hurricane Irene in 2011. The variation in scour depth with the change in flow velocity (i.e., stream power) is examined by varying the drag, entrainment, and bed load coefficients. On the basis of field results, the detachment rate coefficient and the critical stream power are estimated using ISEEP test data. The bed shear stress values are obtained from FLOW-3D analyses, and the scour depth is calculated on the basis of ISEEP data by using an excess stream power approach. From the parameters and findings of this study, the following observations are advanced:

1. The rate of probe advancement is correlated to jet velocity, and erosion parameters are provided for two subsurface layers. The data reduction approach illustrates the viability of defining soil erosion parameters in terms of critical stream power and modified detachment rate coefficients for the two-layer system at the test site.
2. The parametric analyses indicate that among the parameters commonly used to define scour depth, the entrainment coefficient has the largest effect and the drag coefficient has the smallest effect on the estimated scour depth.
3. The scour depths estimated using ISEEP parameters agree relatively well with values obtained from the 3-D numerical analyses, as these estimates were obtained by accounting for the changes in the properties of the subsurface sand layers. The ISEEP-estimated depth measurements best match with those of FLOW-3D for C_e, C_d and C_b values of 0.009, 2 and 4, respectively.
4. For the case study presented herein, the empirical equations considered in the analysis yield smaller estimates of the scour depth at the pier compared to those from the numerical analysis. These equations do not explicitly account for the variation in soil properties in terms of depth and do not have a provision for a layered soil system or time-dependent scour rate.
5. The use of ISEEP data provides the advantage of *in situ* testing as well as the potential for estimating the scour parameters when soil layers vary with depth. Further laboratory and field validations of the proposed test and data reduction approaches are needed. Such validation should include an investigation of the applicability of the approach in soils with appreciable percentages of fines content.

REFERENCES

1. Lagasse, P. F., E. V. Richardson, J. D. Schall, and G. R. Price. *Instrumentation for measuring scour at bridge piers and abutments.* National Cooperative Highway Research Program (NCHRP) Report No. 396, Transportation Research Board, Washington, D.C., 1997.

2. Briaud, J. -L., F. C. K. Ting, H. C. Chen, Y. Cao, S. -W. Han, and K. Kawk. Erosion Function Apparatus for Scour Rate Predictions. *Journal of Geotechnical and Geoenvironmental Engineering*, Vol. 127, No. 2, 2001, pp. 105-113.

3. Lu, J. -Y, J. -H. Hong, C. -C. Su, C. -Y. Wang, and J. -S. Lai. Field Measurements and Simulation of Bridge Scour Depth Variations during Floods. *Journal of Hydraulic Engineering*, Vol. 134, No. 6, 2008, pp. 810-821.

4. Hanson, G. J., K. M. Robinson, and K. R. Cook. Scour Below an Overfall: Part II. Prediction. *Transactions of the American Society of Agricultural Engineers*, Vol. 45, No. 4, 2002, pp. 957-964.

5. Hanson, G. J., and K. R. Cook. Apparatus, Test Procedures, and Analytical Methods to Measure Soil Erodibility In Situ. *Applied Engineering in Agriculture*, Vol. 20, No. 4, 2004, pp. 455-462.

6. Mehta, A. J. Review Notes on Cohesive Sediment Erosion. In *N.C. Kraus, K.J. Gingerich, and D.L. Kriebel, (eds.), Coastal sediment '91, Proceedings of Specialty Conference on Quantitative Approaches to Coastal Sediment Processes*, 1991, pp. 40–53.

7. Annandale, G.W. *Scour Technology: Mechanics and Practice*. McGraw Hill, New York, 2006.

8. Gabr, M., C. Caruso, A. Key, and M. Kayser. Assessment of In Situ Scour Profile in Sand using a Jet Probe. Journal article accepted in ASTM.

9. Melville, B.W., and S.E. Coleman. *Bridge Scour.* Water Resources Publications, LLC, USA, 2000.

10. Laursen, E. M. and A. Toch. *Scour around Bridge Piers and Abutments*. Bulletin No. 4, Iowa Highway Research Board, 1956.

11. Shen, H. W., V. R. Scheider, and S. Karaki. Local Scour around Bridge Piers. *Journal of Hydraulic Engineering*, Vol. 95, No. 6, 1969, pp. 1919-1940.

12. Melville, B.W., and A.J. Sutherland. Design Method for Local Scour at Bridge Piers. *Journal of Hydraulic Engineering*, Vol. 114, No. 10, 1988, pp. 1210-1227.

13. Melville, B.W. *Local Scour at Bridge Sites*. Report No. 117, University of Auckland, School of Engineering, Auckland, New Zealand, 1975.

14. Richardson, E. V., and S. R. Davis. *Evaluating Scour at Bridges*. Rep. No. FHWA-IP-90-017, Hydraulic Engineering Circular No. 18 (HEC-18), 3rd Ed., Office of Technology Applications, HTA-22, Federal Highway Administration, U.S. Dept. of Transportation, Washington, D.C., 1995.

15. Mueller, D. S. *Local Scour at Bridge Piers in Nonuniform Sediment under Dynamic Conditions*. Ph.D. thesis, Colorado State University, Fort Collins, CO, 1996.

16. Richardson, J. E., and V. G. Panchang. Three-Dimensional Simulation of Scour Inducing Flow at Bridge Piers. *Journal of Hydraulic Engineering*, Vol. 124, No. 5, 1998, pp. 530-540.

17. Ali, K. H. M., and R. Karim. Simulation of Flow around Piers. *Journal of Hydraulic Research*, Vol. 40, No. 2, 2002, pp. 161-174.

18. Salaheldin, T. M., J. Imran, and M. H. Chaudhry. Numerical Modeling of Three Dimensional Flow Field around Circular Piers. *Journal of Hydraulic Engineering*, Vol. 130, No. 2, 2004, pp. 91-100.

19. Roulund, A., B. M. Sumer, J. Fredsoe, and J. Michelsen. Numerical and Experimental Investigation of Flow and Scour around a Circular Pile. *Journal of Fluid Mechanics*, Vol. 534, 2005, pp. 351-401.

20. FLOW-3D (2011). *User Manual*. Flow Science, Inc.

21. Hirt, C., and J. Sicilian. A Porosity Technique for the Definition of Obstacles in Rectangular Cell Meshes. In *Proc. Fourth International Conf.*, Ship Hydro., National Academy of Science, Washington, D.C., 1985.

22. Brethour, J., and J. Burnham. Modeling Sediment Erosion and Deposition with the FLOW-3D Sedimentation & Scour Model. *Flow Science Technical Note*, FSI-10-TN85, 2010, pp. 1-22.

23. Engelund, F., and E. Hansen. A Monograph on Sediment Transport to Alluvial Streams. Copenhagen, Tenik Vorlag, 1967.

24. Meyer-Peter, E. and R. Mueller. Formulas for Bed-Load Transport. In. *Proc*. Second Meeting of the International Association for Hydraulic Research, *IAHR, Stockholm*, Sweden, 1948, pp. 39-64.

25. Nnadi, F. N., and K. C. Wilson. Motion of Contact-Load Particles at High Shear Stress. *Journal of Hydraulic Engineering*, Vol. 118, No. 12, 1992, pp.

26. Ribberink, J. S. Bed-Load Transport for Steady Flows and Unsteady Oscillatory Flows. *Coastal Engineering*, Vol. 34, 1998, pp. 59– 82.

27. Fernandez, L. R., and R. Van Beek. Erosion and Transport of Bed-Load Sediment. *Journal of Hydraulic Research*, Vol. 14, No. 2, 1976, pp. 127-144.

28. Rubey, W. Settling Velocities of Gravel, Sand and Silt Particles. *American Journal of Science*, Vol. 25, No. 148, 1933, pp. 325–338.

29. Wu, W., and S. S. Y. Wang. Formulas for Sediment Porosity and Settling Velocity. *Journal of Hydraulic Engineering*, Vol. 132, No. 8, 2006, pp. 858-862.

30. Yakhot, V., and S.A. Orszag. Renormalization Group Analysis of Turbulence. I. Basic Theory. *Journal of Scientific Computing*, Vol. 1, No. 1, 1986, pp. 3–51.

31. Mastbergen, D. R., and J. H. Van den Berg. Breaching in Fine Sands and the Generation of Sustained Turbidity Currents in Submarine Canyons. *Sedimentology*, Vol. 50, No. 4, 2003, 625-637.

32. Ettema, R. *Scour at bridge piers*. Report No. 216, Dept. of Civil Engineering, University of Auckland, Auckland, New Zealand, 1980.

33. Breusers, H. N. C., G. Nicollet, and H. W. Shen. Local Scour around Cylindrical Piers. *Journal of Hydraulic Research*, Vol. 15, No. 3, 1977, pp. 211-252.

34. Jain, S. C., and E. E. Fischer. *Scour around Bridge Piers at high Froude Numbers*. Report Number FHWA-RD-79-104, Federal Highway Administration, Washington D.C., 1979.

35. Melville, B. W. Pier and Abutment Scour—An Integrated Approach. *Journal of Hydraulic Engineering*, Vol. 123, No. 2, 1997, pp. 125–136.

CHAPTER 4

DEVELOPMENT OF MAXIMUM SHEAR AND SHEAR STRESS PROFILE WITH PROGRESS OF SCOUR

ABSTRACT

Bridge pier scour is one of the major reasons for bridge failures. Understanding the development of shear stresses around bridge piers is vital for proper assessment of scour potential and erosion rates under flow conditions. Scour estimation is a time dependent process and most logical approaches for estimating scour depths are in terms of excess shear stress or excess stream power. Therefore, to estimate bridge pier scour it is necessary to determine the shear stress or stream power in the scour hole as a function of the depth of the scour hole. In the literature, however, a maximum shear stress equation that combines the effect of Reynolds number, mean flow velocity, fluid density and particle diameter is absent. Work in this study investigates the influence of flow phenomena on the bed shear stress around cylinders for live-bed scour and clear water scour using Computational Fluid Dynamics (CFD) software FLOW-3D. A model is developed and calibrated using simulations of results from flume tests data reported in literature. An equation that provides maximum shear stress around piers before scour starts is developed based on the results of a parametric study. The equation is proposed as a function of Reynolds number, mean flow velocity, fluid density and critical shields number. Effect of sediment gradation on maximum shear stress and scour depth is also investigated for live bed scour. It is observed that maximum shear stress does not change with the change of soil gradation, however, equilibrium scour depth decreases with the increase of sediment gradation. Shear stress profile with normalized scour depth is also developed from the simulations. Normalized shear stress profile equations are presented and discussed.

INTRODUCTION

Lagasse et al. (1997) reported that there were 488,750 bridges over stream and river crossings in the United States with an annual cost for scour-related bridge failures estimated at $30 million. Furthermore, it was reported that out of 1,000 bridges that have collapsed in

the United States over the past thirty years, approximately 60% of these failures was caused by excess scour at the supporting foundation system (Briaud et al., 2001). Accordingly scour seems to be one of the major causes of bridges' foundation failure and the monitoring and assessment of scour potential at bridge foundation remains a challenging task. The determination of the erosion rate of foundation soils that support these structures is needed not only during the design phase but also throughout the operational lifetime of the structure. In addition to being critical parameters to assess in the initial design phase, the erosion magnitude and rate are also needed to develop maintenance priorities and establish replacement schedules.

Estimation of scour pattern around piers strongly depends on resolving the flow pattern and the mechanism of sediment movement in and out of the scour holes. The flow field around a vertical circular pier is characterized by the size and pattern of the vortex systems that develop due to the presence of the pier. These vortices are considered as the basic mechanism for scour initiation and development (Laursen and Toch 1956, Shen et al. 1969, Melville 1975, Dargahi 1987, and Raudkivi 1990). As the pier partially blocks the water flow area, the flow decelerates, and the approaching flow separates and spreads around the pier edges. Vorticies are then developed and scour is initiated.

Numerical methods can be applied to study flow pattern s at bridge piers and the corresponding pier scour. Numerical investigations of bridge pier flows have utilized steady Reynolds-Average Navier-Stokes (RANS) models with wall functions (Olsen and Melaaen, 1993, Richardson and Panchang, 1998, Olsen and Kjellesvig, 1998, Wang and Jia, 2000, Ali and Karim, 2002, Salaheldin et al., 2004, Roulund et al., 2005). This method has been reported to be applicable for bridge piers and abutments of complex geometry at field-equivalent Reynolds numbers. Ali and Karim (2002) used Computational Fluid Dynamics (CFD) software FLUENT to simulate flow around piers for clear water scour. Velocity and shear stresses distribution around the pier were obtained from the simulations. They concluded that scour depth depends on pier dimension, sediment size, and time. Salaheldin et al. (2004) also used FLUENT to simulate the separated turbulent flow around vertical circular piers in clear water scour mode. Computations were performed using different

turbulence models including k-ε model and Reynolds Stress Model (RSM). Results were compared with several sets of experimental data available in the literature. Results by Salaheldin et al. (2004) using the k-ε model showed some discrepancy with the measured bed shear stress. On the other hand, the RSM was found to perform well in simulating velocity distribution on flat bed and scour hole as well as in estimating shear stress distribution on flat bed around circular piers.

Studies have been performed to characterize maximum shear stress (τ_{max})before scour starts. By performing extensive numerical simulations, Wei et al. (1997) found that for large water depth (Water depth/Pier diameter > 2), τ_{max} was dependent on the Reynold's number (Re), the mean flow velocity (V), and the mass density of water (ρ). Wei et al (1997) work was performed for pier scour in cohesive soils or clear water scour in sand. The following equation to calculate maximum shear stress around the pier was proposed by Wei et al. (1997):

$$\tau_{\max} = 0.094\rho u^2\left(\frac{1}{\log R_e} - \frac{1}{10}\right) \qquad (1)$$

Rounald et al. (2005) simulated scour process to study the flow and live-bed scour around a circular pile exposed to a steady current in cohesionless sediment. A three-dimensional flow code, EllipSys3D, was employed to simulate the flow, both with a rigid plane bed and with a sediment bed undergoing scour. Vertical and horizontal velocity profiles, with depth, were presented. Bed shear stress profile and the effect of boundary layer thickness, Reynolds number and bed roughness on shear stress were presented. Rounald et al. (2005) concluded that normalized shear stress increases with the increase of Reynolds number upto a value of 500, after that it decreases with the increase of Reynolds number.

Huang et al. (2009) used 3D CFD model to examine scale effects on turbulent flow and sediment scour. For the large-scale numerical model, the physical scale and boundary velocity were set up from the small scale model based on the Froude similarity law. Effects of scale on turbulence flow and sediment scour were investigated by comparing results obtained from a full scale numerical model to those derived from the Froude similarity method.

For the case of a highly unsteady flow, characterized by large-scale unsteady vortex shedding and severe adverse pressure gradients, the use of the wall-function approach (which assumes the validity of the law-of-the-wall near solid boundaries) is questionable. The accuracy of the mean flow and turbulence predictions obtained using steady Reynolds Average Navier Stokes (RANS) simulations is relatively poor due to the flow complexity. Several attempts have been reported in literature (e.g., Wei et al., 1997, Nurtjahyo et al., 2002, Chen, 2002, Nagata et al., 2005) to use RANS methods coupled with a movable bed module to characterize the flow field and the bed evolution. Several of the authors indicated that the major disadvantages of the RANS approach is that it cannot accurately predict massively separated flows and flows in which large adverse pressure gradient are present. Large Eddy Simulations (LES) using subgrid-scale models and fine meshes (e.g., Kirkil et al, 2008, Koken and Constantinescu, 2008a-b) have allowed the investigation of the role of regions of concentrated vorticity in the scouring process. These simulations were found to robustly predict the flow patterns and turbulence compared to other numerical methods (Kirkil et al, 2008, Koken and Constantinescu, 2008a-b). Kirkil et al. (2008). reported on the use of LES to investigate coherent structures present in the flow field around a circular cylinder located in a scour hole, and characterize the interaction of the horseshoe vortex (HV) system with the separated shear layers formed from the cylinder, and the near bed turbulence. Significantly large values of the mean bed shear stress were observed under the primary necklace vortex, as well as beneath the small junction vortex at the base of the cylinder.

The main objective of the work presented herein is to investigate the influence of flow phenomena on the development of the bed shear stresses around cylinders for live-bed and clear water scour. The context of the investigation is to develop an approach to predict the maximum bed shear stresses with the progression of the scour process. These shear stresses along with the soil erosion parameters can then be used to estimate the magnitude of scour for a given flow pattern. The analyses are conducted using the Computational Fluid Dynamics (CFD) software FLOW-3D. The developed model was calibrated using laboratory flume tests data obtained from the literature. The Large Eddy Simulation (LES) technique is used in the simulations as it can better predict massively separated flows in which large

adverse pressure gradient are present. Results from a parametric study are used in the development of an equation that provides maximum shear stress around piers with flow and soil parameters is pursued. Varied parameters include Reynolds number, mean flow velocity, fluid density and critical shields number. Effect of sediment gradation ($\sigma = \sqrt{(d_{84}/d_{16})}$) on maximum shear stress around bridge piers and equilibrium scour depth is investigated for live bed scour. Normalized shear stress profile versus normalized scour depth are presented and discussed.

NUMERICAL SIMULATIONS

The CFD software, FLOW-3D, was used to perform the numerical simulations of scour around bridge piers. FLOW-3D (FLOW-3D, 2011) is based on the fundamental laws of mass, momentum and energy conservation. It simulates the flow process using the standard Navier-Stokes flow equation. The domain is discretized using finite difference blocks, and the governing equation is solved for each computational cell. The fractional area-volume obstacle representation (FAVOR) method is utilized for modeling solid obstacles within the domain. Sediment scour model and large Eddy Simulations (LES) turbulence model were used to simulate the scour around cylindrical bridge pier.

Sediment Scour Model

According to Brethour and Burnham (2010), the sediment scour model can simulate the deposition and entrainment of sand, silt and other non-cohesive soils as suspended and packed sediment. In FLOW-3D (FLOW-3D, 2011), suspended sediments are typically of low concentration and advect with fluid. Packed sediments exist in the computational domain at the critical packing fraction, as defined by the user. The input parameters of the sediment scour model are: diameter and density of the sediment (d, ρ), the critical Shields parameter, drag coefficient (C_d), entrainment coefficient (C_e), bed load coefficient (C_b) and angle of repose (ϕ).

Drift velocity is computed from the relative velocity using the definition of the drift and relative velocities (FLOW-3D, 2011)

$$u_{drift,i} = (1 - f_{s,i})u_{r,i} - \sum_{j=1}^{N(-i)} f_{s,j}u_{r,j} \quad (2)$$

Where relative velocity is expressed as (FLOW-3D, 2011):

$$u_{r,i} = \frac{g}{\frac{3f_{s,i}}{4d_{s,i}}\left[C_{D,i} \| u_{r,i} \| + 24\frac{\mu_f}{\rho_f d_{s,i}}\right](\rho_{s,i} - \rho_f) f_{s,i}} \quad (3)$$

$f_{s,i}$ is the volume fraction of sediment species i, $d_{s,i}$ is the diameter of sediment species i, $\rho_{s,i}$ is the density of the sediment material, $C_{D,i}$ is the drag coefficient for ith sediment and μ_f is the dynamic viscosity.

Entrainment is the picking up and re-suspension of packed sediment. According to Brethour and Burnham (2010), entrainment needs to be computed only at the packed sediment interface. Since it is not possible to compute the flow dynamics about each individual grain of sediment and it is often difficult to compute the boundary layer at the interface, an empirical model must be used. The model used in FLOW-3D is based on Mastbergen and Von den Berg (2003). The local Shields parameter at the bed interface is computed based on the local shear stress, τ, as follows:

$$\theta_i = \frac{\tau}{\|g\| d_{s,i}(\rho_{s,i} - \rho_f)} \quad (4)$$

The entrainment lift velocity (volumetric flux) of sediment is then computed as (Mastbergen and Von den Berg, 2003)

$$u_{lift,i} = \alpha_i n_s d_*^{0.3}(\theta_i - \theta_{cr,i})^{1.5}\sqrt{\frac{\|g\| d_{s,i}(\rho_{s,i} - \rho_f)}{\rho_f}} \quad (5)$$

where d^* is the dimensionless mean particle diameter, and is defined as:

$$d_* = d_{50}\left[\frac{\|g\| \rho_f (\rho_{s,i} - \rho_f)}{\mu^2}\right]^{\frac{1}{3}} \quad (6)$$

α_i is an empirical lifting parameter, whose default value is 0.018 (representative for submarine sands), n_s is the outward pointing normal to the packed bed interface and $\theta_{cr,i}$ is the critical Shields parameter.

Bed-load transport describes the movement of large sediment along the surface of the bed without being entrained into the bulk fluid flow. For bed-load transport, the model used in FLOW-3D is developed by Meyer-Peter and Muller (1948). This model predicts the volumetric flow rate of sediment per unit width over the surface of the packed bed. Bed-load velocity was described by van Rijn (1984) as:

$$u_{bedload,i} = \frac{\beta_i(\theta_i - \theta_{cr,i})^{1.5}[\|g\|(\frac{\rho_{s,i} - \rho_f}{\rho_f})d_{s,i}^3]^{1/2}}{0.3d_{50}d_*^{0.7}(\frac{\theta_i}{\theta''_{cr,i}} - 1)^{0.5} f_{b,i}} \frac{\bar{u}}{\|\bar{u}\|} \qquad (7)$$

where θ_i is the dimensionless local bed shear and $\bar{u}/\|\bar{u}\|$ is the direction of the fluid-sediment mixture adjacent to the packed interface and $f_{b,i}$ is the volume-fraction of the bed-load layer. The value of β_i is a dimensionless fitting parameter, generally 5.0 - 5.7 for low transport, 8.0 for intermediate transport, and up to 13.0 for very high transport. The default value is 8.0, which is also the most common value found in the literature (Meyer-Peter and Muller, 1948).

Large Eddy Simulation Model

The LES model in FLOW-3D is based on the work of Smagorinsky (1963). The filter is the cell size, and the sub-grid model is also from Smagorinsky (1963). In the LES model, the effects of turbulence that is too small to compute are represented by an eddy viscosity, which is proportional to a length scale times a measure of velocity fluctuations on that scale. For the length scale, (Smagorinsky, 1963) proposed a geometric mean of the grid cell dimensions as follows,

$$L = (\delta x \delta y \delta z)^{1/3} \qquad (8)$$

Smagorinsky (1963) scales velocity fluctuations by the magnitude of L times the mean shear stress. These quantities are combined into the LES kinematic eddy viscosity (Smagorinsky, 1963).

$$\nu_T = (cL)^2 \sqrt{2e_{ij}2e_{ij}} \qquad (9)$$

Where c is a constant having typical value in the range of 0.1 to 0.2 and e_{ij} denotes strain rate tensor components. This kinematic eddy viscosity is incorporated into the dynamic viscosity used throughout FLOW-3D in exactly the same way as it is for the turbulence transport models:

$$\mu = \rho(\nu + \nu_T) \qquad (10)$$

Model Domain

For the clear water scour simulations, dimensions of the domain are obtained from the laboratory flume tests performed by Ettema et al. (2006). In these tests, the cylindrical pier was placed in a 4.88 m long, 3.0 m wide and 1.0 m deep sediment recess with uniform sand having a median particle diameter of 1.05 mm. The model domain for the simulation of the experimental geometry is shown in Figure 1. For live bed scour simulations, domain dimensions from laboratory flume tests performed by Sheppard and Miller (2006) are used. Domain for live-bed scour is 1.5 m wide, 1.2 m deep, and 45 m long. The reason for choosing Ettema et al. (2006) and Sheppard and Miller (2006) study is dimension of the piers are larger compared to the other model laboratory flume testing data available in the literatures.

Even though the convergence, overall accuracy, and stability of the numerical solution can be found to be insensitive to the grid size away from the solid boundaries, Salaheldin et al. (2004) suggested that finer mesh is required near solid boundaries including the pier, in order to resolve the flow details near the interfaces. In this study, a total 199,328 cells were used for the live-bed scour simulations. In the vicinity of the pier, 3.6 cm size cells were used, and these extended from 6 cm above the soil surface to 40 cm below the surface. Comparatively coarser mesh was used for cells away from the pier. Figure 2 shows mesh sensitivity analysis for live-bed scour simulations. Results show that after a specific mesh size, scour depth value remains the same. In the case of the clear water scour, 193,602 cells were used. Since pier diameter is varied during clear water scour analyses, different cell sizes were used in the vicinity of the pier. Flow properties, sediment size and pier dimensions are presented in Table 1. Values for FLOW-3D sediment scour model parameters were used

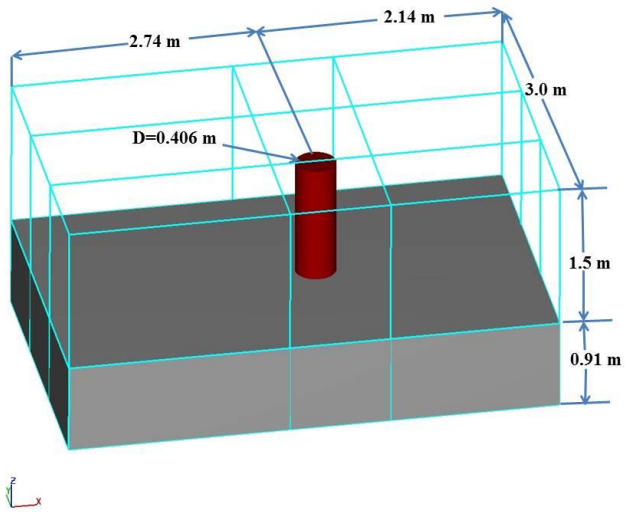

Figure 1. Geometric Domain for Clear Water Scour Simulations

Table 1: Flow properties, Pier Dimension and Sediment Size as was used in Flume Testing by Ettema et al. (2006) and Sheppard and Miller (2006)

	Simulation no.	**Flow Velocity (cm/s)**	**Pier Diameter (cm)**	**Depth of Flow (cm)**	**Critical Velocity (cm/s)**	**V/V_c**	**D_{50} (mm)**	**σ**
Live-bed scour	1	62	15.2	42	28	2.21	0.27	1.33
	2	88	15.2	43	28	3.14	0.27	1.33
	3	110	15.2	40	28	3.93	0.27	1.33
	4	126	15.2	40	28	4.50	0.27	1.33
	5	143	15.2	40	27	5.30	0.27	1.33
	6	164	15.2	40	27	6.07	0.27	1.33
Clear water scour	7	46	40.6	100	36.8	0.8	1.05	-
	8	46	30.5	100	36.8	0.8	1.05	-
	9	46	17.2	100	36.8	0.8	1.05	-
	10	46	6.4	100	36.8	0.8	1.05	-
Live-bed scour (Gradation variation)	11	164	15.2	40	27	6.07	0.32	1.14
	12	164	15.2	40	27	6.07	0.32	1.35
	13	164	15.2	40	27	6.07	0.32	1.60
	14	164	15.2	40	27	6.07	0.32	2.00

from Kayser and Gabr (2013) and are Drag coefficient = 2.0, Entrainment Coefficient = 0.009 and Bed load coefficient = 4. For all simulations, the inlet boundary is defined as a specific velocity condition and the outlet boundary is specified as outflow condition. Both side boundaries are defined as pressure boundaries with fluid height as depth of flow.

RESULTS AND DISCUSSION

Scour depth values obtained from the numerical simulations agreed well with the laboratory flume testing values. Large bed forms were observed both during numerical simulations and laboratory experiments.

Figure 3 (a, b) shows that the maximum horizontal velocity occurs around the sides of the pier before scour starts. A flow separation occurs behind the pier, where the flow is stagnant. The flow velocity is reduced as it approaches the pier and comes to rest in front of the pier.

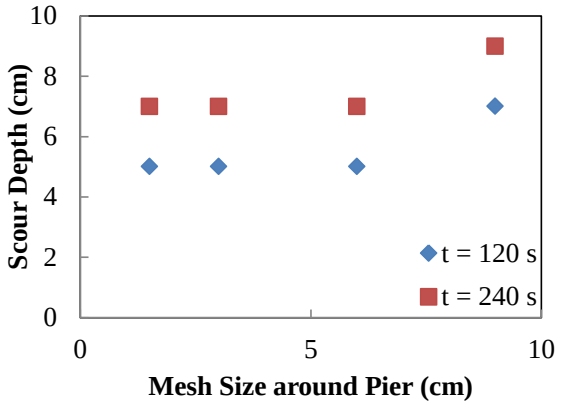

Figure 2. Mesh Sensitivity Analysis

Ali and Karim (2002) depicted stagnation pressures as largest near the pier surface, where the deceleration is greatest, and decrease downwards. With the increase of the inlet flow velocity, the velocity around the pier also increases. Figure 4 shows the vertical velocity profile around the pier before scour starts. In front of the pier, vertical velocity is negative

which depicts downflow impinging on the bed; this impinging flow seems to be the main scouring agent at this point. Negative velocity in front of the pier increases with the increase of inlet flow velocity. The development of the scour hole around the pier also gives rise to a lee eddy, known as the horseshoe vortex. The horseshoe vortex is effective in transporting dislodged particles away past the pier. According to Ali and Karim (2002), the impinging downflow and the horseshoe vortex provide the dominant scour mechanism. Raudkivi (1986), however, noted that the horseshoe vortex is a consequence of scour, not the cause of it.

MAXIMUM SHEAR STRESS BEFORE SCOUR STARTS

During the obstruction of the flow by the pier in an open channel with a flat bottom, the maximum shear stress τ_{max} for scour to start is significantly higher than the shear stress value when there is no obstruction (Briaud et al. 2001). If τ_{max} is larger than the critical shear stress τ_c, scour is initiated. Numerical simulations are performed for both live-bed scour and clear water scour in cohesionless soil to obtain τ_{max}. Results presented in Figure 5 show that before scour starts the maximum shear stress occurs at the side of the the cylindrical pier for live-bed scour.

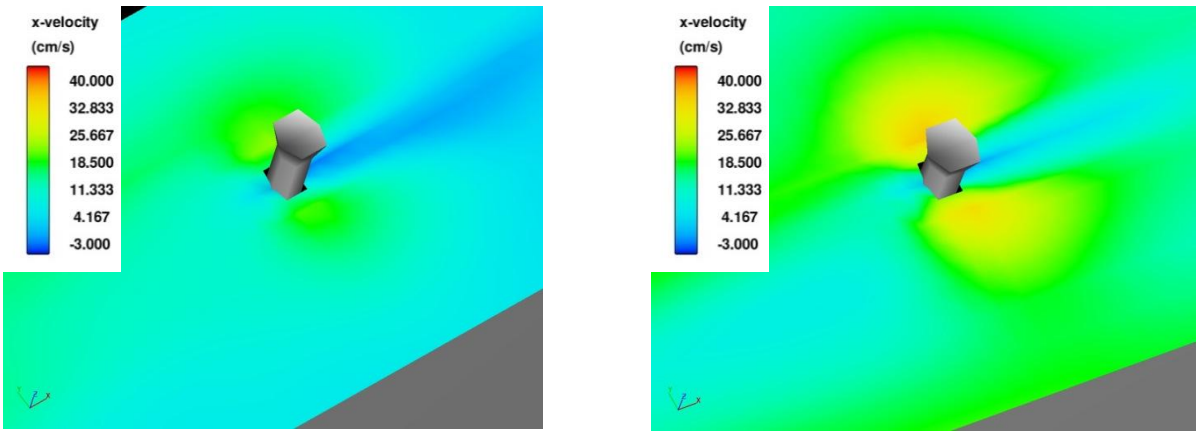

(a) (b)

Figure 3. X-Velocity (cm/s) around the Pier for (a) 0.88 m/s and (b) 1.64 m/s Flow Velocity

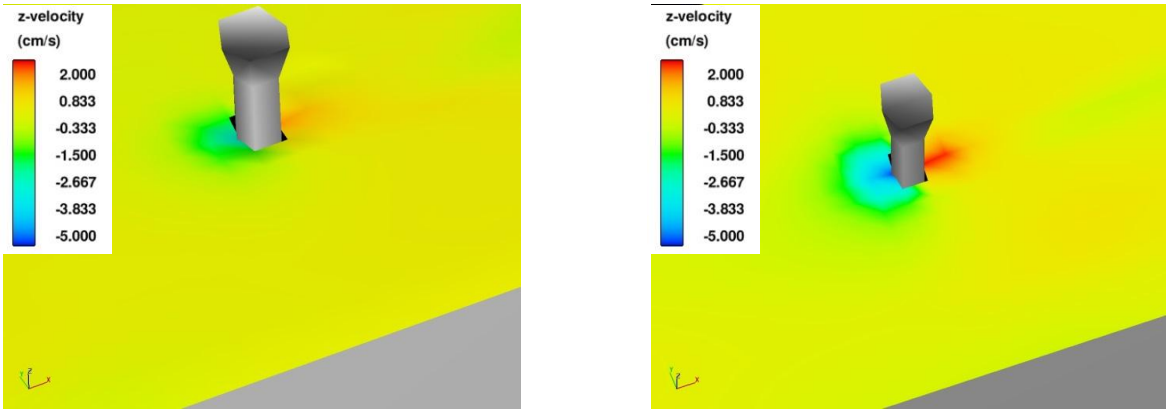

(a) (b)

Figure 4. Z-Velocity (cm/s) around the Pier for (a) 0.88 m/s and (b) 1.64 m/s Flow Velocity

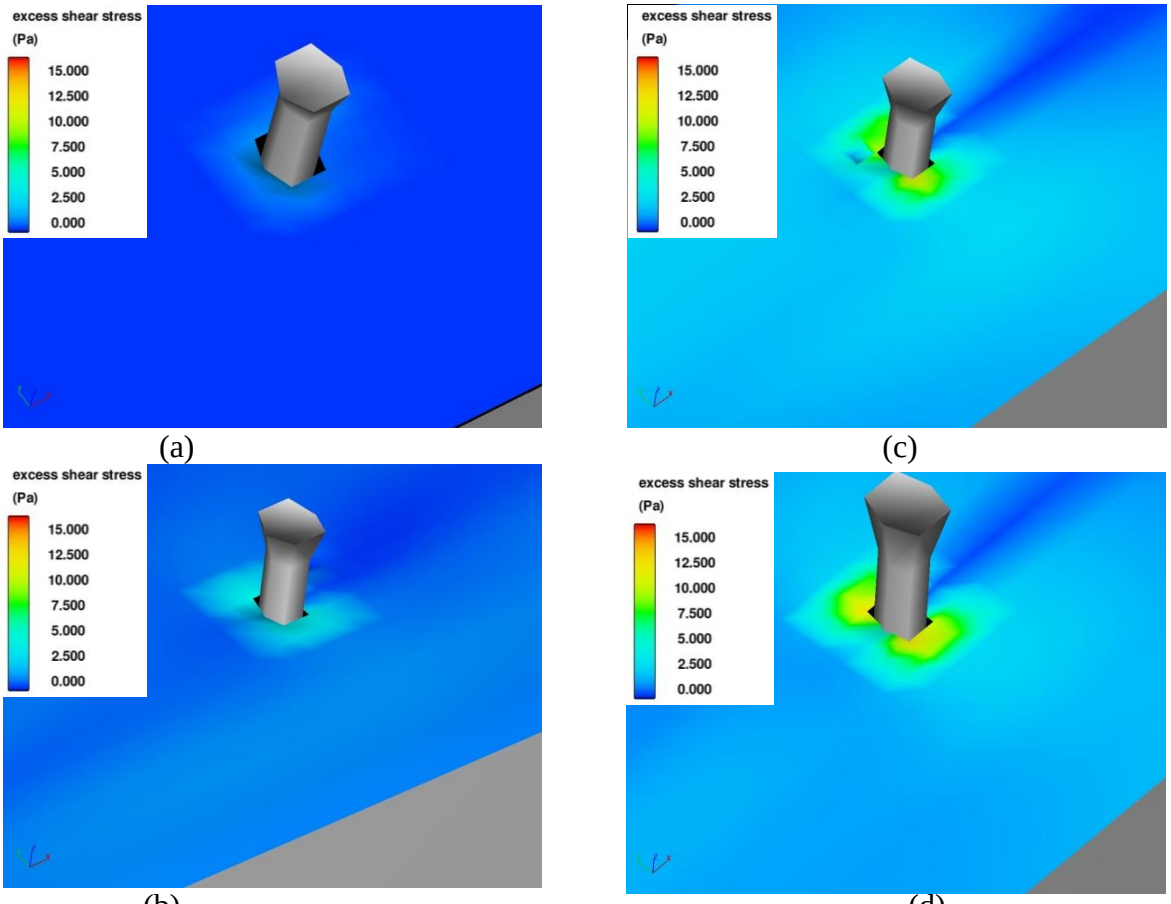

(a) (c)

(b) (d)

Figure 5. Live-bed Scour Shear Stress Contours for Flow Velocity (a) 0.62 m/s (b) 0.88 m/s (c) 1.43 m/s and (d) 1.64 m/s

For a velocity range of 0.62 m/s to 1.64 m/s and pier diameter of 15.2 cm (diameter used in flume testing), maximum excess shear stress (τ-τ_c) varies from 2.0 Pa to 14.0 Pa. The excess shear stress value increases with the increase of flow velocity for a constant pier diameter and constant depth of flow. For clear-water scour simulations, flow velocity and depth of flow were kept constant and pier diameter was varied from 6.4 cm to 40.6 cm. In these cases, the maximum excess shear stress value around the pier varies from 1.4 Pa to 0.85

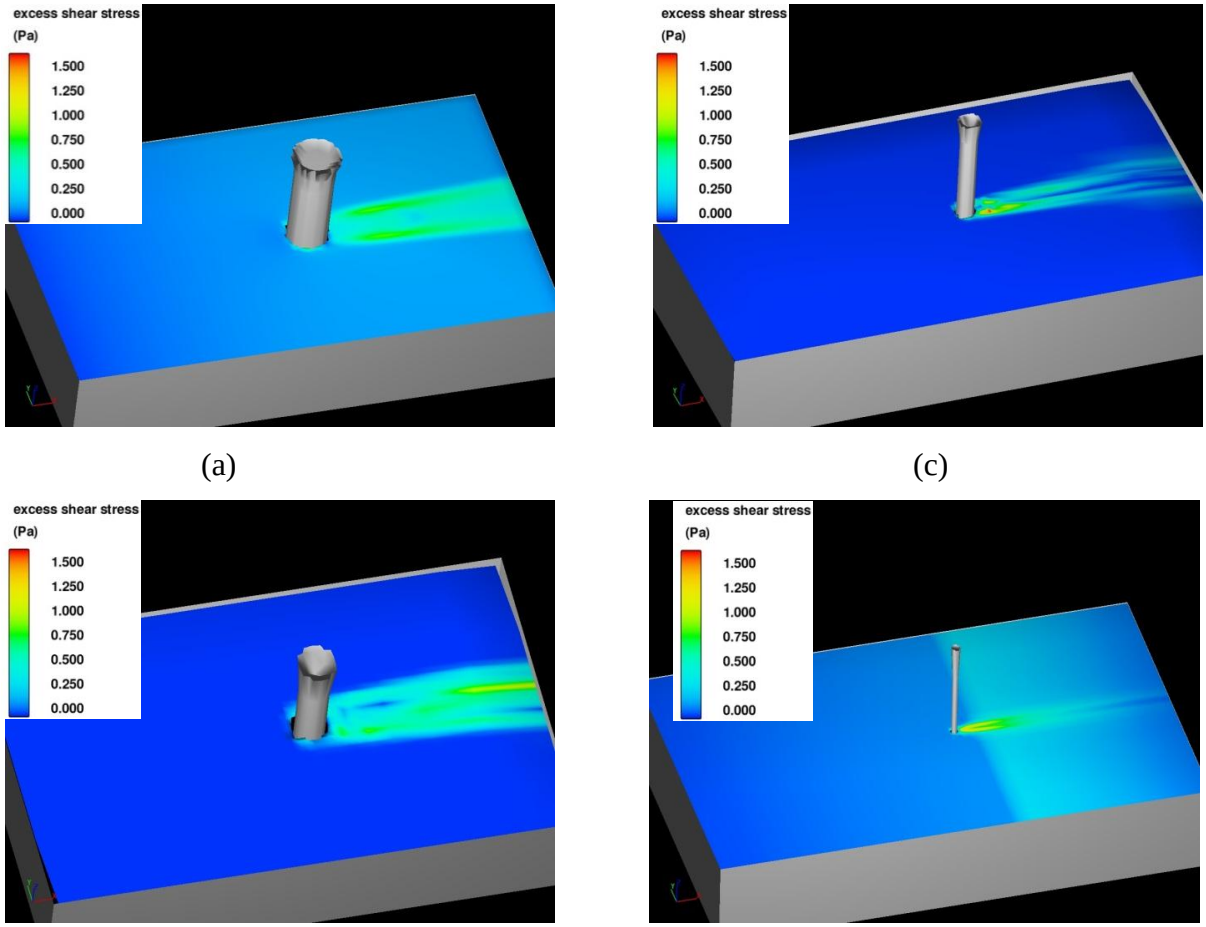

Figure 6. Shear Stress Contours for Clear-water Scour with Pier Diameter (a) 40.6 cm (b) 30.6 cm (c) 17.2 cm and (d) 6.4 cm

Melville (1975) depicted that the scour starts at the location of τ_{max} at about ±100° to the flow direction as a result of the acceleration and separation of the flow on the sides of the pier. Melville concluded that once the scour starts at the pier edges, it spreads towards the upstream and downstream sides of the pier, hence the scour hole develops all around the pier and continues to deepen until equilibrium state is reached.

PROPOSED APPROACH FOR ESTIMATING τ_{max}

Figure 7 shows normalized shear stress value against Reynolds number, as was suggested by Wei et al. (1997), versus results obtained from simulations conducted in this study. In this case τ_{max} for the live bed scour is lower than that estimated for the clear water condition and in both cases, τ_{max} is 15% to 30% lower than results by Wei et al, with the difference increasing with the increase in Reynolds number.

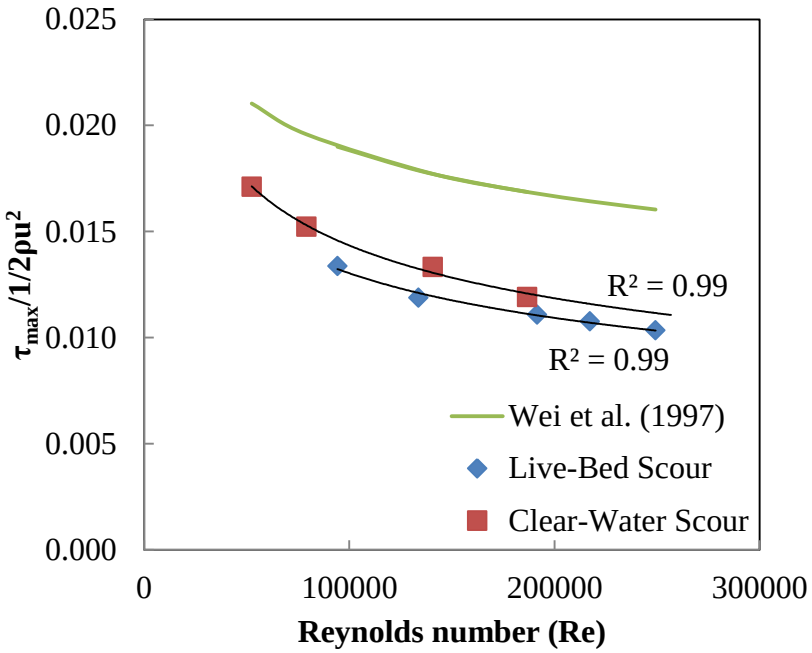

Figure 7: Comparison of Normalized Shear Stress Values versus Reynolds Number

Figure 8 shows a plot of the results with data presented as normalized maximum shear stress versus Reynolds Number that is normalized with respect to the Critical Shields Number. By normalizing the data in the manner, the maximum shear stress value can be defined using a single equation for both live-bed and clear-water scour as follows:

$$\tau_{\max} = 0.5\rho u^2 \left(\frac{R_e}{\theta}\right)^{-0.29} \qquad (11)$$

This equation is valid for cohesionless soil, and for both clearwater and live-bed scour conditions within a Reynolds number range of $5x10^4$ to $2x10^5$.

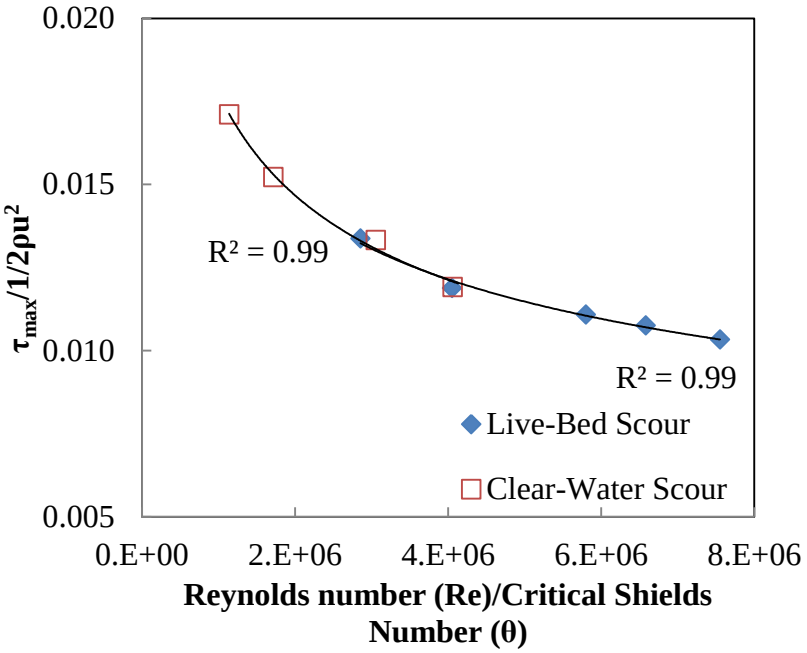

Figure 8: Normalized Maximum Shear Stress vs. Reynolds Number/Critical Shields Number

SHEAR-STRESS PROFILE

Scour estimation is a time dependent process and most logical approaches for estimating scour depths are in terms of excess shear stress or excess stream power. Therefore, to estimate bridge pier scour it is necessary to determine the change in shear stress magnitude as

a function of the depth progression of the scour hole. Normalized shear stress (τ_{max}/τ_{bottom}) profile at the soil surface with the advancement of the scour hole is shown in Figure 9 in the form of the shear stress at the bottom of the scour hole normalized with the maximum shear stress at the onset of the scour versus normalized scour depth (Scour depth/Pier diameter) Normalized shear stress profile was obtained using the maximum shear stress value at a certain depth within an area of a pier diameter distance from the center of the pier. Once the scour hole becomes deep enough, τ_{bottom} becomes equal to the critical shear stress (τ_c), and the final depth of scour z_{max} is reached. After the scouring action had started, the bed shear stress start to decrease as the depth of scour is further developed. In this case, the overall bed shear stress decreases with the increase in the depth of local scour. This rate of decrease is 0.8 times the normalized depth upto a normalized depth ratio of half, after which the decrease rate is less at a value of 0.25 per normalized depth. In general, normalized shear stress profile for the range of flow velocities used in the simulations is similar. According to Ali and Karim (2002), the shear stress value at the brim of the scour hole along the symmetrical plane is essentially less than the critical flat-bed shear stress, marking the boundary of the scour hole. FLOW-3D results show that regions with the highest values of bed shear stress correspond to the region of highest bed velocity, which agrees with the observation mentioned by Ali and Karim (2002). Knowing maximum shear stress around pier before scour starts, the shear stress with the advancement of scour depth can be obtained from the shear stress profile shown in Figure 9. In this case, the best fitted equation is

$$ScourDepth / PierDiameter = 248.4(1-(\tau_{bottom}/\tau_{max})^{3.3E-3}) \qquad (12)$$

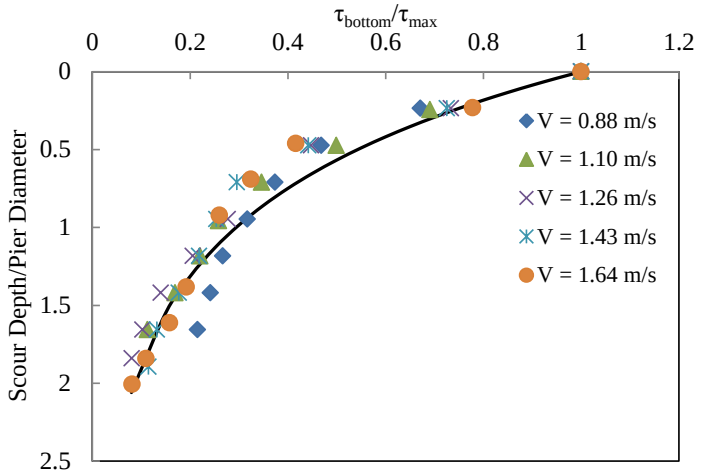

Figure 9. Normalized Shear Stress Profile with Best Fitted Curve

SCOUR PROFILE

According to Ali and Karim (2002) scour hole development commences at the sides of the pier with the two holes rapidly propagating upstream around the perimeter of the cylinder to meet on the centerline. In this way, a shallow hole, concentric with the cylinder, is formed around most of the perimeter of the cylinder, but not in the wake region. Live-bed scour tests were ran in the laboratory by Sheppard and Miller (2006) for a time range of minimum 1.5 hour to maximum 7 hours. However duration of numerical simulations was an hour since during live-bed scour the initial peak is reached early; after the initial peak is obtained sediment moves in and out of the scour hole before equilibrium. For higher flow velocities, equilibrium scour depth was obtained from the the numerical simulation once soil movement in and out of the scour hole around the pier ceased. Figure 10 shows that the maximum scour depth occurred at the midpoint of the upstream face of cylindrical pier for all of the cases. As the scour hole is enlarged with time, the strength of the horseshoe vortices weakened, causing a smaller rate of scour, and the scour depth approached an equilibrium value asymptotically. From the sediment height net change profiles shown in Figure 10, it can be observed that equilibrium is obtained once the scoured bed around the pier is flat.

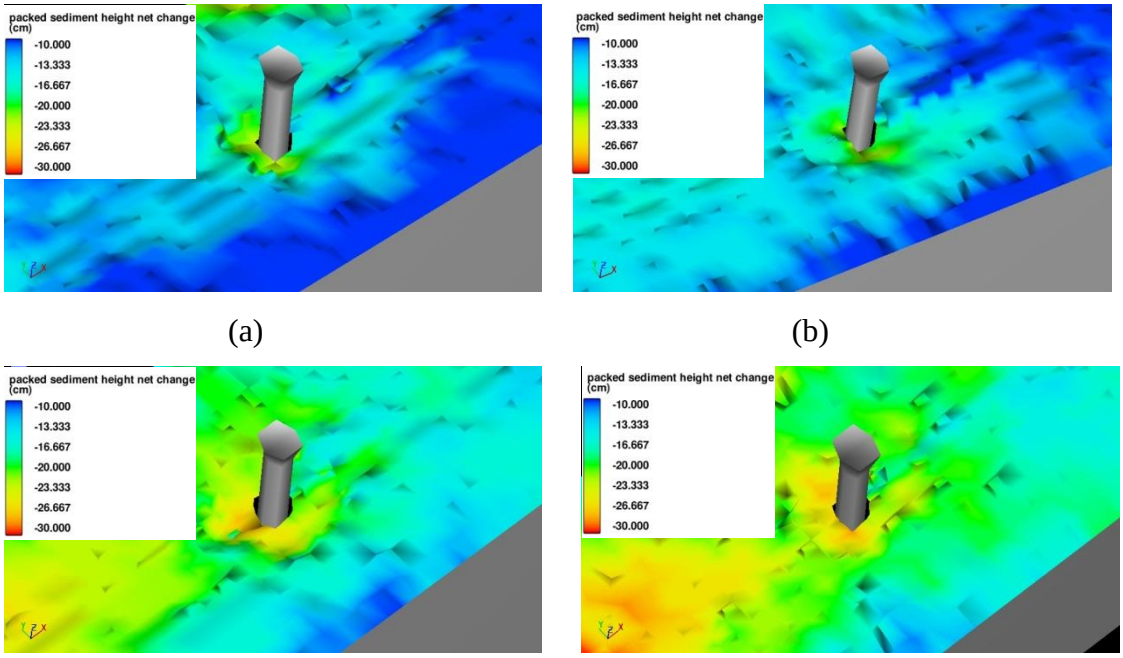

Figure 10. Equilibrium Scour Depth for Flow Velocity (a) 0.88 m/s (b) 1.26 m/s (c) 1.43 m/s and (d) 1.64 m/s

Figure 11 shows scour depth vs flow velocity for live-bed scour. Scour depth values obtained from the numerical simulations agreed well with the laboratory flume testing scour depth values.

EFFECT OF GRADATION ON MAXIMUM SHEAR STRESS AND SCOUR DEPTH

Four different grain size distributions were used to perform numerical simulations, hence understand the effect of gradation, represented by the standard deviation (σ_g) of the grain size distribution the on maximum shear stress, shear stress profile and equilibrium scour depth. The distributions used in the simulations are shown in Figure 12 Geometric Standard deviation (σ) value was varied from 1.14 to 2.0 with a mean soil diameter of d_{50} = 0.32 mm.

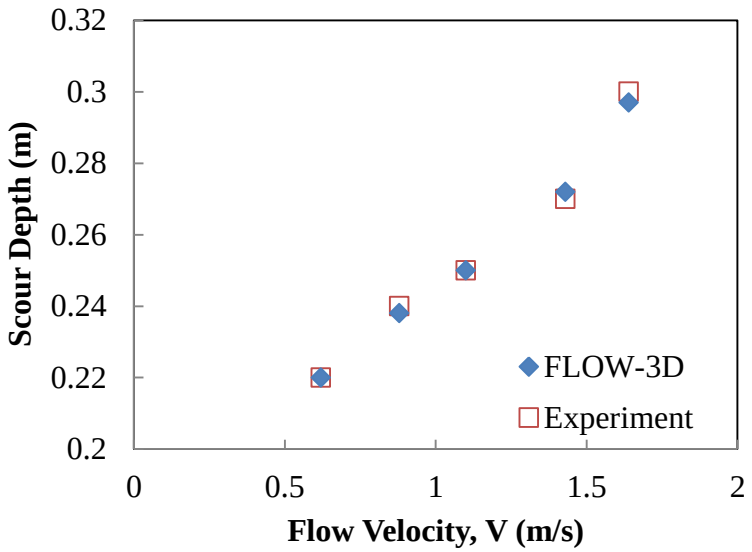

Figure 11. Scour Depth vs. Flow Velocity for Live-Bed Scour

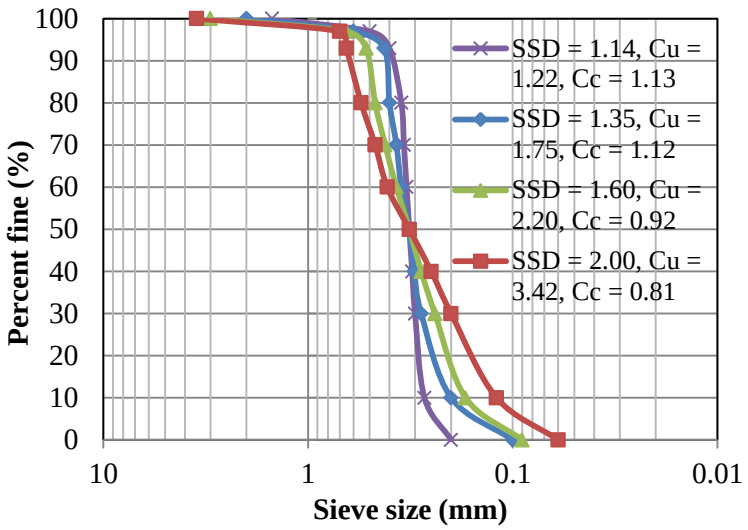

Figure 12. Grain Size Distribution of Four Different Soils with Different Sediment Standard Deviation (SSD)

Four simulations were performed, with the varied parameters presented in Table 1 (simulations No. 11-14). Figure 13 shows the excess shear stress contours for the four SSD values. Results show that the maximum shear stress value that occurs around the pier before scour starts is similar for the four different grain size distributions (but with the same D_{50}) used in the study. Gradation in this case does not have an influence on maximum shear stress before the scour process commences.

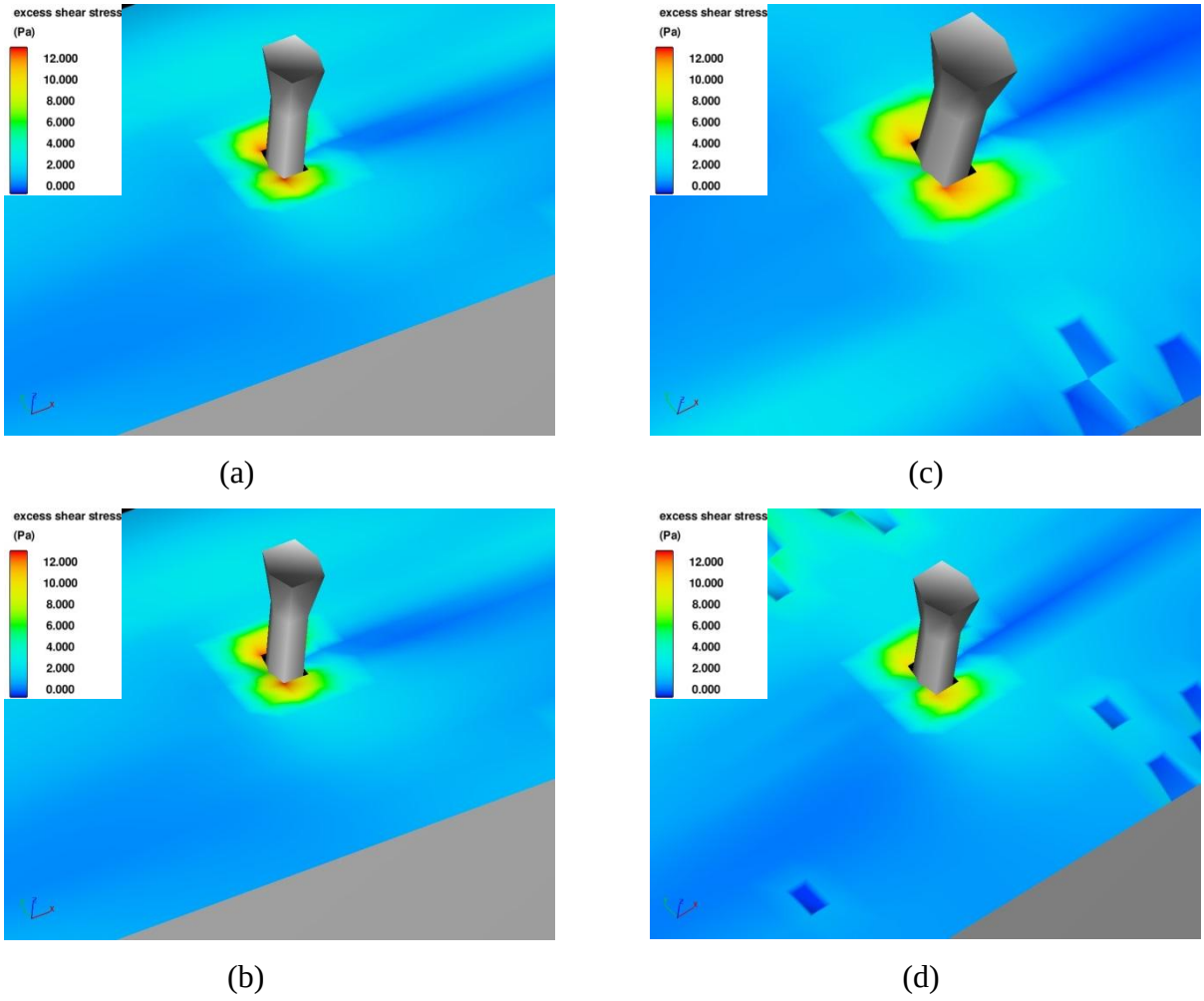

Figure 13. Shear Stress Contours for Live-Bed Scour for Sediment Standard Deviation (a) 1.14 (b) 1.35 (c) 1.6 and (d) 2.0

On the other hand, as shown in Figure 14, with the increase of geometric standard deviation, the scour depth value decreases due to the protection made by the coarser particles as covering material for the finer particles from dislodgement known as "armoring" effect. Ettema et al. (1976) experimentally studied the influence of median grain size (D_{50} =0.55 to 6.0 mm) and gradation (σ/D_{50} upto 1.6) on local scour near a circular pier with pier diameter of 0.1 m and depth of flow 0.6 m. The experiments were carried for clear-water scour. Ettema et al. (1976) found that for σ/D_{50} ratios above 0.3 the scour depth decreases dramatically with the increase of σ/D_{50}. These experiments were performed at or slightly below the critical velocity, so that no general conclusions can be drawn. They concluded that the reduction in scour depth is due to "armoring" effects in the scouring hole. Numerical simulations presented here are performed for live-bed scour. Therefore it can be concluded that maximum scour depth for both live-bed and clear-water scour decreases with the increase of geometric standard deviation.

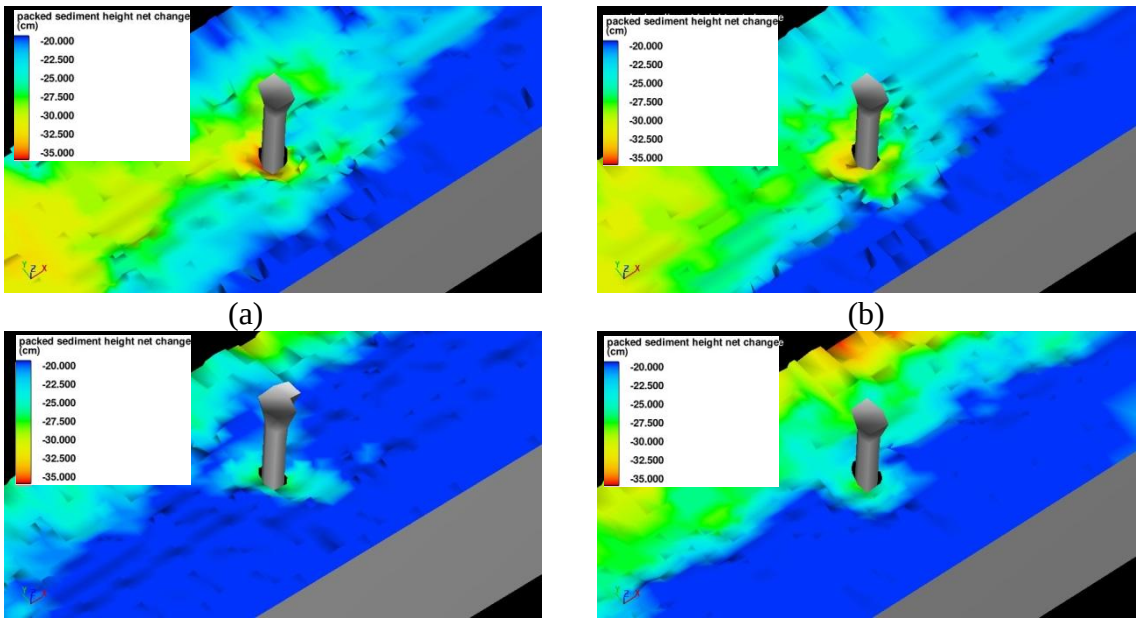

Figure 14. Scour Profile to Understand Effect of Gradation on Equilibrium Scour Depth for SSD (a) 1.14 (b) 1.35 (c) 1.60 and (d) 2.00

Figure 15 shows values of the maximum scour depth decrease with the increase of sediment gradation. From the plot it can be shown that the variation reduces with the increase of standard deviation which is similar to the observation made by Ettema et al. (1976) based on the results from the laboratory flume testing. For an increment of 40% in the sediment standard deviation from a standard deviation value of 1.14, normalized scour depth value decreases about 15%, however this reduction reduces to 7% for an increment in standard deviation of 25% from a value of 2.2.

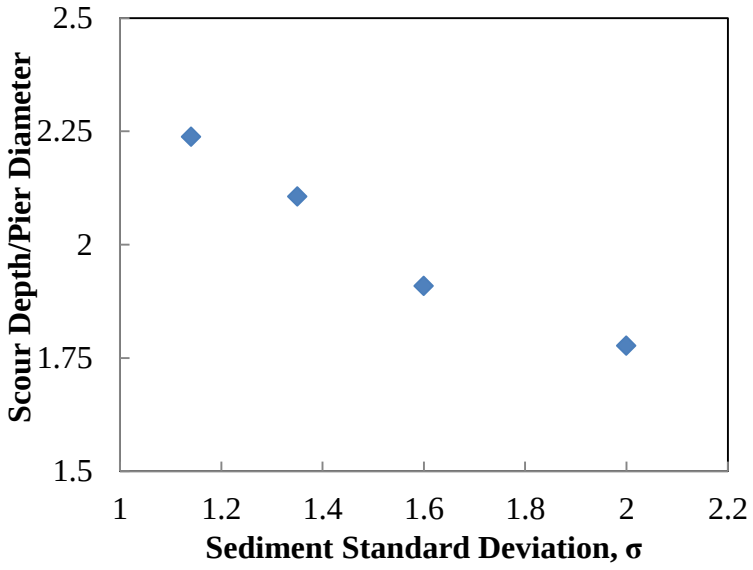

Figure 15. Sediment Standard Deviation vs. Scour Depth

Figure 16 shows that shear stress profile for soils with different sediment standard deviation values. The maximum shear stress value before scour starts in all of the cases is same however it varies afterward. The figure shows that as scour depth increases the shear stress value decreases and for different soil this decrease is different. The critical shear stress value when no more scour happens for different grain size distribution are very close however this value is achieved in different depth for different soils.

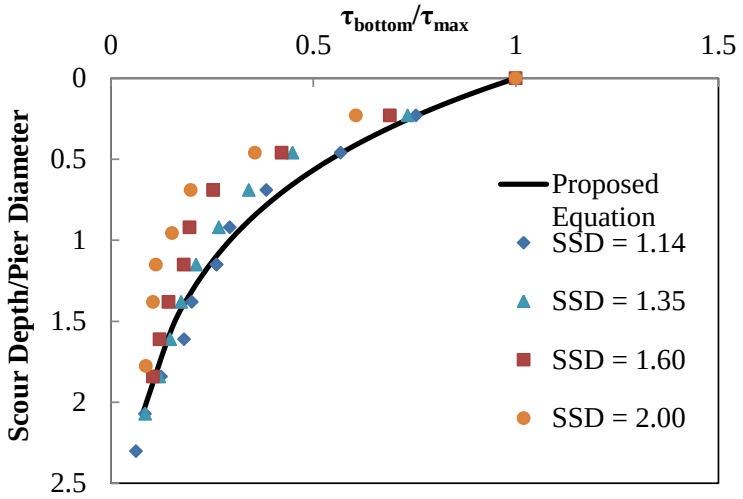

Figure 16. Shear Stress Profile against Normalized Scour Depth for Different Sediment Standard Deviation Values

SUMMARY AND CONCLUSIONS

Bridge pier scour is one of the major reasons for bridge failures. Understanding scour phenomenon around bridge piers is vital for proper assessment of scour potential and erosion rate which are needed to estimate the bridge foundation load carrying capacity. Flow phenomena around cylinders were investigated for live-bed and clear water scour using Computational Fluid Dynamics (CFD) software FLOW-3D. Instead of Reynolds Average Navier Stokes (RANS) model, Large Eddy Simulation (LES) technique was used as it can accurately predict massively separated flows and flows in which large adverse pressure gradient are present. Scour depth values obtained from numerical simulations agreed well with the scour depth values obtained during laboratory tests reported in literature. An equation was proposed to estimate the maximum shear stress around piers before scour starts. The equation was proposed as a function of Reynolds number, mean flow velocity, fluid density and critical shields number. Effect of sediment gradation on the maximum shear stress and scour depth was also investigated for live bed scour. Shear stress profile versus normalized scour depth was obtained from the simulations. Based on the findings of this

study, the following observations are advanced:

a) Shear stress profiles with the progression of scour were presented for live-bed scour by varying flow velocity. The normalized shear stress versus normalized scour depth curve for different flow velocities follow similar trend. Data presented as normalized maximum shear stress versus Reynolds Number that is normalized with respect to the Critical Shields Number allows the estimation off maximum shear stress value using a single equation for both live-bed and clear-water scour
b) Within the scour depth of half of the pier diameter, the reduction of normalized shear stress is very sharp. However this reduction is less pronounced after that depth.
c) Numerical simulations were performed for live-bed scour with four different grain size distributions indicated that maximum shear stress does not change with the change of gradation, however, equilibrium scour depth decreases with the increase of sediment gradation.
d) The maximum shear stress value before scour starts in all of the cases was found to be the same, however, it varies with the progression of scour depth.
e) The decrease of equilibrium scour depth became less pronounced as the geometric standard deviation is increased. With such an increase, the scour depth value decreases due to the protection made by the coarser particles as covering material for the finer particles from dislodgement known as “armoring” effect
f) The shear stress profile for the four simulations followed similar trend, however once scour started the variation in shear stress value increased until the critical shear stress value is reached. This critical value for all of these cases is found to be nearly similar.

REFERENCES

Ali, K. H. M., and R. Karim. Simulation of Flow around Piers. *Journal of Hydraulic Research*, Vol. 40, No. 2, 2002, pp. 161-174.

Briaud, J. -L., F. C. K. Ting, H. C. Chen, Y. Cao, S. -W. Han, and K. Kawk. Erosion Function Apparatus for Scour Rate Predictions. Journal of Geotechnical and Geoenvironmental Engineering, Vol. 127, No. 2, 2001, pp. 105-113.

Brethour, J., and J. Burnham. Modeling Sediment Erosion and Deposition with the FLOW-3D Sedimentation & Scour Model. *Flow Science Technical Note*, FSI-10-TN85, 2010, pp. 1-22.

Engelund, F., and E. Hansen. A Monograph on Sediment Transport to Alluvial Streams. Copenhagen, Tenik Vorlag, 1967.

Ettema, R., Kirkil, G., and Muste, M. (2006). "Similitude of large-scale turbulence in experiments on local scour at cylinders." *J. Hydraul. Eng.*, 132(1), 33–40.

Ettema, R., Constantinescu, G. and Melville, B. (2011). "Evaluation of Bridge Scour Research: Pier Scour Processes and Predictions." NCHRP web-only document 175, Transportation Research Board of the National Academies, Washington, DC.

FLOW-3D (2011). *User Manual*. Flow Science, Inc.

Hirt, C., and J. Sicilian. A Porosity Technique for the Definition of Obstacles in Rectangular Cell Meshes. In *Proc. Fourth International Conf.*, Ship Hydro., National Academy of Science, Washington, D.C., 1985.

Huang, W., Yang, Q., Xiao, H. (2009). CFD modeling of scale effects on turbulence flow and scour around bridge piers. Computers and Fluids 38(5), 1050–1058.

Kirkil, G., S. G. Constantinescu, and R. Ettema (2008). "Coherent structures in the flow field around a circular cylinder with scour hole." Journal of Hydraulic Engineering, 134(5), 572–587.

Koken, M., and G. Constantinescu (2008a). "An investigation of the flow and scour mechanisms around isolated spur dikes in a shallow open channel: 1. Conditions corresponding to the initiation of the erosion and deposition process." Water Resour. Res., 44, W08406.

Koken, M., and G. Constantinescu (2008b). "An investigation of the flow and scour mechanisms around isolated spur dikes in a shallow open channel: 2. Conditions corresponding to the final stages of the erosion and deposition process." Water Resour. Res., 44, W08407.

Lagasse, P. F., E. V. Richardson, J. D. Schall, and G. R. Price. Instrumentation for measuring scour at bridge piers and abutments. National Cooperative Highway Research Program (NCHRP) Report No. 396, Transportation Research Board, Washington, D.C., 1997.

Mastbergen, D. R., and J. H. Van den Berg. Breaching in Fine Sands and the Generation of Sustained Turbidity Currents in Submarine Canyons. *Sedimentology*, Vol. 50, No. 4, 2003, 625-637.

Meyer-Peter, E. and R. Mueller. Formulas for Bed-Load Transport. In. *Proc*. Second Meeting of the International Association for Hydraulic Research, *IAHR, Stockholm*, Sweden, 1948, pp. 39-64.

Melville, B.W., and A.J. Sutherland. Design Method for Local Scour at Bridge Piers. *Journal of Hydraulic Engineering*, Vol. 114, No. 10, 1988, pp. 1210-1227.

Nagata, N., Hosoda, T., Nakato, T. and Muramoto, Y. (2005), "Three dimensional numerical model for flow and bed deformations around river bed structures," Journal of Hydraulic Engineering, ASCE, 131(12), 1074-1087.

Nurtjahyo, P., Chen, H. C., Briaud, J. L., Li, Y. and Wang, J. (2002), "Bed shear stress around rectangular pier: numerical approach," First International Conference on Scour of Foundations, Texas A&M University, TX, 242-256.

Olsen, N. R. B. and Kjellesvig, H. M. (1998), "Three dimensional numerical flow modeling for estimation of maximum local scour depth," Journal Hydraulic Research, IAHR, 36 (4), 579-590.

Olsen, N. B. R., and Melaaen, M. C. (1993), "Three dimensional calculation of scour around cylinders," Journal of Hydraulic Engineering, ASCE, 119 (9), 1048-1054. Chen, H. C. (2002), "Numerical simulation of scour around complex piers in cohesive soil," First International Conference on Scour of Foundations, Texas A&M University,TX.

Raudkivi, A.J., 'Loose Boundary Hydraulics', 3rd Edition, Pergamon Press, 1990, pp. 142-210.

Richardson, J. E., and V. G. Panchang. Three-Dimensional Simulation of Scour Inducing Flow at Bridge Piers. *Journal of Hydraulic Engineering*, Vol. 124, No. 5, 1998, pp. 530-540.

Roulund, A., B. M. Sumer, J. Fredsoe, and J. Michelsen. Numerical and Experimental Investigation of Flow and Scour around a Circular Pile. *Journal of Fluid Mechanics*, Vol. 534, 2005, pp. 351-401.

Salaheldin, T. M., J. Imran, and M. H. Chaudhry. Numerical Modeling of Three Dimensional Flow Field around Circular Piers. *Journal of Hydraulic Engineering*, Vol. 130, No. 2, 2004, pp. 91-100.

Shen, H. W., V. R. Scheider, and S. Karaki. Local Scour around Bridge Piers. *Journal of Hydraulic Engineering*, Vol. 95, No. 6, 1969, pp. 1919-1940.

Sheppard, D. M., and Miller, Jr., W. (2006). "Live-bed local pier scour experiments." J. Hydraul. Eng., 132 (7), 635–642.

Smagorinsky, J. 1963 ‘General circulation experiments with the primitive equations; 1. The basic experiment,’ Mon. Weath. Rev., U.S.W.B., 91, pp. 99–164.

Wei, G., Chen, H. C., Ting, F., Briaud, J.-L., Gudavalli, R., and Perugu, S. (1997). ‘‘Numerical simulation to study scour rate in cohesive soils.’’ *Res. Rep. Prepared for Texas DOT*, Department of Civil Engineering, Texas A&M University, College Station, Texas.

CHAPTER 5
APPLICABILITY OF IN SITU EROSION EVALUATION PROBE (ISEEP) TO FIELD CASES

ABSTRACT: ISEEP is a proposed approach for assessing the soil scour potential with depth through the use of a vertical probe employing a water jet called ISEEP. ISEEP is tested in sand across a range of water velocities and flow rates, and a procedure was proposed for data reduction, based on the stream power approach by Annandale (1995, 2006). Field tests are performed in both marine environment and riverine environment using ISEEP and comparison with the Standards Penetration Test (SPT) data are presented to show the sensitivity of ISEEP measurements to changes in soil density (as reflected by the SPT data). The data reduction approach is described using Penetration rate vs. stream power and critical shields parameter. Soil detachment coefficient is obtained from the penetration rate plots for the different site soils.

INTRODUCTION

Scour evaluation is an integral element in the process of assessing the stability of several types of critical infrastructures during design and post construction stages as well as throughout the structures' operational life. However, within the purview of critical civil infrastructures, the assessment of scour and erosion rates represent a persistent challenge. For example, the occurrence of scour at bridge foundations is considered to be a safety-critical issue; Briaud (2002) suggested that 60 percent of bridge failures in the United States are caused by excess scour at the bridge piers or abutments leading to serious structural damage. Cases where scour evaluation was critically needed for lifelines and flood defense earth structures were cited by Seed et al (2006) after hurricane Katrina. During the design stage, the knowledge of scour potential and depth is critical for specifying and designing various types of foundations and discerning their load carrying capacity. Furthermore, assessment of scour potential and erosion rate is needed for development of maintenance priorities and establishing replacement schedules.

Scour downstream of many hydraulic structures such as culverts and spillways may be treated as analogues to jet scour. Doodiah et al (1953), Sarma (1965), Beltaos, and Rajaratnam (1974), Aderibigbe and Rajaratnam (1997), Hanson et al (2002) and others have all made contributions to this field. Most of these studies were concerned with describing the maximum scour depth, as the jet is held stationary on the surface. There is however little documentation of the erosion behavior produced by a jet that is embedded internally to the material. Niven and Khalili (1998a, 1998b, 2001, 2002) discussed the mechanics and application of vertical, internal jets in a series of papers with their analysis mainly concerned environmental site remediation. In this case, the internal diameter of the jet was 75 mm and it was operated at flow rates on the order 5-13 l/s (80-206 gpm). They showed that jet penetration depth (fluidization zone depth) is proportional to the jet velocity and is a function Froude number.

Bloomquist and Crowley (2010) presented a detail literature review on scour estimation techniques for different types of soils. They depicted that in recent years major scour research focus is not estimation of the maximum scour depth in terms of soil parameters however it focuses on development of relationship between shear stress and erosion rate. Different erosion rate testing devices were described. However, most of these devices are developed for laboratory erosion testing not for field applications. Briaud et al (2001) presented the approach for assessing soil erosion paramters in the laboratory using the Erosion Function Apparatus (EFA). Aberle et al. (2006) presented another approach by limiting the measurements to the exposed surface using inverted flumes. Bloomquist et al. (2012) developed a laboratory tool called RETA (Rotating Erosion Testing Apparatus) to evaluate applied shear stress and soil erosion rate for rock and cohesive soil. In this device sample obtained from field is placed in a cylinder, forming an annular space which is filled with fluid. By rotating the cylinder, torque is produced over the surface area of the soil sample. Shear stress imparted by the flow is evaluated in terms of the torque applied, and measuring eroded soil mass and time duration of the test soil erosion rate was obtained.

For in situ testing of surface layer, Hanson et al. (2002) and Hanson and Cook (2004) presented the resulting stress distribution from impinging jet. This is the case for soils with fines and the data reduction approach was presented on the premise of the excess shear model, where erosion occurs once the shear stresses exceed a critical value. In application of impinging jet, the "potential core" is the part of the jet where water retains its original velocity. At distances greater than the potential core, it is postulated that the velocity decreases linearly with increasing distance from the jet orifice. The shear stress applied to a surface within the potential core of the jet is expressed by Hanson et al. (2002) and Hanson and Cook (2004) as:

$$\tau_o(N/m^2) = C_f \rho U_0^2 \qquad (1)$$

where: τ_o= applied shear stress to bed in N/m^2, U_0 = average velocity of water at the tip (m/s), ρ = density (kg/m^3), and C_f is a friction coefficient = 0.00416

Hanson and Cook (2004) used estimates of the asymptotic state of depth of scour to derive an expression for τ_c. Their ability to accomplish this task was based on the realization by Stein et al. (1993) that, for a fixed jet, as the depth of a scour hole increased, it would reach a depth where the horizontal shear stress becomes equal to τ_c and no more scour takes place.

The rate of erosion is then defined on the basis of the excess shear model, to describe the mass rate of erosion per unit area, or erosion rate (E) as a function of shear stresses exceeding the critical value as follows, Mehta (1991):

$$E = k_d (\tau - \tau_c)^{\alpha} \qquad (2)$$

The k_d coefficient, often called the detachment rate coefficient, and is basically the erosion rate normalized with respect to shear stresses leading to such a rate, and α is usually assumed to be 1 (Hanson and Cook 2004). The Hanson and Cook's approach has been codified as ASTM standard D5852 (ASTM, 1999). On the other hand, Annandale and Parkhill (1995) presented the concept of "Stream Power" as an estimate of the magnitude of the induced flow erosive potential. They indicated this concept is especially useful in the case of turbulent

flow regimes. The input to a system is represented by an applied stream power, P, in Watts per unit area, and is given below for a flow situation with a head drop, H (Annandale, 2006):

$P = \gamma qH$, or in terms of shear stresses as $P = \tau U_o$ (3)

where: P is in the unit of Watts/m^2 (1 Watt = 1 N.m per sec or Kg.m^2 per sec ^{3}), γ = unit weight of water, q = discharge per unit area, and H = energy head, U_o = induced velocity. Annandale (2006) also expressed P in terms of τ for the case of impinging jet and indicated that such an approach accounts for the near boundary turbulent effect and should be used for reducing data from the impinging jet configuration. Based on derivations from the boundary layer theory, Annandale (2006) recommended that the friction factor, C_f (see Equation 1), to estimate the shear stress value, is equal to 0.016.

ISEEP

The impinging jet device used to assess soil erosion potential is termed as In Situ Erosion Evaluation Probe (ISEEP). Figure 1 shows ISEEP setup and cross sectional view of the probe. The probe has a stainless steel body with several removable stainless steel tips. Each section is 1.52 m (5 ft) with a diameter of 50 mm (2.0 inch), so that it may be broken down for transport. The probe has an outer sheathing that is 76 mm (3.0 inch in diameter) with a wall thickness of 1.65 mm (0.065 inches). Different components of the probe and detail test procedure can be found in Gabr et al. (2013).

DATA REDUCTION APPROACH

Figure 2 shows erosion rate vs. stream power plot obtained from data presented Briaud et al. (2014). The data are presented in terms penetration rate and stream power best and the best fitted line using a power function. In this case, the use of the power function yields an r-square value of 0.99 and chi-square value of 7.09; this and chi-square value is lower than the value threshold (see Table 1; Nikulin, 1973) for a degree of freedom of 4 and 95% confidence level. Therefore the values expected falls within the acceptable range.

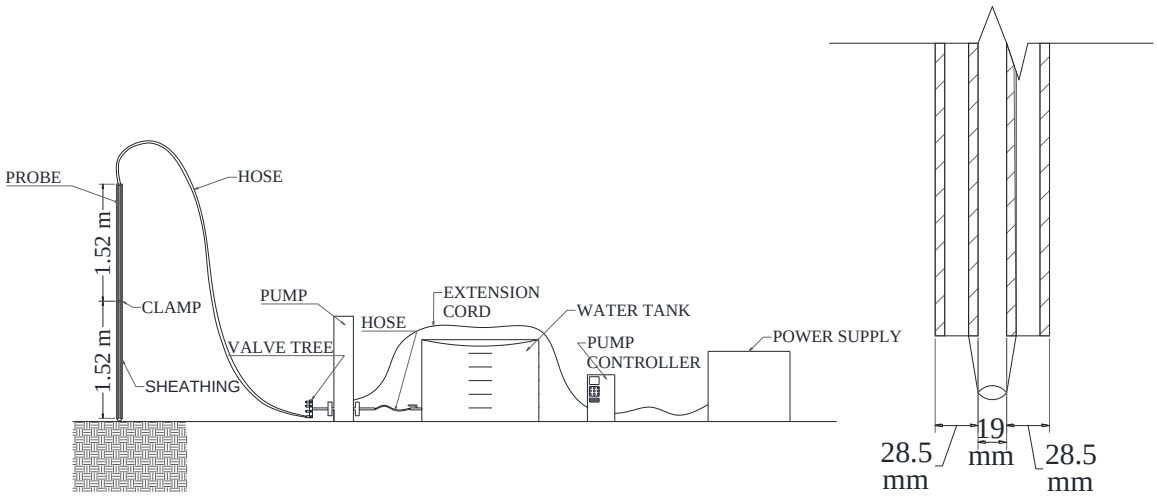

(a) (b)

Figure 1. ISEEP (a) Test Setup and (b) Cross-Sectional View of the Probe with the Tip.

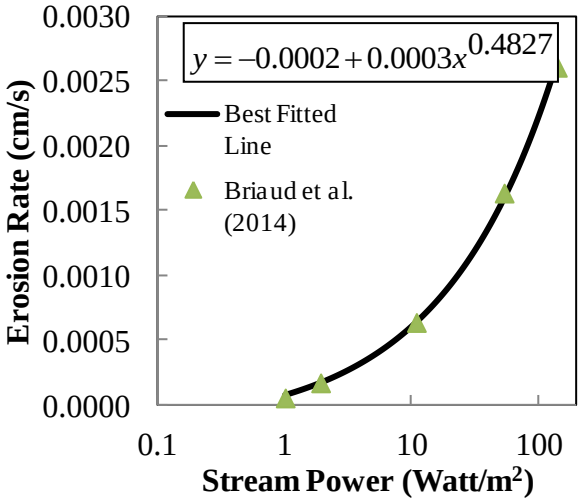

Figure 2. Erosion Rate Versus Stream Power Plot from Briaud et al. (2014) Data with Best Fit Function

Table 1. Chi-Square Test Table (Nikulin, 1973)

df	$\chi^2_{.995}$	$\chi^2_{.990}$	$\chi^2_{.975}$	$\chi^2_{.950}$	$\chi^2_{.900}$	$\chi^2_{.100}$	$\chi^2_{.050}$	$\chi^2_{.025}$	$\chi^2_{.010}$	$\chi^2_{.005}$
1	0.000	0.000	0.001	0.004	0.016	2.706	3.841	5.024	6.635	7.879
2	0.010	0.020	0.051	0.103	0.211	4.605	5.991	7.378	9.210	10.597
3	0.072	0.115	0.216	0.352	0.584	6.251	7.815	9.348	11.345	12.838
4	0.207	0.297	0.484	0.711	1.064	7.779	9.488	11.143	13.277	14.860
5	0.412	0.554	0.831	1.145	1.610	9.236	11.070	12.833	15.086	16.750
6	0.676	0.872	1.237	1.635	2.204	10.645	12.592	14.449	16.812	18.548
7	0.989	1.239	1.690	2.167	2.833	12.017	14.067	16.013	18.475	20.278
8	1.344	1.646	2.180	2.733	3.490	13.362	15.507	17.535	20.090	21.955
9	1.735	2.088	2.700	3.325	4.168	14.684	16.919	19.023	21.666	23.589
10	2.156	2.558	3.247	3.940	4.865	15.987	18.307	20.483	23.209	25.188

Assuming linear relationship between penetration rate and log stream power, Gabr et al. (2013) and, Kayser and Gabr (2013) evaluated critical stream power value by back calculating stream power value from the penetration rate versus stream power plot. However the critical stream power value obtained using this approach was higher than the critical stream power value suggested in the literature. A power function exponential correlation between penetration rate and stream power was observed by including critical stream power value calculated from shields parameter. This is similar to what was observed in Figure 2 from flume test data by Briaud etal (2014). Detail ISEEP data reduction approach is described as follows:

1. Penetration rate for different layers: Penetration rate for different soil layers is obtained from penetration depth versus time plot (see Figure 3).
2. Bed Shear Stress: Shear stress produced by the jet is calculated as:

$$\tau\left(N/m^2\right) = C_f \rho U^2 \qquad (4)$$

where: τ = applied shear stress to bed in N/m^2, U = average velocity of water at the tip (m/s), ρ = density (kg/m^3), and C_f is a friction coefficient = 0.00416

3. Stream Power: Stream power is calculated using the following equation

$$P = \tau U \qquad (5)$$

where: P is in the unit of Watts/m^2 (1 Watt = 1 N.m per sec or Kg.m^2 per sec ^{3}) and U = induced velocity.

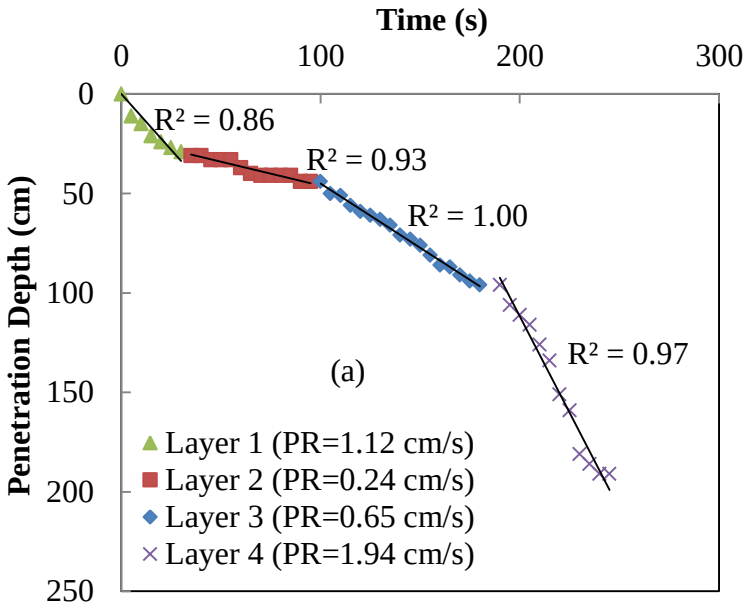

Figure 3. Penetration Versus Depth Plot for a 1400 RPM Test

4. Critical Stream Power: Critical stream power at which no erosion will occur is critical shear stress multiplied by the critical velocity.

$$P_c = \tau_c v_c \qquad (6)$$

Where[1], $\tau_c = D_{50}$ and $v_c = 0.35(D_{50})^{0.45}$

τ_c is in N/m^2, D_{50} is in mm and v_c is in m/s

5. Stream power vs. penetration rate plot: Penetration test should be repeated minimum of three times for three different jet velocities. Along with the critical stream power all testing points for a specific soil layer should be plotted (Figure 4).

6. Erosion rate: The rate of erosion describes the mass rate of erosion per unit area, or erosion rate (E) as a function of stream power exceeding the critical stream power value (P_c) as follows,

$$E = k_d'(P - P_c)^{\alpha} \qquad (7)$$

The k_d' coefficient, often called the detachment rate coefficient, and is basically the erosion rate normalized with respect to stream power leading to such a rate, and α is usually assumed to be 1.

7. Detachment rate coefficient: Detachment rate coefficient (k_d') depends on stream power magnitude. For a given applied stream power value, the detachment rate coefficient (k_d') can be obtained by calculating slope of the best fitted penetration rate versus stream power plot within a zone of the curve that will cover the desired stream power value.
8. Erosion value: For a known applied stream power value and duration of its application, scour depth can be evaluated using equation 7.

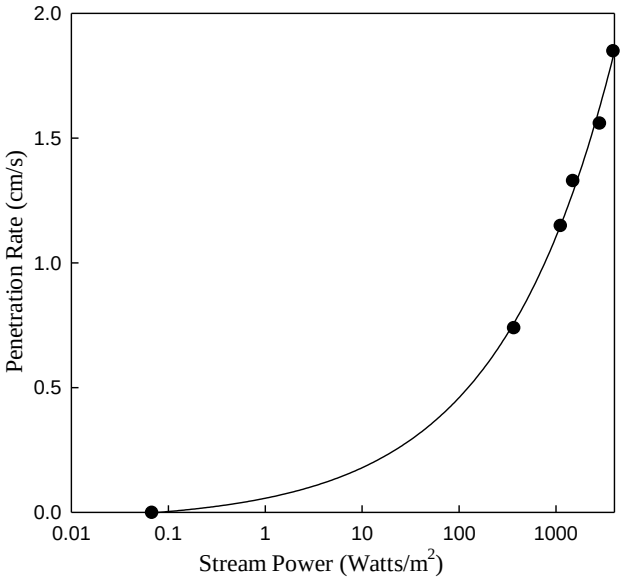

Figure 4. Penetration Rate Versus Stream Power Plot

Figure 5 shows penetration rate variation with the change of best fit function parameters within a range of ±25% to observe the variation of the power function. From the figure it can be observed that the variation is more sensitive to the "b" parameter compared to "a" parameter value. However, compared to the effect of changing the "a" parameter, changing the b parameters by ±25% would lead to significantly lower r-square value.

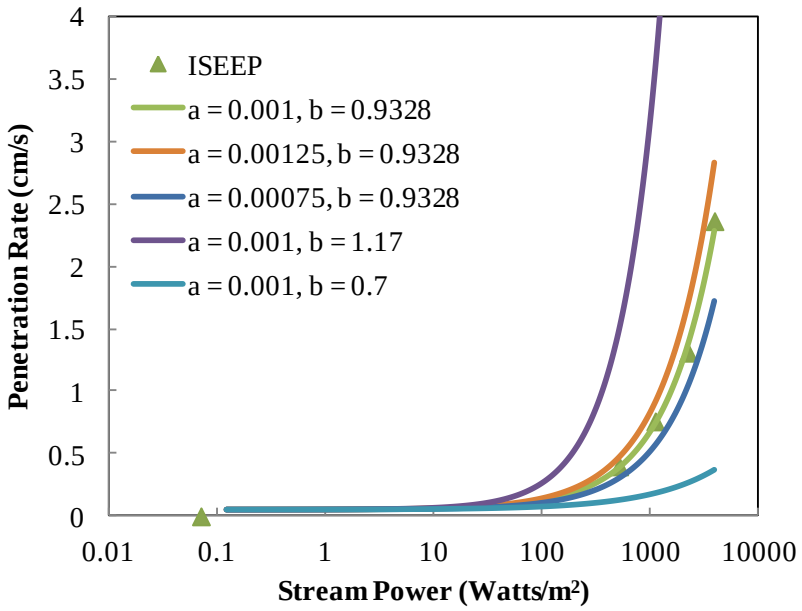

Figure 5. Best Fit Function Variation $y = c + ax^b$ Where c is Constant, a and b are the Best Fit Parameters

ISEEP REPEATABILITY

The precision for measuring soil erosion parameters by the ISEEP method has been determined through the performance of multiple testing under the same conditions. These tests were conducted in the laboratory using a liquefied sand bed, having dimensions of diameter= 3.3m and depth= 6.8 m. Table 2 shows test results for a 60 sec duration experiment performed by ISEEP in the laboratory for a sandy soil. The soil in the laboratory

was a single layered soil and therefore test duration of 60 sec was considered as reasonable to achieve rational penetration rate. The results in Table 2 indicate a Coefficient of variation (COV%) on the average of 2.9% with a one value of approximately 6.5%.

Table 2: Summary of Laboratory ISEEP Testing (Penetration depth for a test duration = 60 sec)

RPM	Velocity (cm/s)	Soil Type	Number of Tests	Average Value (cm)	Standard Deviation (cm)	Coefficient of variation (COV%)
1400	285	SP	4	59.00	1.58	2.68
1600	324	SP	4	74.00	2.55	3.45
1800	374	SP	4	85.00	1.87	2.20
2000	425	SP	5	98.70	2.68	2.72
2200	453	SP	3	119.33	7.72	6.47
2800	580	SP	3	143.67	2.49	1.74
3400	710	SP	3	152.67	1.25	0.82

FIELD TEST SITES

Field testing with ISEEP was performed in both marine and riverine environment in North Carolina. In collaboration with North Carolina Department of Transportation and the Coastal Studies Institute, ISEEP tests were performed in the following six locations:

Marine Environment:

a) Outer banks - Pea island,

b) Jennett's Pier,

c) Costal Studies Institute (CSI) campus,

Riverine Environment:

a) Lake Wackena Road Bridge in Goldsboro city- Wayne County,

b) Moore county bridge

MARINE ENVIRONMENT

TEST LOCATIONS AND SOIL PROPERTIES

Field testing locations in the marine environment are shown on the google map (Figure 6). One of the field testing was conducted at outer banks barrier island site, along NC-12, that was breached during Hurricane Irene. The occurrence of Hurricane Irene led to the erosion of 274 m (900 ft) section of NC 12. Figure 7 shows Pea Island field testing locations (left photo; with a temporary bridge installed) and the ISEEP set up (right photo) prior to the testing at the same location.

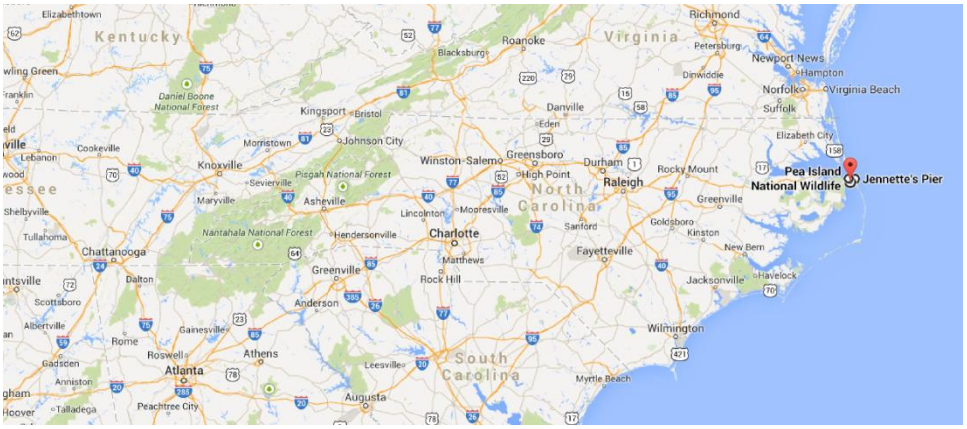

(a)

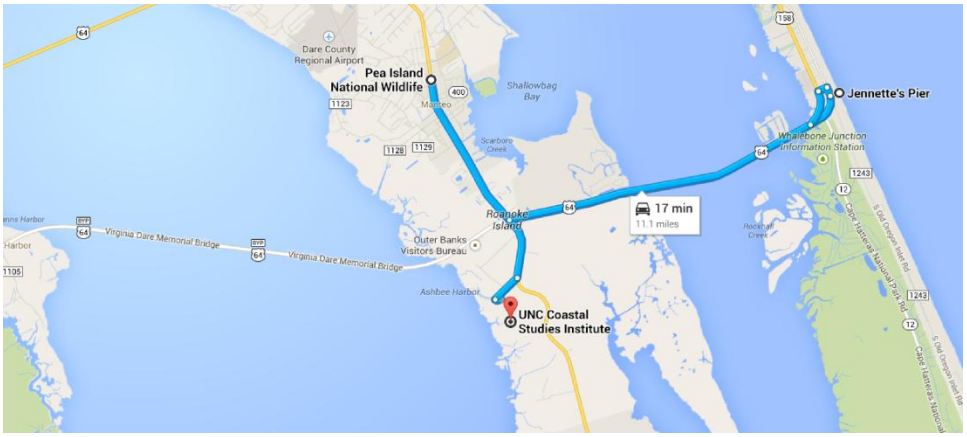

(b)

Figure 6. Map Showing (a) Location of the ISEEP Marine Test Sites (b) Zoomed Locations.

Field tests were also performed at Jennett's pier (Nags Head, NC) and Coastal Studies Institute (CSI) campus in North Carolina. Figure 8 shows Jennett's pier and CSI campus test sites.

Figure 7. Location of Breach along NC-12 and Set Up for Testing using ISEEP

(a) (b)

Figure 8. (a) Jennett's Pier and (b) CSI Campus Site

The grain size distribution for the Pea Island soil is shown in Figure 9 (a). The test soil at the site has a D_{50} of 0.32 mm with some of the samples include organic materials and shells; these yielded an indication of a coarser distribution, as shown in Figure 9 (a). The sand is poorly graded with a coefficient of uniformity of approximately 1.5. According to NCDOT (2011) the sand is described as loose, gray, fine sand (A-3) with uncorrected N-value of 20 blows per foot near the surface reducing to zero at a depth of 4.5m. Figure 9 (b, c) shows the grain size distribution of Jennett's Pier and CSI campus site soils, respectively. These show D_{50} = 0.2 mm for the bottom layer and 0.3 mm for the top layer. At the CSI test site, a very stiff organic layer was observed. The organic content after the layer broke up is visually shown in figure 9 (d). In both sites the sand is poorly graded with a coefficient of uniformity of approximately 1.4 and 1.7, for Jennett's Pier and CSI campus sites, respectively.

TEST RESULTS

Following the data reduction approach presented earlier, the critical stream power and detachment rate coefficient values were obtained from the field data. Figure 10 shows the penetration rate versus stream power plot for the three test sites. Detachment coefficient can be obtained by calculating slope of the best fitted power plot within a relatively zone of the curve that corresponds with the desired stream power value. From the penetration rate vs. stream power plot for Pea Island for a stream power value of 5 Watts/m^2 the detachment rate coefficient value of 0.0217 Watts/m^2 is computed, for example. Due to the existence of organic materials in the bottom soil layer, a low detachment coefficient value is observed with the advancement of the probe for the Jennett's pier testing location. Similarly low detachment coefficient value is obtained for the middle soil layer in CSI campus site.

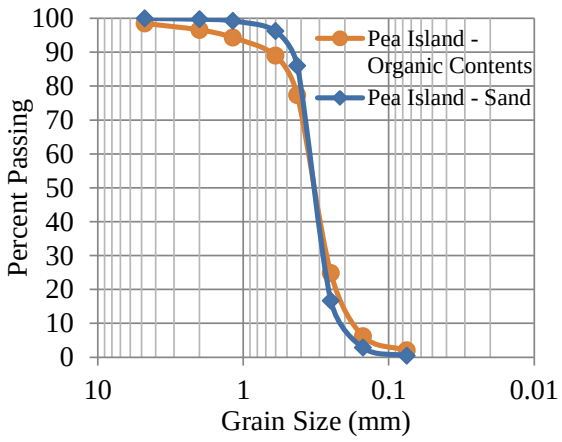

(a)

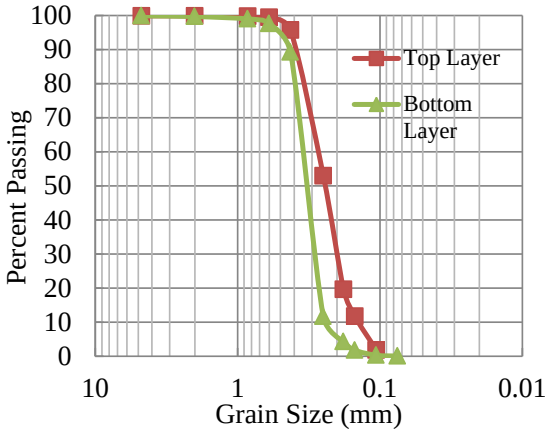

(b)

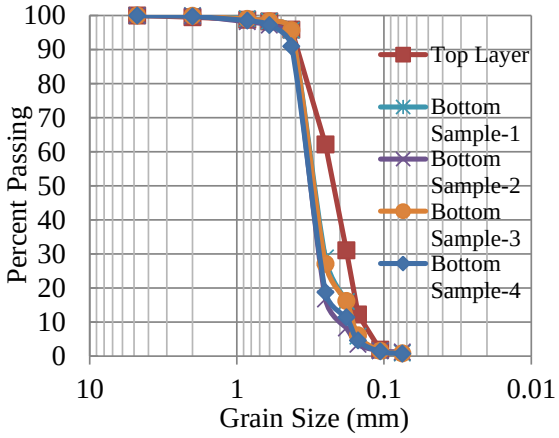

(c)

(d)

Figure 9. Grain Size Distribution of (a) Pea Island, (b) Jennett's Pier, (c) CSI Campus Soil and (d) Stiff Organic Soil in CSI Campus

RIVERINE ENVIRONMENT

TEST SITE AND SOIL CONDITIONS

Field tests were also performed in riverine locations in the North Carolina area. By collaborating with North Carolina Department of Transportation (DOT) field tests were performed in two different locations shown on Figure 11. Figure 12 shows ISEEP test setup in the field. In these test sites, significant vegetations were observed on the top soil layer.

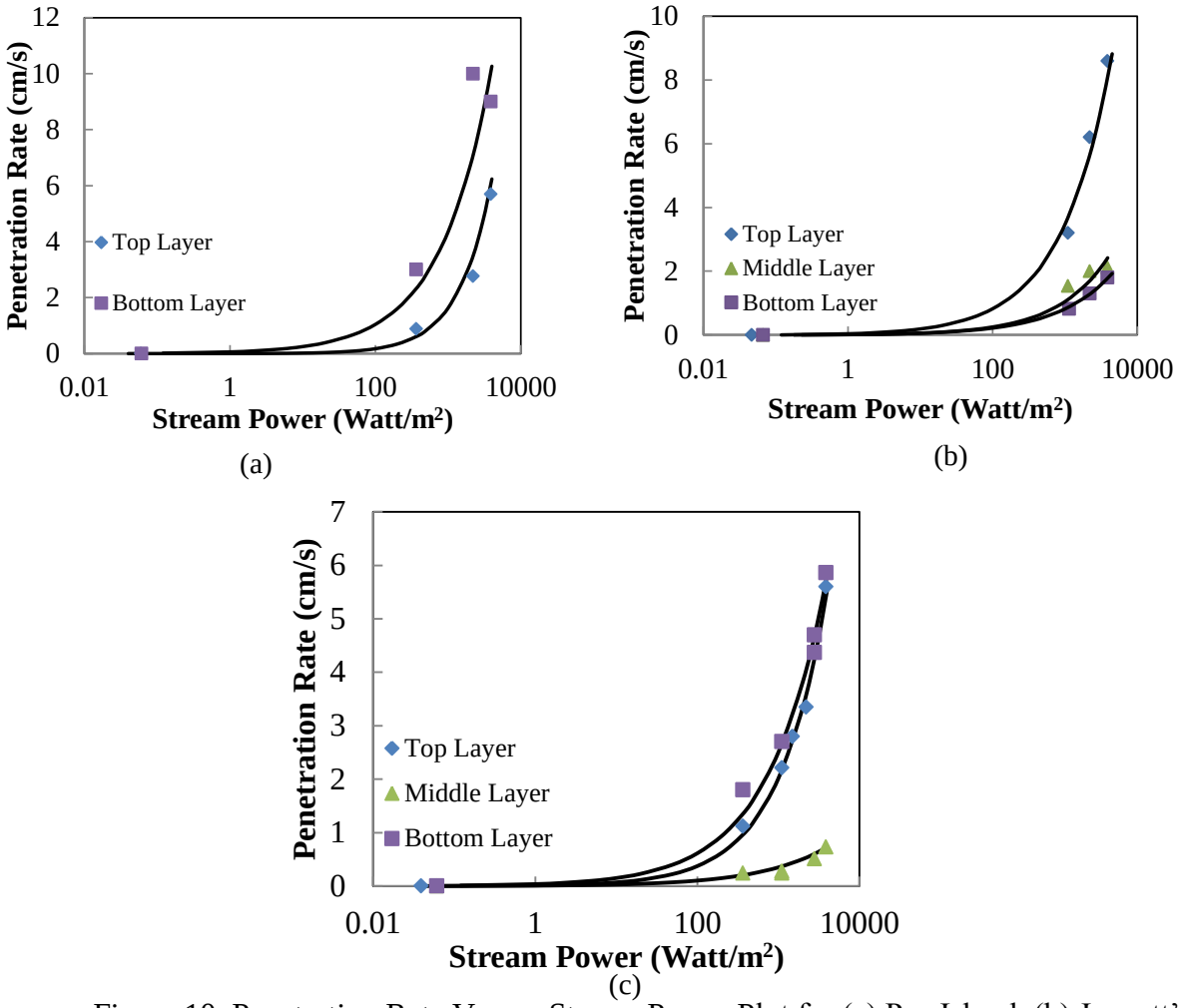

Figure 10. Penetration Rate Versus Stream Power Plot for (a) Pea Island, (b) Jennett's Pier, (c) CSI Campus

Figure 13 shows grain size distribution of the two test sites. Mean diameter (D_{50}) for Goldsboro, NC site varied within a range of 0.3 mm to 0.45 mm and the soil is poorly graded. The soil observed at the Moore County site has a D_{50} of 0.47 mm and is well graded with a Cc higher than 1 and Cu greater than 6.

Figure 11. Locations of the ISEEP Field Test Sites (A) 1728 Lake Wackena Rd, Goldsboro, NC 27534 (B) 3968 Cypress Church Rd, Cameron, NC 28326

(a)

(b)

Figure 12. (a) Goldsboro, NC and (b) Moore County, NC Field Test Site

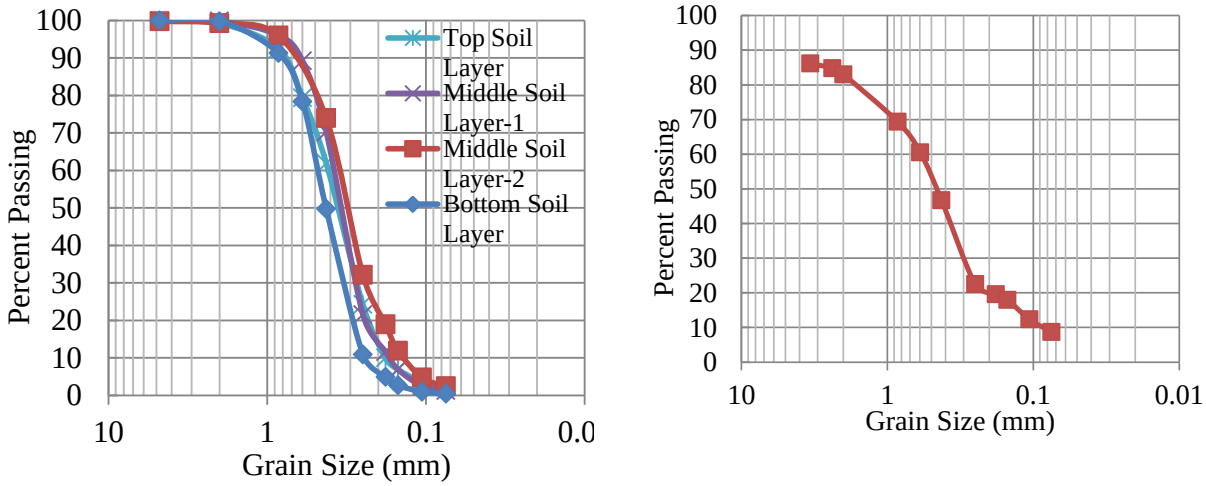

Figure 13. Grain Size Distribution of (a) Goldsboro, NC and (b) Moore County, NC

TEST RESULTS

Figure 14 shows penetration rate vs. stream power plot for the two test sites. High detachment coefficient values are observed for the middle soil layer in Goldsboro site. For

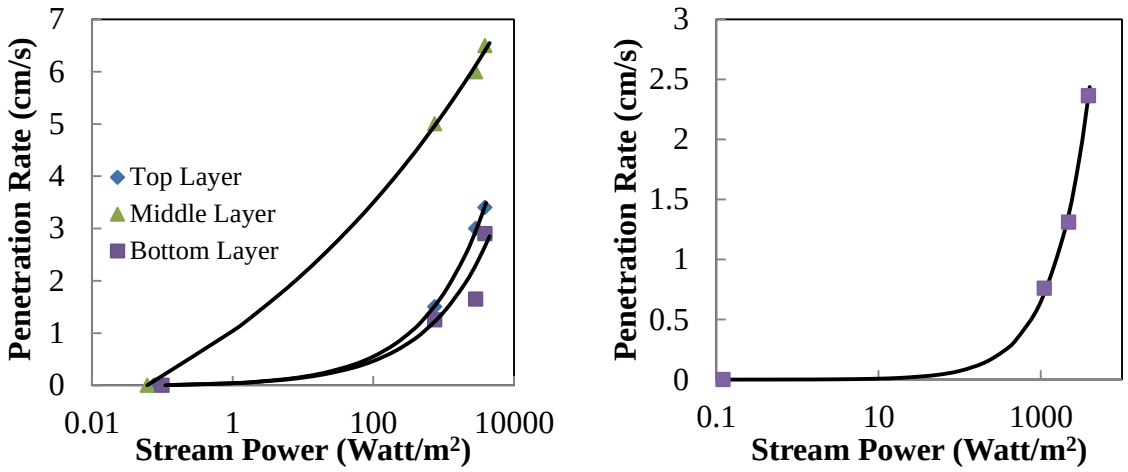

(a) (b)

Figure 14. Penetration Rate Versus Stream Power Plot for (a) Goldsboro, NC and (b) Moore County, NC

top and bottom layers the detachment coefficient values are close. Since no variation in soil was observed in the Moore county field site, a single stream power vs. penetration plot was obtained.

COMPARISON OF ISEEP WITH EROSION FUNCTION APPARATUS (EFA)

Figure 15 shows a comparison of erosion rate versus stream power using Erosion Function Apparatus (EFA) developed by Briaud et al. (2001) and ISEEP data from Jennett's pier and Goldsboro sites. In this case, none of the field sites clearly matched with Briaud et al. (2001) estimated scour depth. Even though for most of these sites the mean particle diameter was very much similar within a range of 0.3 to 0.35, however densities might be different which can lead to difference in ISEEP data as will be shown later.

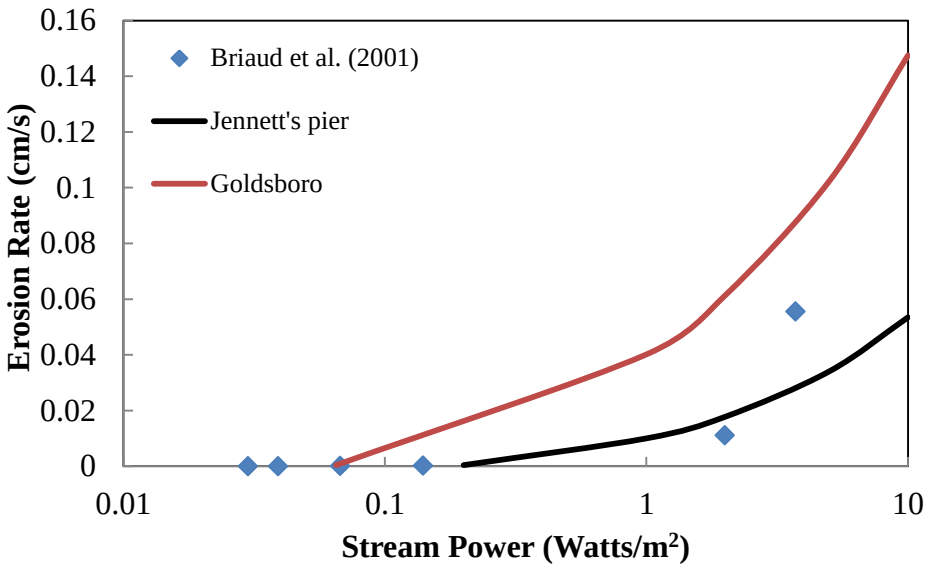

Figure 15. Erosion Rate against Stream Power Plot for EFA and ISEEP Field Sites

PENETRATION RATE VERSUS CORRECTED SPT N VALUE

SPT N values of the CSI campus and Goldsboro sites were the only data available for the test sites. These values were corrected to account for the effect of overburden pressure on

penetration. Figure 16 and 17 show ISEEP's penetration rate versus SPT N value for different stream power values for the Goldsboro and CSI campus field test sites. For both sites, with the increase of corrected SPT N value the probe's rate of penetration decreases. The increase in N value reflects the increase of soil density, and therefore in this case the soil erosion parameters are influenced by the soil density, in addition to the grain size distribution.

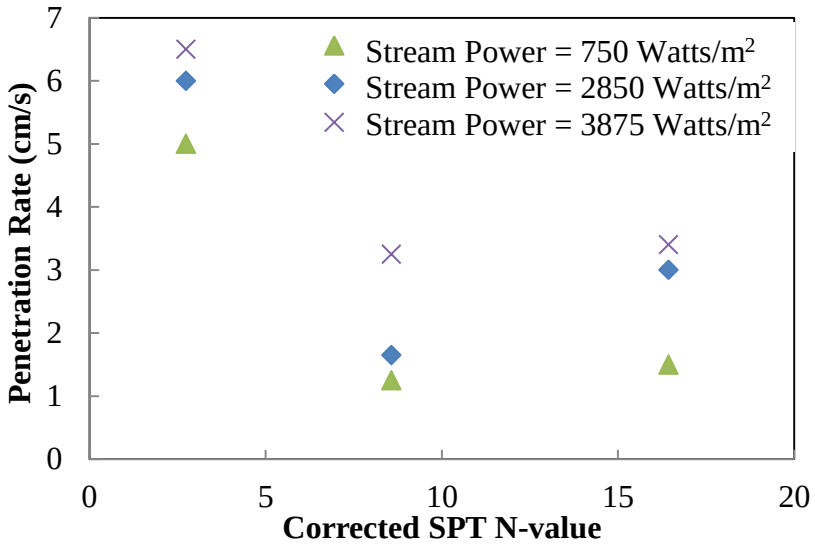

Figure 16. Corrected SPT N Value Versus Penetration Rate Goldsboro Site

DEPENDENCY ON COEFFICIENT OF CURVATURE AND COEFFICIENT OF UNIFORMITY

The coefficient of uniformity and coefficient of curvature represents the gradation of soil. The criteria for well graded soils are $C_u \geq 6$ & $1 < C_c < 3$. Other than Moore county test site soil, all of the test site soils are poorly graded. Figure 18 shows relationship between Cc and Cu with detachment coefficient for three different stream power values. From these figures no clear correlation can be observed.

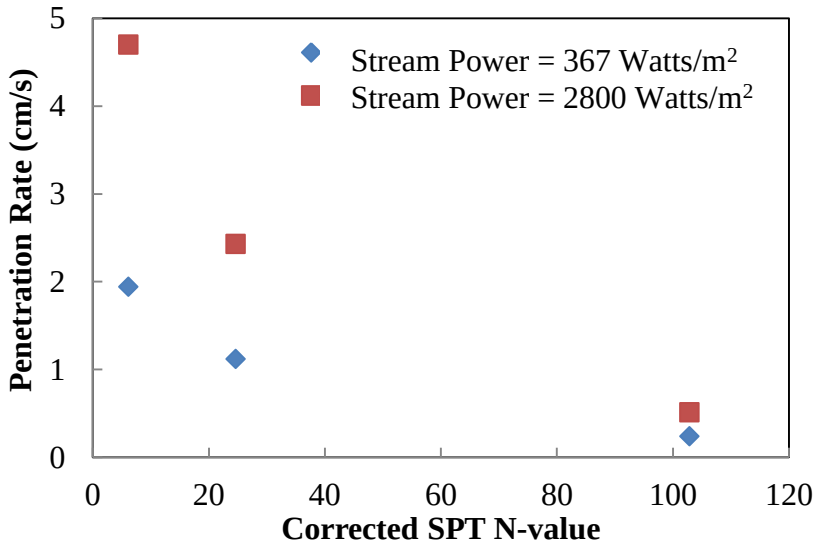

Figure 17. Corrected SPT N Value Versus Penetration Rate CSI Site

ISEEP EXAMPLE APPLICATION

Kayser and Gabr (2014) performed extensive numerical study to understand the flow around bridge piers. They proposed equations to calculate maximum shear stress before scour starts and normalized shear stress profile equation to calculate shear stress around pier with the progression of scour. For a pier diameter (D) bed shear stress, (τ) a scour depth (S) can be found using following equation

$$S / D = 248.4(1-(\tau / \tau_{Max})^{3.3E-3}) \quad (8)$$

$$\tau_{Max} = 0.5\rho u^2 (\frac{R_e}{\theta})^{-0.29} \quad (9)$$

ρ is density of water, u is approaching flow velocity, R_e is Reynolds number and θ is critical shields parameter. Knowing the critical stream power and detachment coefficient value from the field erosion rate vs. stream power plot erosion rate can be calculated using equation 7.

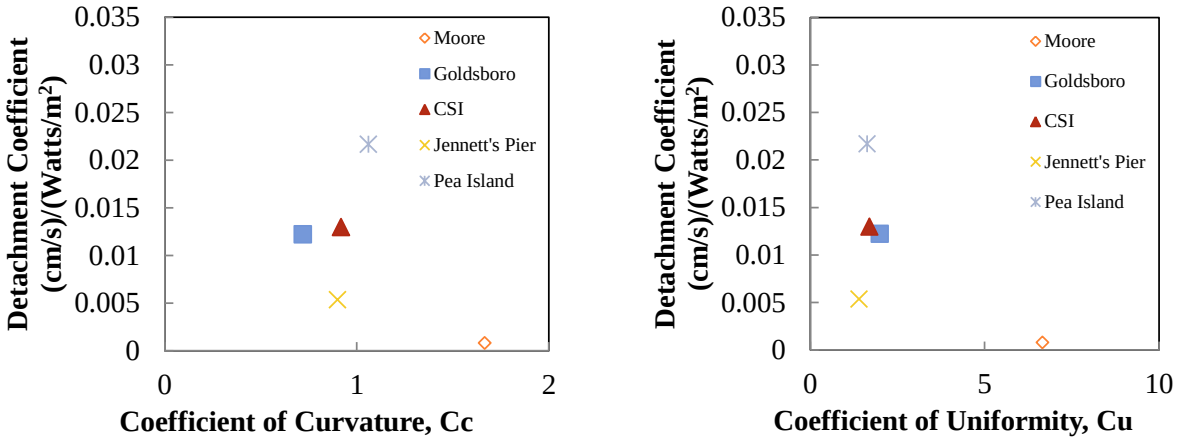

(a) Stream Power = 5 Watts/m^2

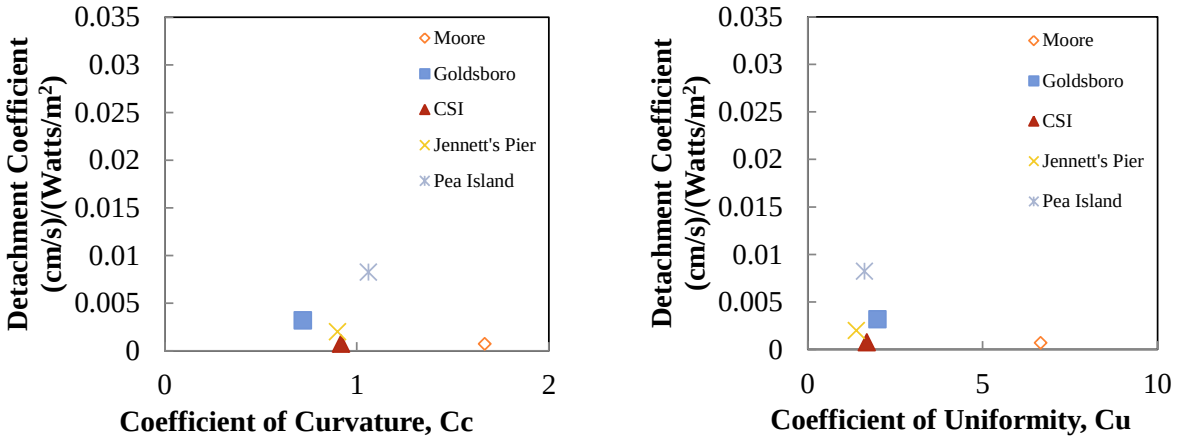

(b) Stream Power = 50 Watts/m^2

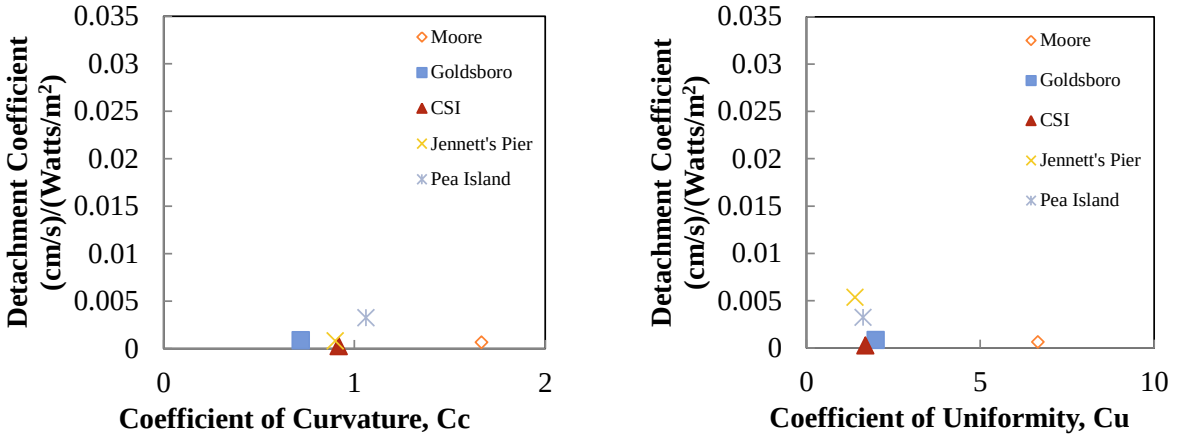

(c) Stream Power = 500 Watts/m^2

Figure 18. Detachment Coefficient Versus Coefficient of Curvature and Coefficient of Uniformity for Different Stream Power Values

Using small time steps, scour depth can be obtained hence the shear stress at that depth can be obtained using equation 8. Repeating these steps total scour depth after a certain time can be obtained. Federal Highway Administration (FHWA) referred following equation, proposed by Oliveto and Hager (2002), to estimate temporal scour depth for clear water scour condition

$$\frac{y_s(t)}{b^{2/3}h^{1/3}} = 0.068\frac{H^{1.5}}{\sqrt{\sigma}}\ln\frac{t\sqrt{(\rho_s/\rho - 1)gD_{50}}}{b^{2/3}h^{1/3}} \qquad (10)$$

Where, $y_s(t)$ scour depth at time, t, b is pier diameter, h is depth of flow, σ is sediment gradation effect, ρ_s is soil density, ρ is water density, g is gravitational acceleration, D_{50} is mean particle diameter and H is Froude number which was described as

$$H = \frac{V}{\sqrt{(\rho_s/\rho - 1)gD_{50}}} \qquad (11)$$

Where V is approaching flow velocity.

For a pier of diameter = 0.5 m, depth of flow = 0.4 m, $\rho_s/\rho = 2.65$, $D_{50} = 0.3$ mm, $\sigma = 1.5$ and known time, t scour depth can be calculated using Oliveto and Hager (2002) equation. Approach flow velocity was varied from 0.25 m/s to 0.5 m/s. Since Oliveto and Hager (2002) equation is valid for clear water scour condition higher flow velocity was not used. Two major assumptions made in this study are D_{50} for all test sites and Oliveto and Hager (2002) equation are 0.3 mm and flow duration for ISEEP field sites, and Oliveto and Hager (2002) equation is same. Since Moore county field site had a D_{50} different than 0.3 mm it is not shown here for comparison. Scour depth comparison between ISEEP and Oliveto and Hager (2002) equation is shown in figure 19. From the figure it shows the equation proposed by Oliveto and Hager (2002) is almost linear however for all the field sites ISEEP estimates same scour depth i.e. equilibrium scour depth is reached at 0.5 m/s.

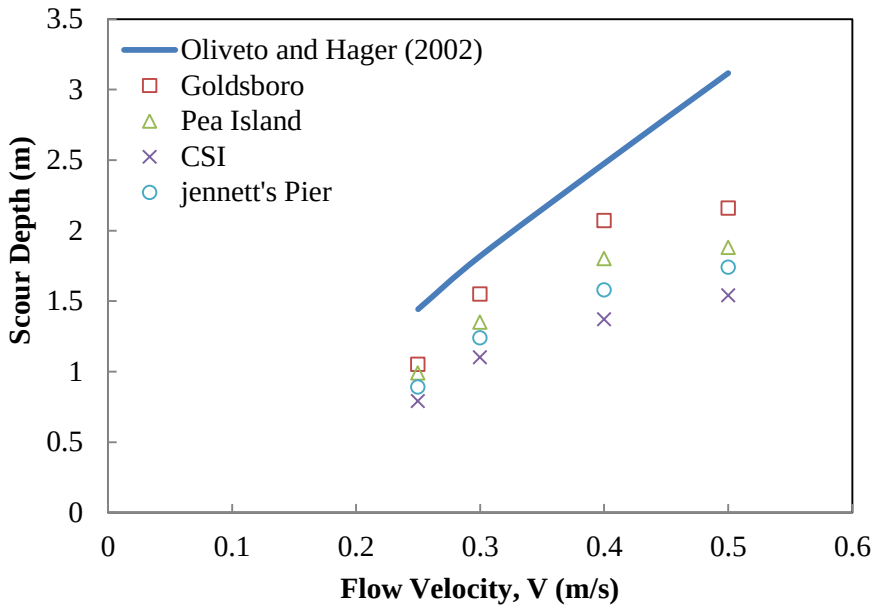

Figure 19. Comparison of ISEEP with Oliveto and Hager (2002) Equation

SUMMARY AND CONCLUSIONS

Gabr et al. (2013) proposed an approach for assessing the scour potential with depth through the use of a vertical probe employing a water jet called ISEEP. The device was tested in sand across a range of water velocities and flow rates. This study described the data reduction approach of ISEEP data using power function to fit the penetration rate versus applied stream power data and the critical shields parameter to estimate the critical stream power value. Field testing was conducted at five sites with SPT data available to compare with ISEEP data at two sites. Penetration rate vs. stream power plot was developed and soil erosion parameters i.e. critical stream power and detachment coefficient were presented. Correlations between penetration rate and soil parameters were explored. Dependency of penetration rate on SPT N values was also explored. Field deployment served to illustrate the viability of performing the approach and collect data to estimate erosion parameters. Based on the findings of this study, the following observations are advanced:

1. Testing has been conducted in both marine and riverine locations on sand since these types of soils are the most difficult to sample in the field. The ISEEP approach provided various penetration rates of the probe with increasing jet velocity for the different profiles.
2. The rate of advancement of the probe provided an indication of the erosion potential of the soil. The data reduction approach illustrated the viability of assessing soil erosion parameters for all the field sites ISEEP was able to predict different penetration rate for different soil layer. ISEEP estimated detachment coefficient values agreed relatively well with the field SPT N values. With the increase of SPT N value penetration rate decreased for the field test soils. Since SPT N values depends on the density of soil, the ISEEP data seems to reflect changes in density as well.
3. Correlation between ISEEP estimated penetration rate and soil's grain size distribution parameters was explored. However no relationship between penetration rate and soil parameters i.e. coefficient of uniformity and coefficient of curvature was observed.
4. An example problem to calculate scour depth was presented using soil erosion parameters estimated using ISEEP and an empirical equation in literature. The equation proposed by FHWA shows a linear relationship between scour depth and velocity. It has been found that ISEEP data yield a non-linear relationship between scour depth and flow velocity. Such a relationship is more in line with data presented in literature based on flume testing (Shen et al. (1969), Melville (1975), Melville and Sutherland (1988), Melville and Coleman (2000)).

REFERENCES

Aderibigbe, O. and Rajaratnam, N., 1997, "Erosion of Loose Beds by Submerged Circular Impinging Vertical Turbulent Jets," *Journal of Hydraulic Research/De Recherches Hydrauliques*, Vol. 35, No. 4, pp. 567-574.

Annandale, G. W. and Parkhill, D. L., 1995, "Stream Bank Erosion: Application of the Erodibility Index Method," *International Water Resources Engineering Conference Proceedings*, Vol. 2, pp. 1570-1574.

Annandale, G.W., 2006, Scour Technology: Mechanics and Practice, McGraw Hill, New York, pp. 430.

ASTM Standard D5852-95, 1999, "Standard Test Method for Erodibility Determination of Soil in the Field or in the Laboratory by the Jet Index Method," *Annual Book of ASTM standards*, Vol. 04.08, ASTM International, West Conshohocken, PA, pp. 686-690.

Beltaos, S. and Rajaratnam, N., 1974, "Impinging Circular Turbulent Jets," *Journal of Hydraulic Engineering*, Vol. 100, No. 10, pp. 1313-1328.

Bloomquist, D., Sheppard, M., Schofield, S. and Crowley, R. 2012, "The Rotating Erosion Testing Apparatus (RETA): A Laboratory Device for Measuring Erosion Rates versus Shear Stresses of Rock and Cohesive Materials." *Geotechnical Testing Journal*, Vol. 35, No. 4, pp. 641-648.

Bloomquist, D. and Crowley, R. (2010). "Enhancement of FDOT's SERF device and a study of erosion rates of rock, sand, and clay mixtures using FDOT's RETA and SERF equipment." Final Report No. BDK75 977-09, Florida DOT, Tallahassee, FL.

Briaud, J. L., Ting, F., Chen, H. C., Han, S.-W. and Kwak, K (2001). "Erosion function apparatus for scour rate prediction." *J. Geotech. Geoenviron. Eng*., 127 (2), 105–113.

Briaud, J. L., 2002, TTI Researcher, V38, #4.

Briaud, J. L., 2014, Time Rate of Scour at Bridges: A Method Including Soil Properties, *J. Geotech. Geoenviron. Eng*., Accepted.

Doddiah, D., Albertson, M. L., and Thomas, R., 1953, "Scour from Jets," *Proceedings Minnesota International. Hydrology Convention*, International Association for Hydraulic Research, Minneapolis, 161–169.

Gabr, M., Caruso, C., Key, A. and Kayser, M. 2012. Assessment of In Situ Scour Profile in Sand Using a Jet Probe. *Geotechnical testing journal*, 36 (2), 0149-6115.

Guo, J., Suaznabar, O., Shan, H. and Shen, J. (2012). "Pier Scour in Clear-Water Conditions with Non-Uniform Bed Materials." FHWA-HRT-12-022, Federal Highway Administration, Washington, DC.

Hanson, G. J., Robinson, K. M., and Cook, K. R., (2002), 'Scour Below an Overfall: Part 2. Prediction', *Transactions of the American Society of Agricultural Engineers*, 45 (4), 957-64.

Hanson, G. J. and Cook, K. R., 2004, "Apparatus, Test Procedures, and Analytical Methods to Measure Soil Erodibility in Situ," *Applied Engineering in Agriculture*, Vol. 20, No. 4, pp. 455-462.

Hanson, G. J. and Hunt, S. L., 2007, "Lessons Learned Using Laboratory Jet Method to Measure Soil Erodibility of Compacted Soils," *Applied Engineering in Agriculture*, Vol. 23, No. 3, pp. 305-312.

Hanson, G. J., Robinson, K. M., and Cook, K. R., 2002, "Scour Below an Overfall: Part II. Prediction," *Transactions of the American Society of Agricultural Engineers*, Vol. 45, No. 4, pp. 957-964.

Kayser, M. and Gabr, M., 2014, "Development of Maximum Shear Stress Equation and Shear Stress Profile: Numerical Approach." To be submitted.

Mehta, A. J., 1991, "Review Notes on Cohesive Sediment Erosion," In: N.C. Kraus, K.J. Gingerich, and D.L. Kriebel, (eds.), Coastal sediment '91, *Proceedings of Specialty Conference on Quantitative Approaches to Coastal Sediment Processes*, pp. 40–53.

Melville, B.W. *Local Scour at Bridge Sites*. Report No. 117, University of Auckland, School of Engineering, Auckland, New Zealand, 1975.

Melville, B.W., and A.J. Sutherland. "Design Method for Local Scour at Bridge Piers." *Journal of Hydraulic Engineering*, Vol. 114, No. 10, 1988, pp. 1210-1227.

Melville, B.W., and S.E. Coleman. *Bridge Scour.* Water Resources Publications, LLC, USA, 2000.

Nikulin, M.S. (1973). "Chi-squared test for normality". In: *Proceedings of the International Vilnius Conference on Probability Theory and Mathematical Statistics*, v.2, pp. 119–122.

Niven, R. K. and Khalili, N., 1998a, "In Situ Fluidization by a Single Internal Vertical Jet," *Journal of Hydraulic Research*, Vol. 36, No. 2, pp. 199-228.

Niven, R. K. and Khalili, N., 1998b, "In Situ Multiphase Fluidization (" Upflow Washing") for the Remediation of Hydrocarbon Contaminated Sands," *Canadian Geotechnical Journal*, Vol. 35, No. 6, pp. 938-960.

Niven, R. K., 2001, "In Situ Fluidization for Solids Addition to Permeable Reactive Barriers," *2001 International Containment and Remediation Technology Conference and Exhibition*, Orlando, FL, June, pp. 10-13.

Niven, R. K., and Khalili, N., 2002, "In Situ Fluidization for Peat Bed Rupture, and Preliminary Economic Analysis," *Journal of contaminant hydrology*, Vol. 59, No. 1-2, pp. 67-85.

Oliveto, G., and Hager, W. H. (2002). "Temporal evolution of clear-water pier and abutment scour." *J. Hydraul. Eng.* , 128 (9), 811–820.

Sarma, K. V. N., 1965, "Simple Empirical Formula for Scour under Vertical Jets," *Irrigation and Power (India),* Vol. 22, No. 1, pp. 27-33.

Seed, R. B., and 34 others, 2006, "Investigation of the Performance of the New Orleans Flood Protection Systems in Hurricane Katrina on August 29, 2005," Report to National Science Foundation under Grants No. CMS-0413327 and CMS-0611632.

Shen, H. W., V. R. Scheider, and S. Karaki. "Local Scour around Bridge Piers." *Journal of Hydraulic Engineering*, Vol. 95, No. 6, 1969, pp. 1919-1940.

Shields, A., 1936, Anwendung der aenlichkeitsmechanik und der turbulenzforschung auf die geschiebebewegung. Mitteilungen der Preussischen Versuchsanstalt fur Wasserbau und Schiffbau, Berlin, Germany, translated to English by W. P. Ott and J. C. van Uchelen, CalTech, Pasadena, CA.

Smith, A. (2003) "Jetting Techniques for Pile Installation and Environmental Impact Minimization," M. S. Thesis, North Carolina State University, Raleigh, 155pp.

Stein, O. R., Alonso, C. V., and Julien, P. Y., 1993, "Mechanics of Jet Scour Downstream of a Headcut," *Journal of Hydraulic Research,* Vol. 31, No. 6, pp. 723-738.

Vardoulakis, I., Stavropoulou, M., and Papanastasiou, P., 1996, "Hydro-mechanical Aspects of the Sand Production Problem," *Transport in Porous Media,* Vol. 22, pp. 225–244.

CHAPTER 6
SUMMARY AND CONCLUSIONS

An approach for assessing the scour potential with depth is proposed through the use of a vertical probe employing a water jet. The probe, termed ISEEP, has been tested in sand across a range of water velocities and flow rates. One advantage of ISEEP is the ability to quickly deploy it and collect data (less than an hour once on site), and being self-contained with all equipment necessary fitting well in a full size Van. A proposed procedure for data reduction, based on the stream power approach by Annandale (1995, 2006), is presented. Results from large scale laboratory testing, field testing and modeling using sand as the test soil are presented and discussed. Field deployment served to illustrate the viability of performing the approach and collect data to estimate erosion parameters. An illustrative example is presented demonstrating the application of the proposed approach for assessing erosion depth. Based on the findings of this study, the following observations are advanced:

1. The viability of obtaining various penetration rates of the probe with increasing jet velocity is demonstrated. The rate of advancement was correlated to the vertical velocity of the water and provides an indication of the erosion potential of the soil.
2. The probe is capable of applying various velocities at the same flow rate as well as various flow rates at the same velocity through changing the size of the jet orifice. This feature is important when erosion through "cutting" versus particle mobilization is induced as in the case of fine grained soils.
3. The combined probe and outer sheathing has a weight of approximately 15 kg per m. Assuming a dynamic coefficient of friction of 0.25-0.35, at 1m depth, the skin friction force is estimated equal to 7-10 kg. The probe is in continuous movement and the amount of skin friction force is estimated to be less than the weight of the probe for the test sand. A stick-slip behavior was however observed at times. The issue of skin friction is being further assessed at this time.
4. The data reduction approach illustrated the viability of obtained soil erosion parameters in terms of critical stream power and modified detachment coefficient. Testing has been conducted in sand since these types of soils are the most difficult to

sample in the field and the simpler to test in a laboratory setting with reconstituted samples.

The CFD software, FLOW-3D, is used to study the potential scour magnitude at a bridge pier with soil properties obtained from a site at a North Carolina Outer Banks site where a breach occurred during Hurricane Irene in 2011. The variation in scour depth with the change in flow velocity (i.e., stream power) is examined by varying the drag, entrainment, and bed load coefficients. Based on field test results, the detachment rate coefficient and the critical stream power are estimated using ISEEP test data. The bed shear stress values are obtained from FLOW-3D analyses, and the scour depth is calculated based on ISEEP data using an excess stream power approach. Based on the parameters and findings of this study, the following observations are advanced:

1. The rate of probe advancement is correlated to jet velocity, and erosion parameters are provided for two subsurface layers. The data reduction approach illustrates the viability of defining soil erosion parameters in terms of critical stream power and modified detachment rate coefficients for the two-layer system at the test site.
2. The parametric analyses indicate that among the parameters commonly used to define scour depth, the entrainment coefficient has the largest effect and the drag coefficient has the smallest effect on the estimated scour depth.
3. The scour depths estimated using ISEEP parameters agree relatively well with values obtained from the 3-D numerical analyses, as these estimates were obtained by accounting for the changes in the properties of the subsurface sand layers. The ISEEP-estimated depth measurements best match with those of FLOW-3D for C_e, C_d and C_b values of 0.009, 2 and 4, respectively.
4. For the case study presented herein, the empirical equations considered in the analysis yield smaller estimates of the scour depth at the pier compared to those from the numerical analysis. These equations do not explicitly account for the variation in soil properties in terms of depth and do not have a provision for a layered soil system or time-dependent scour rate.

Bridge pier scour is one of the major reasons for bridge failures. Understanding scour phenomenon around bridge piers is vital for proper assessment of scour potential and erosion rate which are needed to estimate the bridge foundation load carrying capacity. Flow phenomena around cylinders were investigated for live-bed and clear water scour using Computational Fluid Dynamics (CFD) software FLOW-3D. Instead of Reynolds Average Navier Stokes (RANS) model, Large Eddy Simulation (LES) technique was used as it can accurately predict massively separated flows and flows in which large adverse pressure gradient are present. Scour depth values obtained from numerical simulations agreed well with the scour depth values obtained during laboratory tests reported in literature. An equation was proposed to estimate the maximum shear stress around piers before scour starts. The equation was proposed as a function of Reynolds number, mean flow velocity, fluid density and critical shields number. Effect of sediment gradation on the maximum shear stress and scour depth was also investigated for live bed scour. Shear stress profile versus normalized scour depth was obtained from the simulations. Based on the findings of this study, the following observations are advanced:

1. Shear stress profiles with the progression of scour were presented for live-bed scour by varying flow velocity. The normalized shear stress versus normalized scour depth curve for different flow velocities follow similar trend. Data presented as normalized maximum shear stress versus Reynolds Number that is normalized with respect to the Critical Shields Number allows the estimation off maximum shear stress value using a single equation for both live-bed and clear-water scour
2. Within the scour depth of half of the pier diameter, the reduction of normalized shear stress is very sharp. However this reduction is less pronounced after that depth.
3. Numerical simulations were performed for live-bed scour with four different grain size distributions indicated that maximum shear stress does not change with the change of gradation, however, equilibrium scour depth decreases with the increase of sediment gradation.
4. The maximum shear stress value before scour starts in all of the cases was found to be the same; however, it varies with the progression of scour depth.

5. The decrease of equilibrium scour depth became less pronounced as the geometric standard deviation is increased. With such an increase, the scour depth value decreases due to the protection made by the coarser particles as covering material for the finer particles from dislodgement known as “armoring” effect.
6. The shear stress profile for the four simulations followed similar trend, however once scour started the variation in shear stress value increased until the critical shear stress value is reached. This critical value for all of these cases is found to be nearly similar.

Gabr et al. (2013) proposed an approach for assessing the scour potential with depth through the use of a vertical probe employing a water jet called ISEEP. The device was tested in sand across a range of water velocities and flow rates. This study described the data reduction approach of ISEEP data using power function to fit the penetration rate versus applied stream power data and the critical shields parameter to estimate the critical stream power value. Field testing was conducted at five sites with SPT data available to compare with ISEEP data at two sites. Penetration rate vs. stream power plot was developed and soil erosion parameters i.e. critical stream power and detachment coefficient were presneted. Correlations between penetration rate and soil parameters were explored. Dependency of penetration rate on SPT N values was also explored. Field deployment served to illustrate the viability of performing the approach and collect data to estimate erosion parameters. Based on the findings of this study, the following observations are advanced:

1. Testing has been conducted in both marine and riverine locations on sand since these types of soils are the most difficult to sample in the field. The ISEEP approach provided various penetration rates of the probe with increasing jet velocity for the different profiles.
2. The rate of advancement of the probe provided an indication of the erosion potential of the soil. The data reduction approach illustrated the viability of assessing soil erosion parameters for all the field sites ISEEP was able to predict different penetration rate for different soil layer. ISEEP estimated detachment coefficient values agreed relatively well with the field SPT N values. With the increase of SPT N

value penetration rate decreased for the field test soils. Since SPT N values depends on the density of soil, the ISEEP data seems to reflect changes in density as well.

3. Correlation between ISEEP estimated penetration rate and soil's grain size distribution parameters was explored. However no relationship between penetration rate and soil parameters i.e. coefficient of uniformity and coefficient of curvature was observed.
4. An example problem to calculate scour depth was presented using soil erosion parameters estimated using ISEEP and an empirical equation in literature. The equation proposed by FHWA shows a linear relationship between scour depth and velocity. It has been found that ISEEP data yield a non-linear relationship between scour depth and flow velocity. Such a relationship is more in line with data presented in literature based on flume testing (Shen et al. (1969), Melville (1975), Melville and Sutherland (1988), Melville and Coleman (2000)).

CHAPTER 7
FUTURE WORK

Estimation of Skin Friction around the Probe

A penetration friction model will be developed to account for the skin friction around the probe surface during penetration. Since the sand is often saturated, an effective stress approach similar to the Beta Method will be used here for a first approximation of the frictional force per unit area. Skin friction zone around the probe will be estimated by subtracting the scoured zone from the probe embedment. Soil erosion rates estimated by ISEEP with and without skin friction will be compared. Friction is one of the controlling forces on the kinetic behavior of the ISEEP.

The model for studying the frictional force on the probe in the test pit is similar to that used in calculation of skin friction of a pile in sand. As the probe is buried in the test pit, the unit frictional resistance will increase approximately linearly with depth to a depth between 10 and 20 times the diameter of the probe. For depths greater than 10 and 20 times the diameter of the probe, the unit value of frictional force will remain constant per classical approaches (Kezdi, 1975). There are several different cases that will be investigated based on the location of the water table. The end-member cases are where the soil is dry and where the soil is saturated.

For data collected with the ISEEP, the assumption is made that the sand around the probe will be in the active condition; that is, the sand is being displaced toward the probe. The reason for this is that as the probe enters the sand, the size of the hole excavated by the water jet is slightly larger than the size of the shroud.

The friction force per unit surface area in contact with soil between the soil and the probe can be described using a sliding friction model as given in Coduto (2000):

$$f_s = \sigma'_x \tan \phi_f \qquad \text{Equation 1}$$

where: f_s = unit side friction, σ_x' = horizontal effective stress, $\tan \phi_f$ = coefficient of friction between soil and probe. This model can be rewritten as shown in equation of Coduto (2000) as:

$f_s = K_0 \sigma'_z (K/K_0) [\tan(\phi'(\phi_f/\phi'))]$ Equation 2

where: f_s = unit side friction, σ_z' = vertical effective stress, K_0 = coefficient of lateral earth pressure before probe is inserted, K = coefficient of lateral earth pressure after probe is inserted, ϕ_f = soil-probe interface angle, and ϕ' = effective friction angle of the soil. The ratios of ϕ_f/ϕ' and K/K_0 can be found in Coduto (2001). For friction angle values between soil and the smooth steel of the probe, ϕ_f/ϕ', values between 0.5 and 0.7 are suggested in Coduto (2001). f_s multiplied by the surface area in contact with the soil will give the skin friction.

Scour Assessment for Different Structures with ISEEP

Using ISEEP estimated data, numerical simulations were performed to simulate bridge pier foundation scour. However, ISEEP has not been used to assess scour in other types of critical structures, for example levee and floodwalls. During high water rise incidents, levees and floodwalls provide protection to large areas and protect the areas from inundation. Therefore, understanding scour mechanism in levee system is vital. ISEEP will be used to estimate soil erosion parameters for levee system and FLOW-3D will be used to simulate levee overtopping (Figure 1). Numerical simulation will help to understand the mechanism of levee scour during overtopping and identify the most vulnerable location of a levee during storm surge.

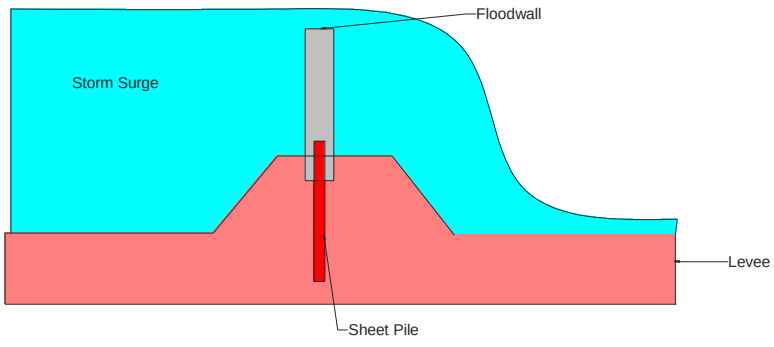

Figure 1. Levee Overtopping

APPENDIX

Standard Test Method for Erodibility Parameters Determination of Soil in the Field by the In Situ Erosion Evaluation Probe

1. Scope

1.1 This test method describes the process for in situ assessment of erosion potential with depth by employing a device In Situ Erosion Evaluation Probe (ISEEP). Tests can be performed either in a field site or in a laboratory peat for the determination of the erodibility of soil.

1.2 The jet flow velocity and the advancement rate of the probe are correlated with a stream power value, and used to estimate soil erodibility parameters critical stream power and detachment rate coefficient.

1.3 Units-The values stated in SI units are to be regarded as the standard. The values given in parentheses are for information only.

1.4 *This standard does not purport to address all of the safety concerns, if any, associated with its use. It is the responsibility of the user of this standard to establish appropriate safety and health practices and determine the applicability of regulatory limitations prior to use.*

2. Referenced Documents

2.1 *ASTM Standards:*

D 422 Test Method for Particle-Size analysis of Soils

D 653 Terminology Relating to Soil, Rock, and Contained Fluids

D 698 Test Methods for Laboratory Compaction Characteristics of Soil Using Standard Effort (12400 ft-lbf/ft^3 (600kN-m/m^3))

D 854 Test Methods for Specific Gravity of Soil Solids by Water Pycnometer

D 1140 Test Methods for Amount of Material in Soils Finer than No. 200 (75-μm) Sieve

D 1557 Test Methods for Laboratory Compaction Characteristics of Soil Using Modified Effort (56,000 ft-lbf/ft^3 (2,700 kN-m/m^3))

D 2216 Test Methods for Laboratory Determination of Water (Moisture) Content of Soil and Rock by Mass

D 2487 Practice for Classification of Soils for Engineering Purposes (Unified Soil Classification System)

D 2488 Practice for Description and Identification of Soils (Visual-Manual Procedure)

D 5852 Standard Test Method for Erodibility Determination of Soil in the Field or in the Laboratory by jet Index Method

3. Terminology

3.1 *Definitions:*

3.1.1 For standard definitions of common technical terms, refer to Terminology D653.

4. Significance and Use

4.1 Increased flow events such as storm surges or alteration of the river's channel cause increased stresses on the bottom of the rivers channel resulting in increased removal of material from the bottom of the channel. This increased loss of sediment is a type of erosion called scour.

4.2 During operational lifetime, assessment of scour potential and erosion rate is needed for development of maintenance priorities and establishing replacement schedules. Within the purview of civil infrastructures, the assessment of scour and erosion rates is critical not only for bridge foundations but also for other structures such as culverts, dams, levees, and stream banks.

4.3 Current techniques for assessing in situ erosion potential with depth require either removal of soil samples for laboratory testing or limiting the measurements to the surface of the sediment. However undisturbed sandy soil is difficult to collect and there is no in-situ technique to predict soil erosion for layered soil system. ISEEP can predict in-situ soil erosion for layered cohesionless soil system.

4.4 Tests in laboratory or field site need to be performed in saturated soil condition.

5. Apparatus

5.1 Probe: The probe is a stainless steel body. Each probe section is 1.52 m (5 ft) with a diameter of 50 mm (2.0 inch), so that it may be broken down for transport.

5.2 Tip: Tips are also made with stainless steel. Several tips and configurations can be used to obtain different flow rates. Three different types of tips can be used for testing, a 1/8 inch orifice in a 60° conical tip, a flat-topped tip with 6-1/4 inch orifices and a 1/2 inch orifice in a 60° conical tip. These tips can cover a velocity range from 2 to 12 m/s, which also corresponds to jet Reynolds number between 5000 and 155,000.

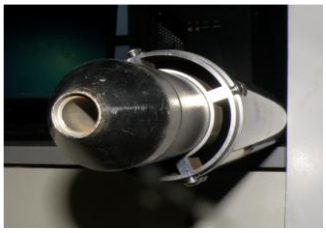

(a) Scale 1 cm = 0.05 m (b) Scale 1 cm = 0.20 m (c) Scale 1 cm = 0.05 m

Figure 1. Probe with (a) Outer Shroud, (b) Bottom end and (c) Tips

5.3 Speed Controller: The ITT PumpSmart pump controller controls the rotational speed of the pump and is calibrated in RPM. Determination of the relationship between pump rpm and the water velocity at the tip of the pump is required before starting tests. This can be done by measuring the flow rate at the probe's tip first and then converting it into water velocity.

5.4 Flow Pump: The flow pump is a Gould GLSSV2 variable speed centrifugal pump coupled to the variable speed controller. The system is capable of applying a flow rate of 2000 ml/sec (32 gpm) and velocities as high as 12 m/s depending on the tip size.

5.5 Sheathing: During testing the probe refuses to penetrate much below 1 m unless the site soil is completely saturated. In the fully saturated case, the probe tends to free-fall into the sand of the peat as the sand becomes fluidized by the water jet. This behavior suggests that an over-pressurized zone built up within the sand and when water flow ceased, the decreasing pressure allows the probe to settle into the formerly pressured region. Therefore

an outer sheathing that is 76 mm (3.0 inch) in diameter with a wall thickness of 1.65 mm (0.065 inch) should be used to dissipate the pore water pressure in the tip area.

5.6 Tripod: To support the shrouded ISEEP a new, larger tripod made of steel is required. The tripod needs to support a probe that could be up to 20 feet tall and weighing in excess of 200 pounds. It should have an upper and a middle shelf and is primarily used to guide the ISEEP during setup and as it enters the soil.

5.7 Valve Tree: Ball valves and hose segments for returning water to the supply tank should be used. Several different ball valve configurations can be tried until water velocities below 1 m/s are obtained. The valve configuration dives the flow in half using a 2-way valve and then divide the flow by 4 using a 4-way valve. In all cases, unused water returns to the tank. Calibration runs should be performed relating pump rpm and valve configuration to water velocity at the nozzle. Using the valve tree the available upper velocity can be decreased to about 6 m/s. The decrease in the upper velocity occurs because the valves do not have the same internal diameter as the rest of the discharge system of the pump.

5.8 Hose: Two long hoses are required for ISEEP setting. One hose needs to be connected from the tip of the probe to the flow pump and the other one needs to be connected from the water source to the tank. First hose should have an inside diameter equal to that of the tip diameter.

5.9 Stopwatch: To determine an average flow rate at a given rpm of the pump, a stopwatch can be used to determine the amount of time necessary to pass a known volume of water.

5.10 Camera: Penetration depth timing with the stopwatch is often difficult. Timing intervals of less than 1 second needs to be avoided since errors expected in the time measurements are desired to be less than 20 % assuming a reaction time of 0.1 second. The vast majority of time measurements need to be made of probe movements of 1 cm. However, the velocity with which the probe buried itself is sometimes too fast for a meaningful time measurement of a 1 cm change to be made. Therefore Flip video cameras can be useful. These cameras will work very well for recording the experiments since they recorded in a video format that is native to the computer and the files can be transferred directly to the

computer.

5.11 Generator: During field testing to run the controller and the flow pump generator is required.

5.12 Pump for water source: Water source can be obtained directly from nearby water front in the site. The tank can be filled up with this pump. For laboratory testing, water fountain or any other water source can be used to fill up the tank.

5.13 Hood: A 15 cm stainless steel hood can be used to connect with the bottom part of the probe. The hood helps to guide the probe straight into the soil.

5.14 Clamps: Steel clamps need to connect the probe sections.

5.15 Marker: Marker is required to mark the sheathing portion of the probe in cm to get the penetration readings.

5.16 Miscellaneous Equipments: Duct tape, Shovel, Clamp, Flathead, wrenches, plastic bags or basket to collect soil sample for soil testing.

6. Summary

6.1 A vertical probe employing a water jet used to estimate scour potential and erosion rates of sediments. The premise is that analysis of the probe penetration rate into the soil correlates with scour rate and hence, erosion potential. This method aims to measure the scour rate in situ and as a function of depth. The assumption is made that there is a 1-to-1 replacement of sand by probe as the probe advances into the sand.

The proposed approach is based on assessment of scour potential with depth by applying a vertical water jet and monitoring the rate of advancement and depth of erosion hole. As the water jet is induced through the cone tip, it mobilizes the soil particles. The sand particles are in a liquefied state while being transported from the annulus to the surface. The probe advances once an erosion of a sufficient area of soil beneath the tip occurred. During this process, the sand is displaced into the annulus, and the erosion process continued.

7. Procedure

7.1 Test bed setup: The surface of the test site needs to be leveled and voided from vegetation. To level the surface rack should be used. The hood connected with the probe needs to be touched with the soil surface before starting the test.

7.2 Probe assembling: Depending on desired depth of penetration, probe sections need to be connected. Attached probe sections will be inserted into the sheathing and the sheathings will be connected by steel clamps. The clamps will be connected with the sheathing by screws.

7.3 Water source and pump setup: Using a suction pump water needs to be extracted, with the help of a hose, from nearby water source and the tank needs to be filled up to ¾ of its volume. The controller connected with the flow pump should be connected with the generator when performing field testing or to socket in the laboratory.

7.4 Hose connection: A long hose needs to be connected from the flow pump to the tip of the probe. The hose should be inserted into the hollow probe.

7.5 Testing: The pump can run from 800 rpm to 3400 rpm. Using the calibration chart specific rpm can be found for desired water flow velocity. Time count will start when water will hit the soil surface.

7.6 Data extraction: The velocity of flow can be changed each time by changing the flow rate, with the diameter of the tip being the same for all cases (19 mm). Due to the speed with which depth change occurs during experimental measurements of the erosion rate, data should be collected through the use of videotaping. Measurements can be made by slowing the playback speed and using image processing software that will allow the timing interval to be 1/30 second.

7.7 Soil testing: After finishing depth tests in the field, soil samples need to be extracted from different layers to perform laboratory soil properties testing.

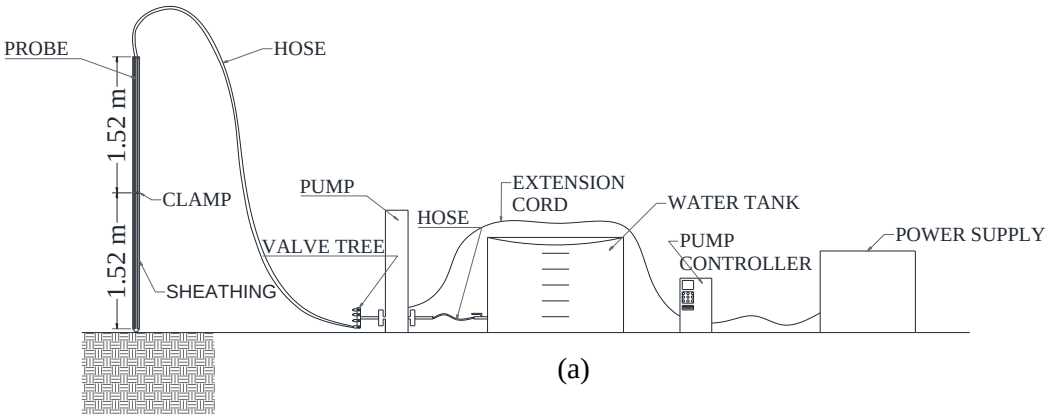

(a)

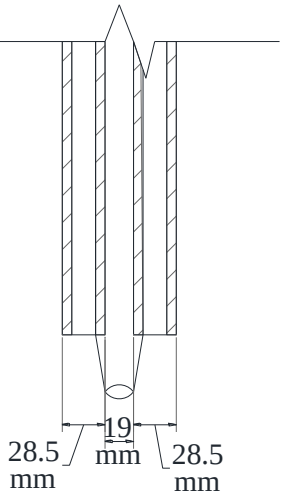

(b)

Figure 2. ISEEP (a) test setup and (b) cross-sectional view of the probe with the tip.

8. Calculation

8.1 Penetration rate for different layers: Penetration rate for different soil layers can be obtained from penetration depth against time plot (figure 3).

8.2 Bed Shear Stress: Shear stress produced by the jet can be calculated as

$$\tau\left(N/m^2\right) = C_f \rho U^2 \qquad (1)$$

where: τ = applied shear stress to bed in N/m^2, U = average velocity of water at the tip (m/s), ρ = density (kg/m^3), and C_f is a friction coefficient = 0.00416

8.3 Stream Power: Stream power can be calculated using the following equation

$$P = \tau U \qquad (2)$$

where: P is in the unit of Watts/m^2 (1 Watt = 1 N.m per sec or Kg.m^2 per sec ^{3}) and U = induced velocity.

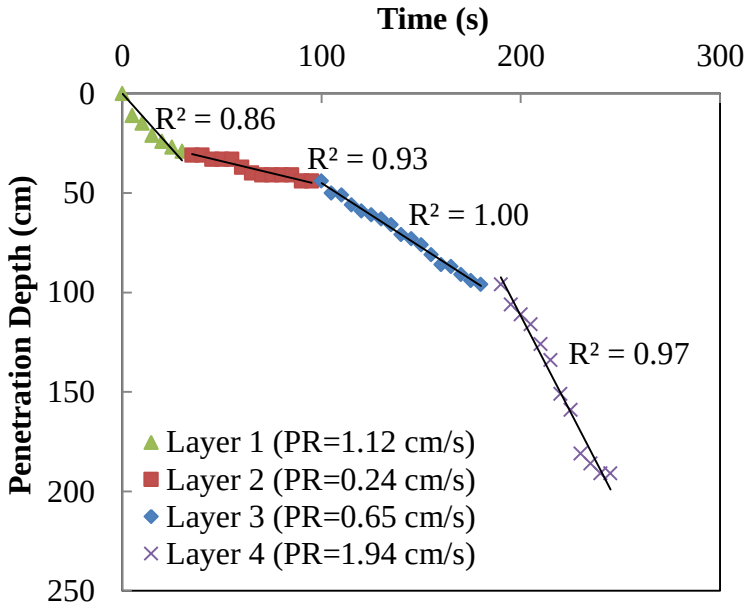

Figure 3. Penetration vs. Depth plot for a 1400 rpm test

8.4 Critical Stream Power: Critical stream power at which no erosion will occur is critical shear stress multiplied by the critical velocity.

$$P_c = \tau_c v_c \qquad (3)$$

Where[1], $\tau_c = D_{50}$ and $v_c = 0.35(D_{50})^{0.45}$

τ_c is in N/m^2, D_{50} is in mm and v_c is in m/s

8.5 Stream power vs. penetration rate plot: Penetration test should be repeated minimum of three times for three different jet velocities. Along with the critical stream power all testing points for a specific soil layer should be plotted (Figure 4).

8.6 Erosion rate: The rate of erosion describes the mass rate of erosion per unit area, or erosion rate (E) as a function of stream power exceeding the critical stream power value (P_c) as follows,

$$E = k_d'(P - P_c)^{\alpha} \qquad (4)$$

The k_d' coefficient, often called the detachment rate coefficient, and is basically the erosion rate normalized with respect to stream power leading to such a rate, and α is usually assumed to be 1.

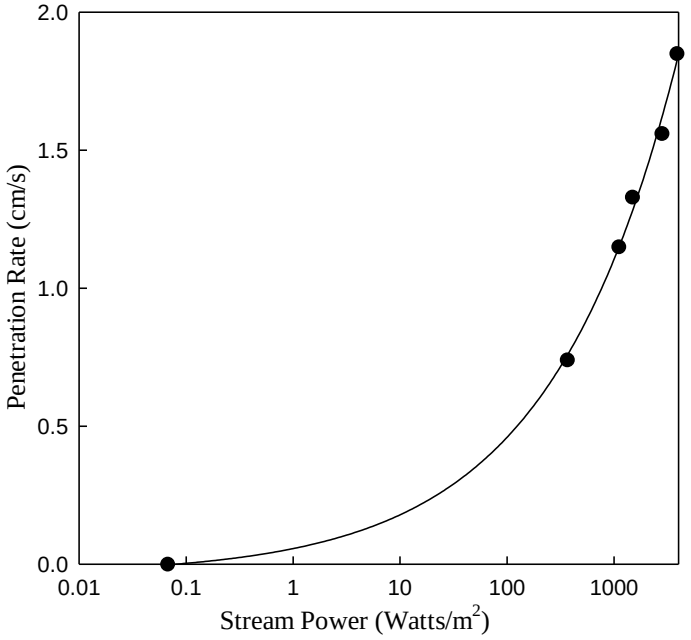

Figure 4. Erosion rate vs stream power for the top soil layer

1 Briaud J.-L., Chen H.-C., Chang K.-A., Oh S.J., Chen S., Wang J., Li Y., Kwak K., Nartjaho P., Gudaralli R., Wei W., Pergu S., Cao Y.W., Ting F. (2011). "The SRICOS-EFA Method." Summary Report, Texas A&M University, College Station, TX.

8.7 Detachment rate coefficient: Detachment rate coefficient (k_d') depends on stream power. For an applied stream power value detachment rate coefficient (k_d') can be obtained by calculating slope of the best fitted erosion rate versus stream power plot within a relatively straight zone of the curve that will cover the desired stream power value.

8.8 Erosion value: For a known applied stream power value and duration of the stream power value, using the detachment coefficient value calculated from erosion rate vs. stream power plot total scour depth can be evaluated using equation 4.

9. Report

9.1 Report the following items:

9.1.1 Location of the test;

9.1.2 Record the depth from which soil samples were collected, to evaluate soil properties in different layers;

9.1.3 The water content, particle size distribution and unit weight of the sample;

9.1.4 Grain size distribution of the soil sample obtained from the field in accordance with Practice D422;

9.1.5 Size of the tip.

9.1.6 ISEEP test results.

10. Precision and Bias

10.1 *Precision*—The precision for measuring soil erosion by the ISEEP method has been determined. Since erosion rate estimation using ISEEP has several steps therefore by being

Table 1 Summary of Laboratory ISEEP Testing at 2000 RPM (Penetration depth for a test duration =60 sec)

Soil Type	Number of Tests	Average Value (cm)	Standard Deviation (cm)	Coefficient of Variation (COV%)
SP	5	98.7	2.68	2.7

careful enough the data precision can be assured. Again the repeatability of the testing was performed in the laboratory where similar peat testing condition can be achieved by draining and saturating the peat. Table 1 shows test results for a 60 sec duration experiment performed by ISEEP in the laboratory for a sandy soil. Since the soil in the laboratory was a single layered soil therefore test duration of 60 sec was considered as reasonable time duration to achieve rational penetration rate.

10.2 *Bias*—There is no accepted reference value for this test method, therefore bias cannot be determined.

11. Keywords

11.1 erosion; iseep; soil; layered soil system; water; critical stream power; detachment rate coefficient.